Deltares
Enabling Delta Life

TU Delft

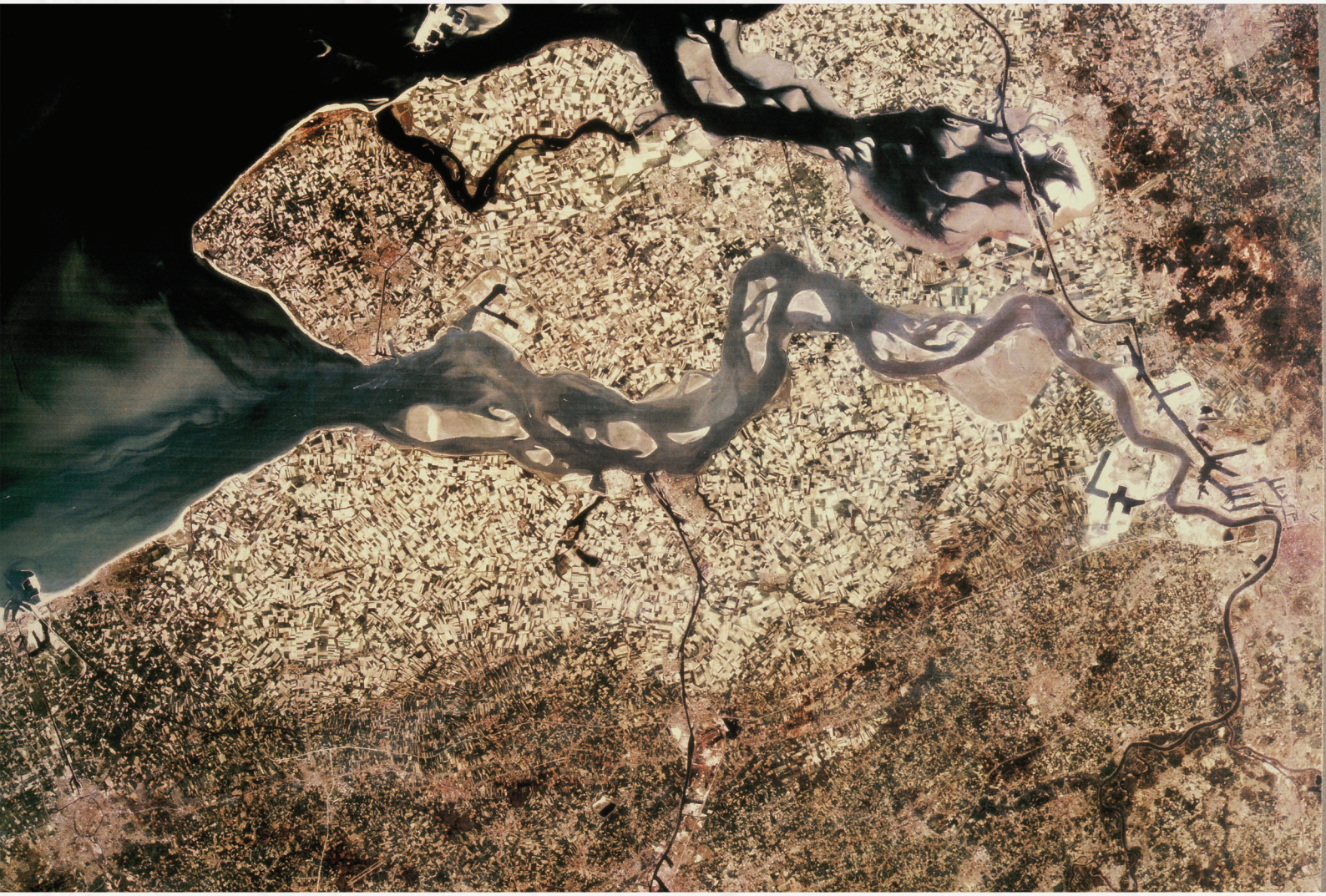

The role of mud on the long-term morphological development of a tidal basin

MSc Thesis

George Fotis

January 2017

The role of mud on the long-term morphological development of a tidal basin

By George Fotis

In partial fulfillment of the requirements for the degree of

Master of Science in Civil Engineering,
track of
Hydraulic Engineering

at Delft University of Technology

January 2017,
Delft, The Netherlands

Graduation Committee

Prof. dr. ir. Z. B. Wang	TU Delft / Deltares
Prof. dr. ir. J. C. Winterwerp	TU Delft / Deltares
Dr. ir. B. Van Maren	TU Delft / Deltares
Dr. ir. M. Van Der Wegen	Deltares / UNESCO IHE
Ir. G. Dam	Deltares / Svasek Hydraulics

PREFACE

This MSc thesis concludes the Master of Science of Hydraulic Engineering within the programme of Civil Engineering, at Delft University of Technology (TUDelft).

This has been a long journey and I would like to take this opportunity and thank all the people who have helped me through.

First of all, I would like to thank my graduation committee for their valuable advice and guidance throughout my thesis. I am very grateful to my daily supervisor Mick van der Wegen, who has provided me with everyday guidance and whose consistent way of thinking has always made things easier for me. Special thanks to Bas van Maren for sharing his knowledge with me and providing useful feedback. In addition, I would like to thank Gerard Dam for the discussions we had and for guiding me towards the right directions.

Moreover, I would like to thank my friends Pedro, Geert and Jennifer for the useful conversations we had, relevant to my thesis, as well as for the time we spent together getting to know each other better.

Finally, all of this would not have been possible without the unconditional support of my family and friends. Ευχαριστώ Μιχάλη, Γεωργία και Ελεάνα που δεν σταματήσατε να πιστεύετε σε μένα, να με στηρίζετε έμπρακτα, και να μου δίνετε θετική ενέργεια και κίνητρο κατά την διάρκεια των σπουδών μου. Ευχαριστώ επίσης όλους του φίλους μου που με στήριξαν ψυχολογικά και ιδιαίτερα τον Μίλτο, που έκανε τα προβλήματα μου και δικά του.

George Fotis
Delft, January 2017

ABSTRACT

The Scheldt estuary has been historically of great importance to The Netherlands and Belgium due to the fact that it serves a threefold purpose: safety, navigation and ecology. The numerous interests involved have increased the relevance of the area, urging the development of predictive tools (e.g. numerical models) in order to investigate the behavior of the estuary on the long-term.

Over the last years, process-based models have been used towards predicting future estuarine morphology. Comparison between measured and modeled parameters has pointed out the predictive accuracy of these models. However, most of these models have used sand as the representative sediment diameter, thus, neglecting finer grains.

The physical system of the Western Scheldt consists also of fluvial and marine mud imported from the river and the tide respectively. Mud is settling at the shallow areas leading to a direct reduction of the accommodation space. This change can be related to a change in residual transport and hence, a change in morphology. Furthermore, the geometry of the basin is altered as a result of mud deposition; the latter is coupled to the hydrodynamics and through sediment transport, a feedback loop is initiated leading to morphological change.

In order to investigate the effect of mud on the long-term morphological development of a tidal basin under fluvial and tidal forcing, a two-dimensional depth-averaged schematized model is set up, using the process-based Delft3D software. The specifications of this model are chosen such that it reflects the Western Scheldt estuary thereby increasing the relevance of this study.

The idea behind this model is to investigate the influence of mud on the mechanisms responsible for morphological change. Residual sediment transport is considered as a main driver of morphological development. Therefore, the impact of mud on the parameters that influence residual sediment transport is tested. The approach used is as follows: the model is initially forced by sand so that a reference bathymetry is created. Using this bathymetry as a starting point, mud is implemented. Accordingly, four scenarios are formed by varying the boundary conditions. Comparison between scenarios and further analysis on specific parameters, that influence residual transport, highlights the importance of mud on each of the parameters.

Model results indicate a decreased export of sand when mud is applied in the domain. Analysis proves that this decrease can be associated with three mechanisms: the reduction of tidal storage, the hiding effect and the reduction of Stokes Drift return current, all of them induced by mud. Furthermore, it is concluded that the effect of mud on tidal asymmetry is minor and hence, tidal asymmetry cannot be considered as a mechanism responsible for the change in morphology.

Furthermore, a sensitivity analysis is done in order to realise the influence of input parameters (e.g. fall velocity, critical shear stress for erosion, river discharge and others) on the model output. Model results are then, qualitatively, compared to the physical system of interest.

CONTENTS

1

INTRODUCTION

1.1 Background information

The Scheldt estuary is situated at the border of The Netherlands and Belgium. It consists of three main parts: the tidal river, extending from Ghent to about Antwerp, the Western Scheldt estuary, located between Antwerp and Vlissingen and the ebb-tidal delta. At Ghent the tidal wave is impaired in the upstream direction by the use of sluices.

Looking at geological timescales (millions of years), the morphology of the area of Zeeland has not been constant; reconstruction of Holocene evolution has proved it was part of the North Sea that later on silted up almost completely (by 3100BC). Since 200AD, the peat bog deteriorated and finally large basins and estuaries appeared. In the following years, land reclamation and land loss due to severe storms in the North Sea changed the morphology into the one we know in the recent days (Figure 1):

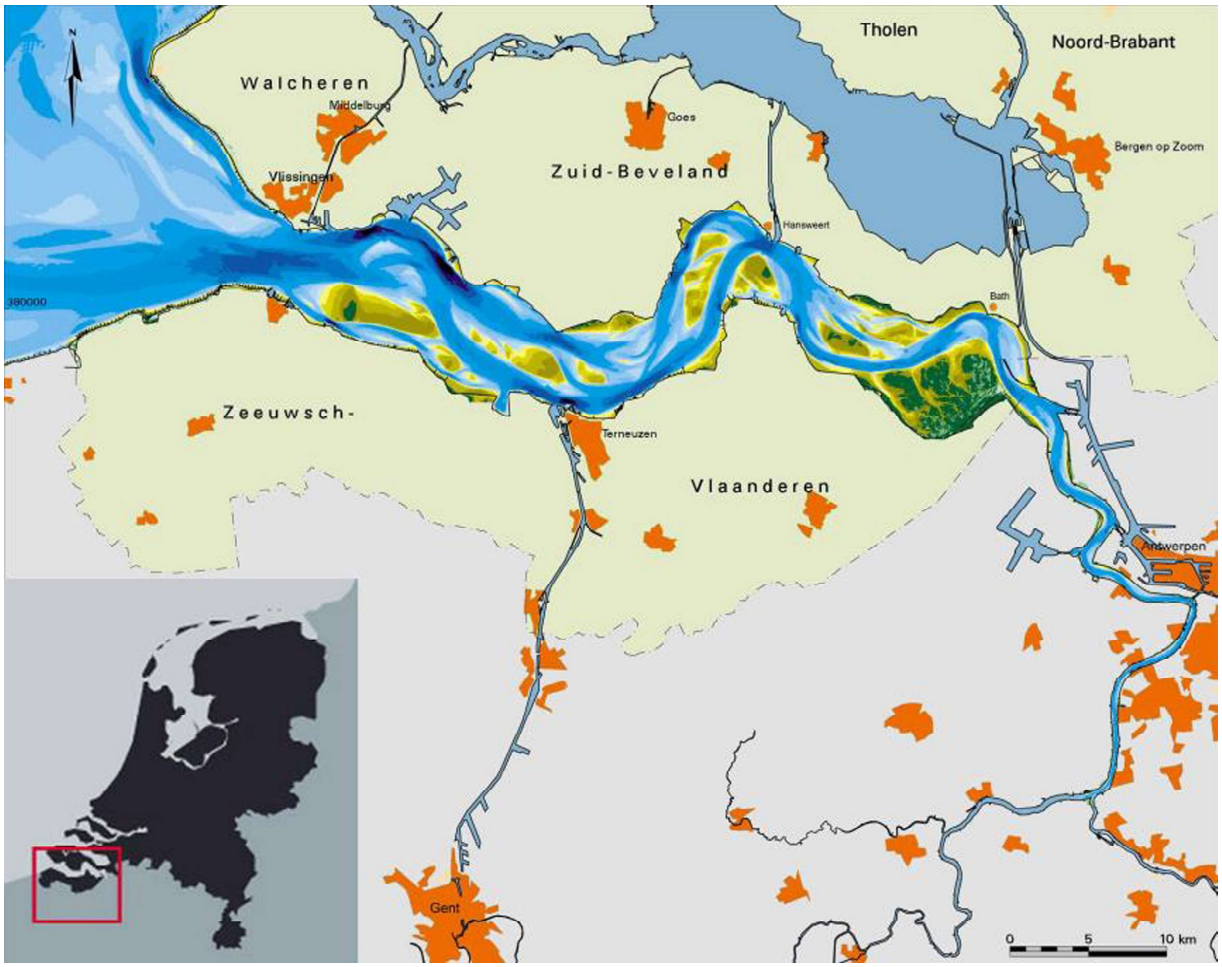

Figure 1 – The Scheldt estuary (From van der Werf and Briere, 2013)

Presently, the Western Scheldt exhibits a well-developed system of channels and shoals. It has a funnel-shaped geometry and covers an area of about 370 km^2. Its cross-sectional area decreases exponentially from the estuary mouth at Vlissingen to the estuary head near Ghent. The width averaged depth decreases from about 15 m at Vlissingen to only 3 m near Ghent while the width of the estuary reduces from 6 km to less than 100 m.

The estuary can be characterized as a multiple channel system, separated by elongated tidal flats. The large channels form a more or less continuous meandering channel, constrained by fixed points along the estuary (e.g. dikes). Due to the meandering of the channels, shallow areas are formed (i.e. sills), positioned at the transitions between channel bends.

There has been extensive research related to the Scheldt estuary over the past years. The reason behind this is related to the numerous interests involved, sometimes conflicting with each other. The purpose that it serves in principle is threefold: safety, navigation and ecology.

In 1953 a flood inundated Netherlands; this event created the urgent need of an improved national coastal defence system. As a result, under the Delta Works framework, estuaries were closed off from the sea (viz. HaringvlietDam, BrouwersDam) and enormous storm surge barriers were constructed (viz. Eastern Scheldt). Yet, the Western Scheldt was not considered possible to be closed-off due to navigational as well as ecological concerns. Alternatively, the Dutch government constructed dikes of significant height, thereby reducing the possibility of flooding at certain areas adjacent to the estuary (e.g. Vlissingen, Terneuzen).

Because of its distinct morphology, the estuary comprises a number of internationally acclaimed nature reserves. In addition, several fisheries have developed at certain points along the estuary. Consequently, it is of high ecological and commercial importance.

At the same time, the mouth of the estuary serves as an entrance to one of the biggest ports in Europe; the port of Antwerp. It is needless to say that keeping the navigational aspects (e.g. required depth, navigational aids, etc.) to a high level is essential for the economic growth of the port and therefore for Belgium itself. Moreover, the ports of Vlissingen and Terneuzen are found along the banks of the estuary. A large proportion of the working population in Zeeland (10%) depends on port-related activities. Hence, the Scheldt estuary is of major regional economic importance to Netherlands as well.

Although the length of the Belgian coast is limited (i.e. 67km), extensive use from different parties takes place; ports and industries are active by the sea side while the area is also used as a touristic resort. As a result, the need for coastal protection in the area comes first. Until now, yearly nourishments have been taking place along the Belgian coast in order to counteract erosion and ensure the desired safety levels. However, the expected sea level rise in the upcoming years has raised significant safety concerns and made the need of an integrated long-term plan essential. The Flemish government is interested in investigating large-scale interventions at the mouth (Master plan for Flanders Coastal Safety).

The physical processes at the mouth differ significantly compared to the ones taking place in the inner estuary. As a result, the influence of parameters that force morphological development differs as well. Therefore, new prediction tools have to be developed (e.g. numerical models) which take into account the relevant processes and evaluate their respective parameters accordingly.

1.2 Problem statement

Remarkable research around process-based models and their ability to predict long-term estuarine morphodynamics has been done over the past years.

Hibma, 2003 using a two-dimensional depth-averaged numerical model showed how due to nonlinear interactions, an initially perturbed regular-shaped estuarine environment merged to a complex channel shoal system.

Wegen & Roelvink, 2008 investigated the evolution of a tidal embayment using a numerical, process-based model. The 2-D model results clearly depicted distinct pattern formation with different timescales. In addition, comparison of the model results to data from the Western Scheldt showed acceptable results in terms of morphological wavelengths.

Further study (Wegen & Roelvink, 2012) proved the ability of a process-based, numerical model to reproduce the basic pattern formation observed in the Western Scheldt with significant skill. Starting from

a flat bed and imposing the Western Scheldt geometry, two different pattern formations were produced by the model in the long-term; namely, the channel-shoal formation and the longitudinal bed development with timescales in the order of magnitude of decades and centuries respectively.

Most of these studies have deliberately considered only one representative sediment diameter (i.e. sand) to account for the whole sample, thus, neglecting finer grains. However, the impact of mud on the estuarine system of the Western Scheldt should not be overlooked; on the one hand, it is of high environmental and ecological importance to the system (e.g. mudflats) while on the other, knowledge around mud deposition rates at port areas is essential for a successful dredging management. On top of that, the influence of mud on the long-term evolution of the estuary has not been sufficiently investigated yet and as a result, its effect on the physical system is not adequately determined.

Numerous field surveys were conducted in the past with the purpose of determining the origin and concentration of mud along the estuary. Verlaan (2000) proved the existence of significant marine mud volume fraction in the (tidal) river part of the estuary, thus, indicating marine mud import (Figure 2):

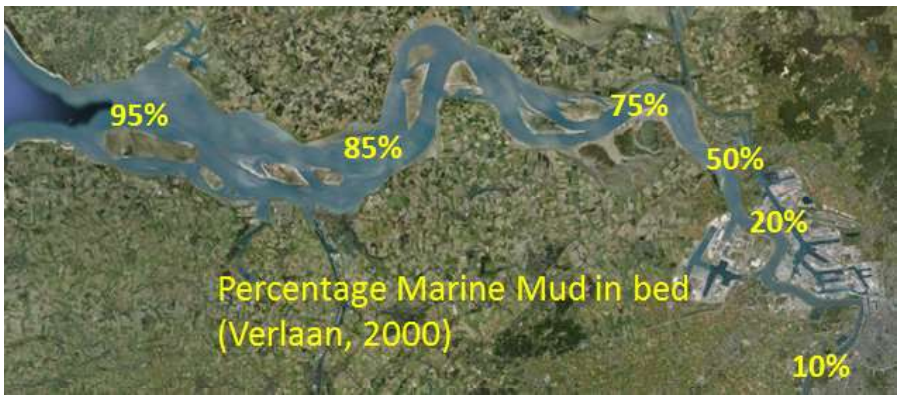

Figure 2 - Percentage of marine mud in bed (Verlaan, 2000)

Several processes, partly strengthening each other, determine the residual transport of fine-grained sediment. Some of them are the following:

- Residual flows including estuarine circulation
- Temporal as well as spatial asymmetries in the tide
- Lag effects introduced by sediment properties in combination with the asymmetric tide

Van Maren and Winterwerp, (2013) mention that the responsible mechanisms behind these lags are two: the asymmetric flow velocity (e.g., slack tide asymmetry) and the asymmetry in sediment properties (viz., in mobilization, vertical mixing and settling). The combination of these asymmetries induces net sediment transport and thus, a change in morphology. Therefore, a thorough understanding of the velocity profile in combination with sediment characteristics is essential towards understanding mud dynamics.

Past studies have pointed out the importance of mud dynamics in the morphological evolution of the Western Scheldt estuary. Observations have proved that finer grains tend to accumulate more at sheltered areas, which are protected against tidal currents and waves, and less at the main channel. Figure 3 indicates the distribution of mud fraction on the bed:

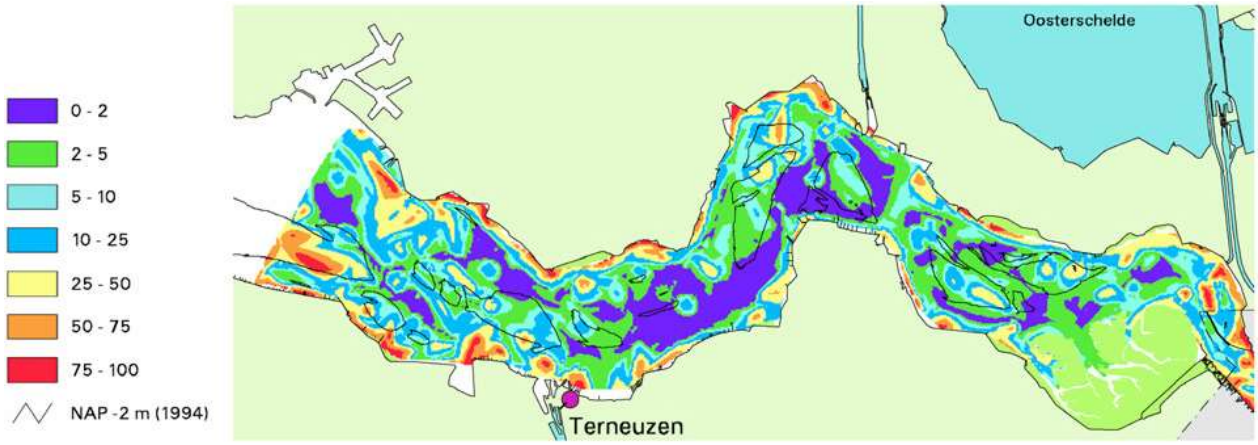

Figure 3 – Observed mud fraction on the bed (McLaren, 1994)

The volume that is contained between surface elevation at high water and the bed, where sediment can accumulate, is defined as the accommodation space of an estuary. As both surface elevation and bathymetry are changing over time, so does the volume, and hence, the accommodation space.

The deposition of fines at the shallow areas of the estuary may have an impact on the sediment budget of the Western Scheldt; mud is settling on the bed leading to a reduction of the accommodation space. This might have an effect on the residual sediment transport of fine as well as coarse sediment, thus, forcing morphological development. Furthermore, basin geometry influences tidal distortion, which in turn has an effect on residual sediment transport. The underlying mechanism is depicted in Figure 4:

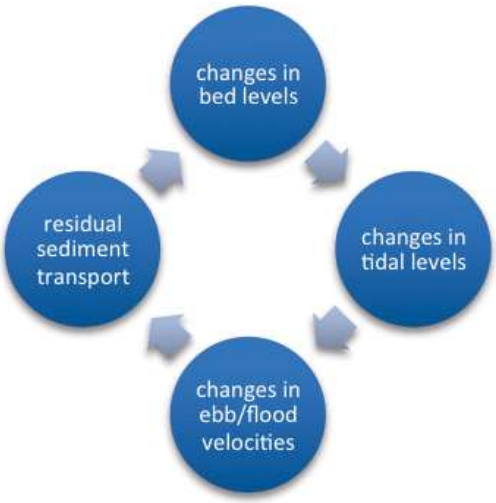

Figure 4 - Schematic representation of the interaction between morphology and tidal asymmetry

The findings of a long-term simulation of the Western Scheldt estuary using sand and mud suggest that mud does have an influence on the sediment budget of the estuary (Dam, Wegen, Bliek and Cleveringa, 2016). In this model, a standard concentration of mud is applied both at the seaward and the landward boundary.

The results initially indicate import of mud (marine and fluvial) and export of sand; the accumulation of mud however leads to a reduction of the accommodation space and hence after 100 years of simulation, export of mud is observed. As a result, the total sediment volume starts decreasing over time. The results of this analysis are visible in Figure 5:

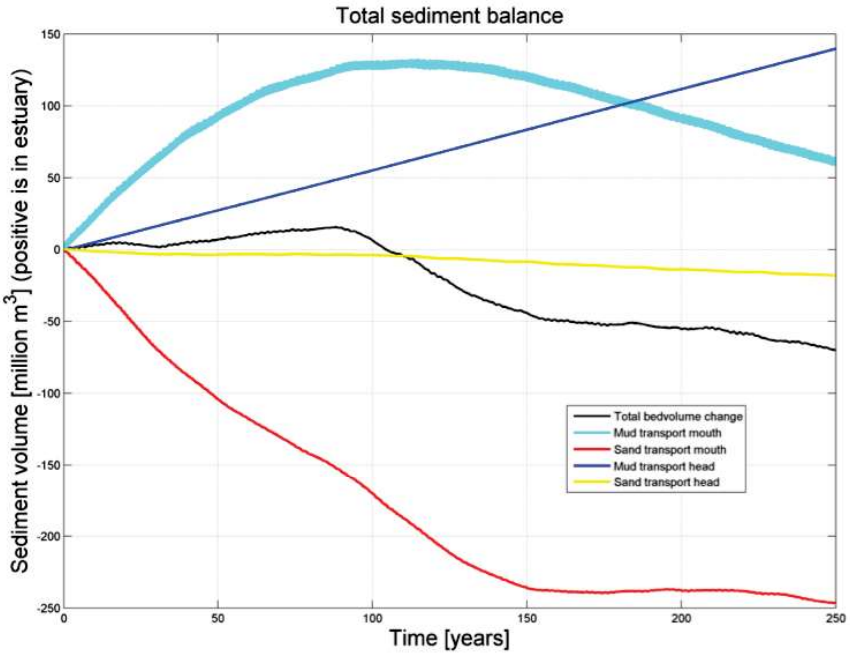

Figure 5 - Sediment Balance (Dam, Wegen, Bliek and Cleveringa, 2016)

The focus of this MSc thesis is to explore the influence of mud on the estuarine morphology; this can be achieved by investigating its impact on the accommodation space and tidal asymmetry.

1.3 Research questions

The aim of this MSc thesis is to determine the role of mud on the long-term morphological evolution of a tidal basin, as the result of tidal and fluvial forcing. For this purpose, use is made of a simple schematized model, set up in Delft3D.

In the process of trying to give an answer to this main question, several aspects have to be clarified. Some of the research questions can be formed as follows:

Q1. What is the influence of mud on the morphological development?

Q2. What is the sensitivity of model output to changes in certain parameters?

Q3. What is the impact of mud on the hydrodynamics?

Q4. What is the impact of mud on the residual sediment transport?

1.4 Approach

A literature review will be done on the physical processes governing the Scheldt estuary. Reference will be made to the influence of morphology on tidal asymmetry and, in turn, the influence of tidal asymmetry on morphological development through residual sediment transport. In addition, numerical modelling aspects are going to be discussed; concepts relative to hydrodynamics and sediment transport in relation to the model will be analysed. Literature review will give an insight into the next stage that has to do with the set up of the model.

When it comes to simulation it is important to start simple and increase complexity step by step. Following this reasoning, a lot of information in terms of which parameters are responsible for a possible model outcome can be obtained. The purpose of this thesis is to determine and explain the importance of mud on the morphological evolution of a tidal basin.

Therefore, use will be made of a simple schematized model, set up in Delft3D, which will be the tool, while attempting to give an answer to following questions:

Q1. What is the influence of mud on the morphological development?

The impact of forcing on the morphological development of the system will be determined by varying the imposed boundary conditions of the model. Hence, the following scenarios can be formed:

S1. Sand
S2. Sand + marine mud
S3. Sand + fluvial mud
S4. Sand + mud at both boundaries (standard scenario)

For instance, the influence of fluvial mud can be realised by comparing S4 to S2. Moreover, comparing S4 to S1 the role of mud (in total) in the system can be assessed.

Q2. What is the sensitivity of model output to changes in certain parameters?

Using a standard scenario, sensitivity analysis will be performed in order to get an idea on how different parameters influence the model results. The following parameters are going to be tested:

Sensitivity Analysis parameters	Units	Scenarios		
Erosion parameter	$kg/m^2/s$	5E-05	1E-05	5E-04
Fall velocity	mm/s	0.1	0.5	1
Critical shear stress for erosion	Pa	0.15	0.25	0.35
River discharge	m^3/s	100	300	600
Mud concentration at the boundaries	kg/m^3	0.025	0.05	0.1

Table 2 - Creating bathymetry specifications

Q3. What is the impact of mud on the hydrodynamics?

Comparison of the flow velocity record between scenario S4 and S1 throughout the years of morphological evolution will highlight the importance of mud on the hydrodynamics. Local horizontal tidal asymmetry can be credited to local bathymetry.

Q4. What is the impact of mud on the residual sediment transport?

Residual sediment transport is driven by changes in morphology induced by mud. There are several mechanisms responsible for residual transport. The role of mud in these mechanisms is going to be examined by comparing different runs (e.g. S4 to S1).

Close attention will be paid on the following:

- The impact on accommodation space and tidal storage
- The impact on slack period
- The impact on peak flow asymmetry

The essential parameters for this analysis are mentioned below:

1. T_{HWS}, T_{LWS}
2. T_{FLOOD}, T_{EBB}
3. α_{M2}/α_{M4}, $2\varphi_{M2}-\varphi_{M4}$
4. Intertidal area

Where,

T_{HWS}=high water slack duration
T_{LWS}=low water slack duration
$T_{(FLOOD/EBB)}$=flood/ebb period
a_{M2}/a_{M4} =amplitude ratio between M2 and M4 tidal constituents
$2\varphi_{M2}-\varphi_{M4}$=phase difference between M2 and M4 tidal constituents

2

LITERATURE REVIEW

2.1 Propagation of the tide

A tidal wave is a long wave (h/L<0.05), which means that following the dispersion relation, its propagation speed can be described by the following equation: $c=(gh)^{1/2}$. This statement implies that the propagation velocity depends solely on the water depth. Consequently, taking into account that the period of the wave is invariant, the wavelength varies linearly with the velocity (i.e. L=cT).

In the open ocean, the tidal wave can be described by the Shallow Water Equations (SWE). Starting from the Navier-Stokes Equations and neglecting friction, advection, horizontal diffusion and short wave effects, we arrive to the following set of equations:

$$\frac{\partial u}{\partial t} = -g\frac{\partial \eta}{\partial x} \quad (1)$$

$$\frac{\partial \eta}{\partial t} = -h\frac{\partial u}{\partial x} \quad (2)$$

Applying a number of mathematical modifications to the above equations, the second degree hyperbolic differential equation that describes the propagation of the wave in the open ocean yields:

$$\frac{\partial^2 \eta}{\partial t^2} = gh\frac{\partial^2 \eta}{\partial x^2} \quad (3)$$

The previous wave is a progressive wave (i.e., there is no phase difference between surface elevation and velocity). In other words, highest velocities are found below wave crests (and troughs) while lowest velocities around MSL.

However, as the wave propagates towards the coast, bed friction as well as wave reflection prevail, leading to a wave whose velocity and surface elevation is out of phase. The exact phase difference cannot be easily determined due to the complex bathymetry and geometry of the basin; measurements suggest that it varies between 0^0 and 90^0, with velocity always leading the surface elevation. In more detail, as the wave enters a funnel shaped estuary (as in the case of the Western Scheldt), it is influenced both by friction and inertia. As the wave propagates up in the estuary, bottom friction dampens its amplitude and as a result the reflected wave does not have the same amplitude as the incoming wave. Overall, it can be stated that the propagation of the wave along the estuary has a partly progressive and partly standing character.

Moving to our area of interest; along the western coast of The Netherlands, a semidiurnal tide propagates from South to North. This tide belongs to the amphidromic system in the Southern Bight of the North Sea.

As the tidal wave propagates northwards it is losing its sinusoidal character becoming steeper and steeper. In addition, the influence of friction on the tide becomes evident by the space decreasing amplitude, which implies damping (Figure 6). This has consequences on the asymmetry of the co-oscillating tides in the Dutch tidal basins and estuaries (J. Dronkers, 1986).

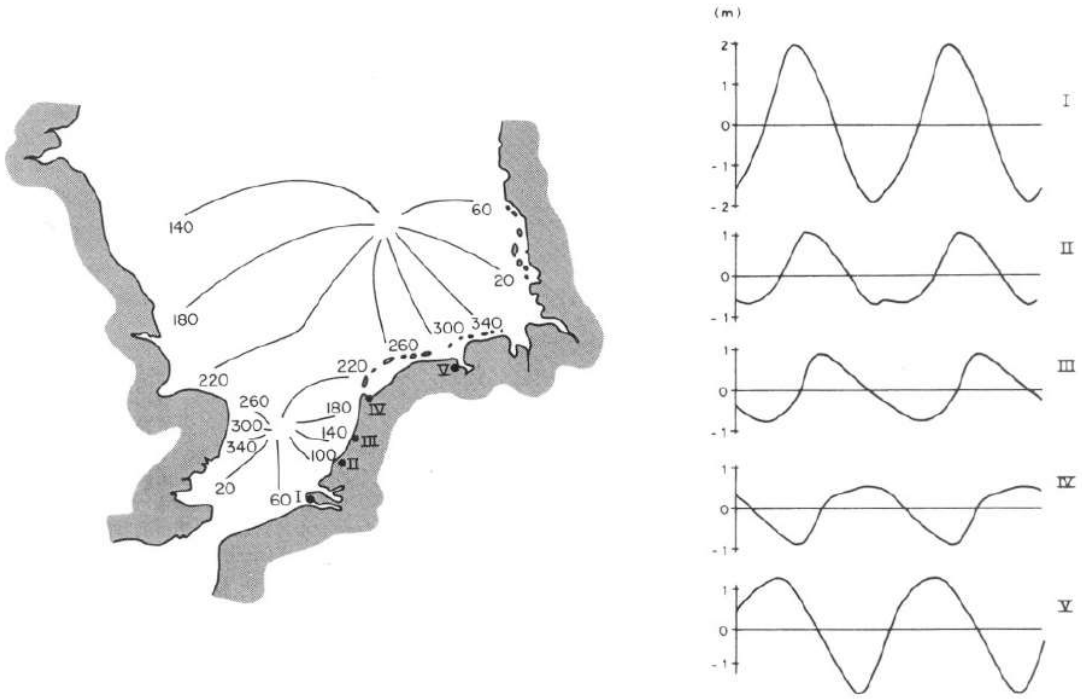

Figure 6- Distortion of the tidal wave propagating along the Dutch coast (Rijkswaterstaat)

2.2 Tidal Asymmetry

2.2.1 Physical description

The number of the physical processes taking place in an estuary urges for consistency in terminology. Throughout this MSc thesis, the terms vertical and horizontal tide are going to be used to describe the surface elevation and the velocity of the tidal wave respectively. The terms rising and falling period will refer to the vertical tide while the terms flood and ebb will relate to the horizontal tide. In addition, high water slack (HWS) and low water slack (LWS) will refer to flow reversal from flood to ebb and from ebb to flood respectively.

According to Linear Wave Theory, the tidal wave can be visualised as a sinusoidal wave with no deformations over the horizontal or the vertical axis; still, this is only the case in deep water. When the wave approaches the shallow part of the estuary, basin geometry as well as reduced bathymetry gives rise to wave distortion. Wave transformation theory suggests that the wave initially shoals and later becomes steeper and steeper until the point of breaking (usually, around $H \approx 0.8h$).

In more detail, the width restriction yields to a slowing-down of the wave, ultimately leading to shoaling. Similarly to width-induced shoaling, depth-induced shoaling takes place, causing even higher wave amplitudes. On the other hand, bed friction acts as a counteracting force by inducing wave damping. The net result depends on the relative influence of each of the above-mentioned effects.

Literature introduces two types of asymmetries; peak flow asymmetry, which is the asymmetry over the horizontal axis and slack tide asymmetry, which is the asymmetry over the vertical axis. Peak flow asymmetry suggests flood (or ebb)-dominance when flood (ebb) velocities exceed ebb (flood) velocities. Slack tide asymmetry is defined as the difference between flood and ebb slack tide period at which flow velocities are below a certain threshold value.

2.2.2 Mathematical description

Tides originate from the gravitational force that celestial bodies (i.e. sun, moon) exert on the earth; as a result their frequencies and periods are exact and relate to the movement of the earth-sun (earth-moon) system. For instance, the main tidal constituents that are used to describe the tide, viz., M2, S2 have a period of 12,42h and 12h respectively.

The mathematical representation of tidal distortion is possible with the employment of the shallow-water tides. The term shallow-water tides or overtides, is used to describe the tidal constituents that are not created by the astronomical forcing but are rather the result of non-linear effects in the shallowing waters. The two most important parameters introducing tidal distortion is continuity and bottom friction.

The 1D representation of tidal motion in a prismatic channel can be given by the following set of equations:

$$\frac{\partial u}{\partial t} + u\frac{\partial u}{\partial x} = -g\frac{\partial \zeta}{\partial x} - c_f\frac{u|u|}{h_0+\zeta} + \frac{\partial}{\partial x}\left(v_t\frac{\partial u}{\partial x}\right) \quad (4)$$

$$\frac{\partial \zeta}{\partial t} + \frac{\partial}{\partial x}[u(h_0+\zeta)] = 0 \quad (5)$$

Where,

$\frac{\partial u}{\partial t}$ local inertia term (A)

$u\frac{\partial u}{\partial x}$ advective inertia term (B)

$g\frac{\partial \zeta}{\partial x}$ pressure term (C)

$c_f\frac{u|u|}{h_0+\zeta}$ friction term (D)

$\frac{\partial}{\partial x}\left(v_t\frac{\partial u}{\partial x}\right)$ horizontal diffusion term (E)

$\frac{\partial \zeta}{\partial t}$ storage term (F)

$\frac{\partial}{\partial x}[u(h_0+\zeta)]$ discharge gradient term (G)

From the above terms, (B), (D), (E) and (G) are not linear; if we assume that ∂u/∂x is small, then the diffusion term can be neglected. Therefore, the main source of non-linearity comes from the three remaining terms, namely, the advective inertia, bottom friction and the discharge gradient (Wang, Jeuken, de Vriend, 1999).

In shallow waters continuity equation yields to: $c=\sqrt{g(h\pm a)}$; this suggests that wave crest propagate faster than wave trough. The latter implies a shorter rising period and hence a shorter flood duration which in turn equals with flood dominance. This distorted signal can be mathematically assigned with the use of a sinusoidal wave with double the frequency of the main tidal constituent (i.e. M4), which is in phase with the basic astronomical constituent (M2); the summation of these waves introduces skewness.

Speer et al (1991) concluded that the relative phase difference between quarter-diurnal components and their parent constituents (i.e. semi-diurnal) is approximately equal for all the components at a certain station; based on this conclusion, tidal distortion can be solely based on the analysis of the M2 component and its overtides (M4, M6). In order to analyze the M2-M4 induced tidal distortion the velocity signal can be written as: $v(t) = \widehat{u_{M2}}\cos(\omega_{M2}t) + \widehat{u_{M4}}\cos(\omega_{M4}t - (\varphi_{M4} - 2\varphi_{M2}))$

The signal will be flood-dominant as long as $270^0 < \varphi_{M4}-2\varphi_{M2} < 90^0$ and ebb-dominant if $270^0 > \varphi_{M4}-2\varphi_{M2} > 90^0$, in which $\varphi_{M4}-2\varphi_{M2}$ is the phase difference between M4 and M2.
Furthermore, saw-tooth asymmetry can be mathematically implemented with the suitable angle φ.

In Figure 7 the asymmetric velocity profile, which is the result of summation of the tidal components M2 and M4, is presented for different values of φ (where $\varphi=\varphi_{M4}-2\varphi_{M2}$).

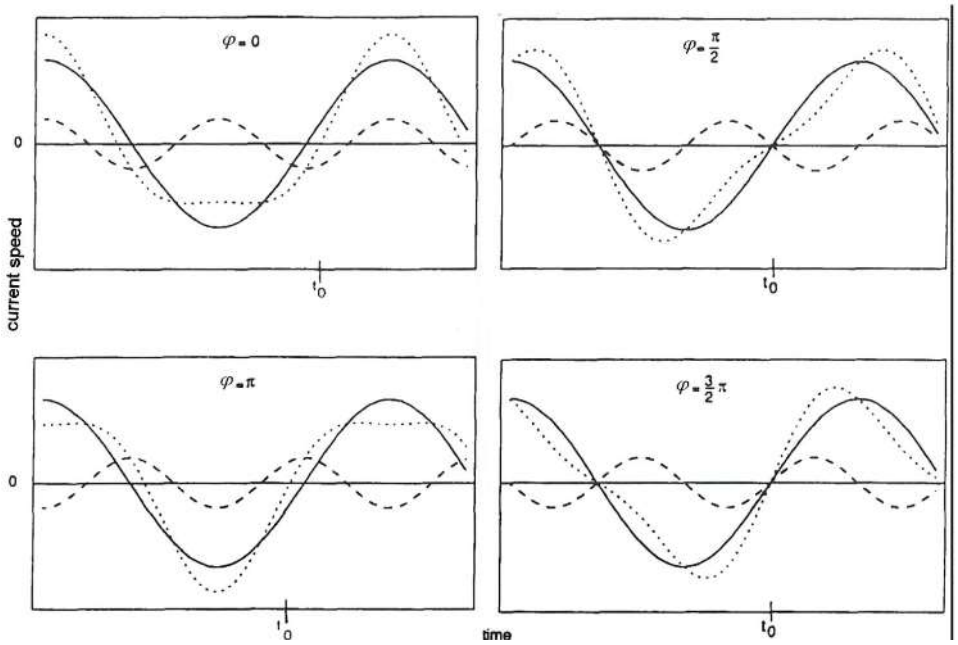

Figure 7 - M2 and M4 tidal constituents. From Bosboom and Stive (2013)

Figure 7 shows that at 0^0 and 180^0 of phase difference the signal is skewed (i.e. positively and negatively respectively) while at 90^0 the signal is appeared distorted over the vertical axis with longer low than high duration of slack water. At 270^0, high water slack is longer than low water slack duration. Figure 8 illustrates the influence of the phase difference between M2 and M4 on the tidal signal:

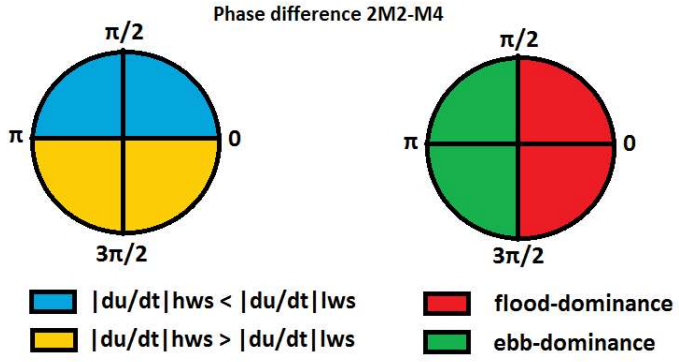

Figure 8 - Phase difference between M2 and M4 horizontal tidal components and the corresponding tidal distortion

Moreover, bottom friction (D) generates tidal constituents with a frequency three times larger than the frequency of the main tidal components (sixth-diurnal); this is due to the quadratic dependence of the bottom shear stress on the current speed: $\tau_b=\rho c_f u|u|$. Therefore, friction produces M6 out of M2 (S6 out of S2).

The above-mentioned conclusions regarding the creation of higher harmonics, are also verified by Wang, Jeuken, de Vriend, (1999); during chapter 4 (Summary, conclusions and recommendations) it is mentioned: "a time-invariant mean effect (rectification) and the overtide M4 originate from the auto-interaction of the M2 via three non-linear terms, viz.: the adjective inertia term, the bottom friction and the discharge gradient. The sixth-diurnal overtide M6 is essentially due to non-linear interaction of M2 with itself and other fundamental constituents (e.g. S2) via bottom friction."

A comprehensive literature survey on local non-linear tidal interaction mechanisms is given in chapter 3 of the book "Tidal Hydrodynamics" edited by B.B. Parker (1991).

2.3 Relation between morphology and tidal asymmetry

2.3.1 Influence of morphology on tidal asymmetry

Speer and Aubrey (1985) and Friedrichs and Aubrey (1988) made use of a 1D numerical model in order to investigate the influence of morphology and bathymetry of a friction dominated, well-mixed, short estuary, on the tidal signal. After conducting this survey they concluded that the most important factors determining tidal distortion are the following: the ratio of the mean tidal amplitude over the water depth (α/h) and the ratio of the volume of water stored at the intertidal flats between high and low water over the volume of water contained in the channels below MSL (Vs/Vc). Consequently, the variation of tidal distortion with (α/h) and (Vs/Vc) can be seen in Figure 9:

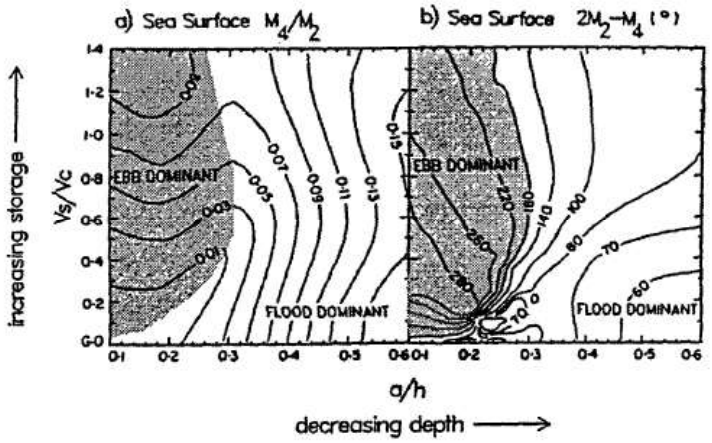

Figure 9 - Contour plots of parameters that determine n-l distortion as a function of α/h and Vs/Vc, resulting from 84 model systems. The 1800 contour separates the plots into flood- and ebb-dominant regions. After Friedrichs and Aubrey (1988)

Two parameters characterizing tidal asymmetry have been defined (Wang et al, 2002): the amplitude ratio M4/M2 and the phase difference 2M2-M4; they relate to the intensity of the asymmetry and the type of the asymmetry respectively. Following this reasoning, the relation between M2 and another higher harmonic (e.g. M6) can be expressed by introducing the respective parameters.

As it can be concluded from Figure 9, an increase in the intertidal area enhances ebb-dominance while larger tidal amplitude combined with smaller depth leads to flood-dominance. This conclusion is also true for the Western Scheldt estuary since it comes to an agreement with the findings of Wang, Jeuken, de Vriend, (1999). Therefore, qualitatively, the results of Speer (1991) are applicable to the Western Scheldt. However, Friedrichs and Aubrey assume a standing wave pattern (i.e. short basin), while the Western Scheldt is not a short basin.

Furthermore, except from peak flow asymmetry, slack tide asymmetry can also be linked with morphology. Literature has showed that, with regards to irregularly shaped estuaries, two types of geometries can be discerned (J. Dronkers, 1987):

a) Estuaries with deep channels throughout and tidal flats above MSL
b) Estuaries with shallow channels (landward depth decreasing) and tidal flats below MSL

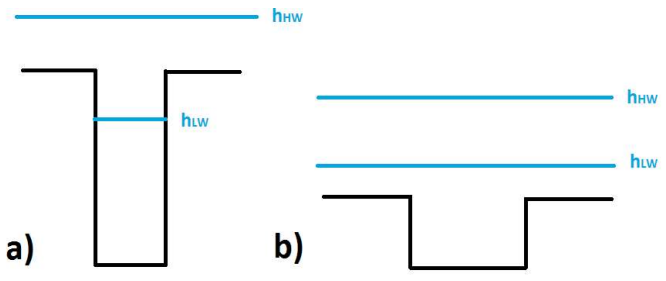

Figure 10 - Type of estuarine cross-sections

Case a) can be associated with a longer low water slack duration while case b) with a longer high water slack duration. The physical interpretation of this can be understood by the non-linear propagation of the tidal wave.

2.3.2 Influence of tidal asymmetry on residual sediment transport

Research has indicated that residual sediment transport has two main components: residual flow velocity as well as higher frequency constituents of the flow velocity (i.e. tidal asymmetry) (Wang, Jeuken, de Vriend, 1999).

The first term can be related to an upstream river discharge, the Stokes drift in case of wind waves (also in tidal waves), a bathymetry-induced residual current, a curvature-induced and Coriolis-induced secondary flow as well as to estuarine circulation (i.e. residual flow pattern induced by the density difference between sea water and fresh water). The second term has already been discussed earlier.

According to Tee (1976) the main drivers of residual currents are: non-linear bottom friction, non-linear terms in the continuity equation as well as non-linear advective terms in the momentum equation (inertia).

Following the reasoning of continuity, the same volume of water that flows into the estuary during flood flow has to flow out during ebb flow. This statement holds as long as water is not stored. The reason that makes tidal asymmetry so important is that velocity scales non-linearly with sediment transport. The latter implies that what holds for water does not necessarily hold for sediment.

In other words, since any sediment transport formula is a power function of flow velocity, higher velocities can lead to higher sediment transport rates. Averaged over the tide, this might lead to a net import or export of sediment and as a result, to erosion or deposition at certain parts of the estuary. Therefore, residual flow and tidal asymmetry may lead to residual sediment transport, thus, urging morphological evolution.

As far as bed load is concerned (mainly coarse sediment), Van de Kreeke and Robaczewska (1993) mention "only the residual flow velocity u_0 and the velocity signal of the M2 overtides viz., uM4 and uM6 are important for the long-term averaged bed load transport rate" (Wang, Jeuken, de Vriend, 1999). The main conclusion of this study is that a flood-dominant velocity signal leads to a net import of coarse sediment while an ebb-dominant to a net export. Therefore, peak flow asymmetry determines the residual transport of coarse sediment.

Sediment transport of fines is much more complicated than coarse. Due to low fall velocity of the grains, most of the fines cannot accumulate during the tidal cycle and as a result they are kept in suspension. Unlike bed load transport, suspended load depends on the memory effect; the flow condition upstream of the area of interest and in the past has to be taken into account, since it has an influence on the suspended sediment concentration.

Maximum suspended sediment concentration (red dotted line) lags behind maximum depth-averaged flow velocity (blue line) (Figure 11); the latter indicates the influence of settling lag.

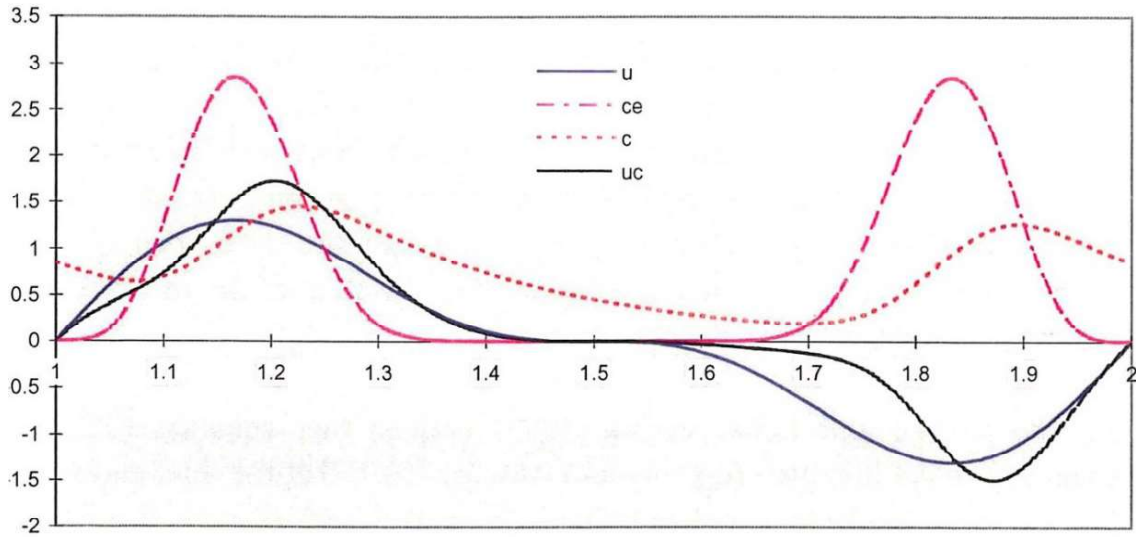

Figure 11 - The influence of lag effects on the residual suspended sediment transport. (Wang et al. 1999)

Fine sediment contrary to coarse, need time to settle when flow is too weak to transport it; this time span is referred to as settling lag. Essentially, this leads to the time lag between maximum flood velocity and maximum concentration (e.g. Figure 11). Slack tide asymmetry is crucial for the residual transport of fine sediment; a longer HWS duration (case b, Figure 10) implies a net import of fines while a longer LWS (case a, Figure 10) implies a net export.

2.4 Relation between vertical and horizontal tide

Due to the abundance of water level measurements all along most of the estuaries, the task of extracting sufficient information regarding the vertical tide becomes trivial. The situation is reversed when we refer to the horizontal tide; long-term measurements are required in order to be able to acquire sufficient information on the tidal constituents. As a result, the procedure of obtaining such data becomes time-consuming as well as costly, thus, making it problematic.

The relation between horizontal and vertical tide is not a linear one; this can be mathematically proved with the use of the continuity equation for the 1D case:

$$\frac{\partial \zeta}{\partial t} + \frac{\partial (\zeta u)}{\partial x} = 0 \xrightarrow{yields} Q_1 - Q_2 = \int_{x1}^{x2} b(x,\zeta)\frac{\partial \zeta}{\partial t} dx \quad (6)$$

Also,

$$u(t) = \frac{Q(t)}{A_b(\zeta(t))} \quad (7)$$

Where:

Q1,2 = discharge at $x_{1,2}$
b = storage width
Ab = cross-sectional area

Velocity scales non-linearly with water elevation, since the storage width as well as the cross-sectional area depends on the water level. This practically means that, for instance, a flood-dominant signal in the vertical tide (shorter rising period) does not necessarily coincide with a flood-dominant signal in the horizontal tide.

2.5 Numerical modelling aspects

2.5.1 Delft3d- Hydrodynamic equations

Delft3D-FLOW solves the Navier Stokes equations for an incompressible fluid under the shallow water and the Boussinesq approximation. Since the current MSc thesis largely relates to the Western Scheldt estuary, which is considered to be a well-mixed environment, density differences over the vertical are not taken into account, thus, density driven currents are neglected; the latter allows for a 2DH approach (depth-integrated). Consequently, the description of the hydrodynamic equations will be with regards to a two-dimensional, depth-averaged sense.

In such a model set up, lag effects (e.g. mixing, settling and scour lag) are much less accurate than in a 3D model. Therefore, sediment transport processes of fine sediment are less reliable as well. However, a 2DH model is much more simplified and as a result, it is easier to relate model results to certain processes. In addition, it is computationally less expensive that makes it favourable when long-term simulation is intended.

Neglecting vertical acceleration terms, wind, waves and density differences, the continuity as well as the horizontal momentum equations read:

$$\frac{\partial \zeta}{\partial t} + \frac{\partial h\bar{u}}{\partial x} + \frac{\partial h\bar{v}}{\partial y} = 0 \quad (8)$$

$$\frac{\partial \bar{u}}{\partial t} + \bar{u}\frac{\partial \bar{u}}{\partial x} + \bar{v}\frac{\partial \bar{u}}{\partial y} + g\frac{\partial \zeta}{\partial x} + c_f \frac{\bar{u}\left|\sqrt{\bar{u}^2 + \bar{v}^2}\right|}{h} - v_e\left(\frac{\partial^2 \bar{u}}{\partial x^2} + \frac{\partial^2 \bar{u}}{\partial y^2}\right) = 0 \quad (9)$$

$$\frac{\partial \bar{v}}{\partial t} + \bar{u}\frac{\partial \bar{v}}{\partial x} + \bar{v}\frac{\partial \bar{v}}{\partial y} + g\frac{\partial \zeta}{\partial y} + c_f \frac{\bar{v}\left|\sqrt{\bar{u}^2 + \bar{v}^2}\right|}{h} - v_e\left(\frac{\partial^2 \bar{u}}{\partial x^2} + \frac{\partial^2 \bar{u}}{\partial y^2}\right) = 0 \quad (10)$$

with

$$c_f = \frac{g}{C^2} \quad (11)$$

$$C = \frac{1}{n} h^{\frac{1}{6}} \quad (12)$$

from (11),(12) it yields

$$c_f = g \frac{n^2}{\sqrt[3]{h}} \quad (13)$$

where,

ζ=water level (m)
h=water depth (m)
$\bar{u}$ =depth averaged velocity in x direction (m/s)
$\bar{v}$ =depth averaged velocity in y direction (m/s)
g=gravitational acceleration (m/s^2)
c_f=friction coefficient (-)
n= Manning coefficient (m$^{-1/3}$ s)
v_e=eddy viscosity (m^2/s)
C=Chezy friction coefficient (m$^{1/2}$/s)

2.5.2 Delft3D - Sediment transport equations

2.5.2.1 Coarse sediment

The velocities acquired from the solution of the continuity and momentum equations are now used for the calculation of sediment transport rate. In more detail, the sediment transport formula of Engelund & Hansen is used (bed and suspended load):

$$S = S_b + S_s = \frac{0.05U^5}{\sqrt{g}C^3\Delta^2 D_{50}} \quad (14)$$

In which,

S_b=bed load
S_s=suspended load
U=magnitude of the depth averaged flow velocity
Δ=relative density
C=Chezy friction factor
D_{50}=median grain diameter

The sediment balance equation (viz. Exner equation) is further used for the determination of the bed level change:

$$(1-\varepsilon)\frac{\partial z_b}{\partial t} + \frac{\partial S_x}{\partial x} + \frac{\partial S_y}{\partial y} = 0 \quad (15)$$

Where,

ε = bed porosity (usually 0,4)
z_b = bed level (m)
S_x = sediment transport per unit width in x direction (m^3/m)/s
S_y = sediment transport per unit width in y direction (m^3/m)/s

2.5.2.1 Coarse sediment

It is generally accepted that coarse sediment (mainly bed load) respond instantaneously to the local flow conditions; thus, an equilibrium transport rate can be assumed. Unlike bed load transport, in suspended load, which is the relevant transport model for fine sediment, the sediment transport rate is not equal to the equilibrium; the reason is that sediment takes time to settle (Wang, 1989).

As far as the numerical practice is concerned, there are some aspects that require due consideration: viz. the exchange of sediment between the bed and the water column and the settling velocity under the effect of gravitational acceleration.

Part of sediment in the water column is deposited on the bed under the effect of gravity, while part of it is eroded from the bed and gets into suspension due to the current-induced bottom shear stress. The eroded sediment together with the sediment already in suspension is horizontally advected by the flow; this process is described by the 3D advection-diffusion equation for suspended sediment:

$$\frac{\partial c}{\partial t}+\frac{\partial uc}{\partial x}+\frac{\partial vc}{\partial y}+\frac{\partial wc}{\partial z}-\frac{\partial}{\partial x}\left(\varepsilon_{s,x}\frac{\partial c}{\partial x}\right)-\frac{\partial}{\partial y}\left(\varepsilon_{s,y}\frac{\partial c}{\partial y}\right)-\frac{\partial}{\partial z}\left(\varepsilon_{s,z}\frac{\partial c}{\partial z}\right)=0 \quad (16)$$

Where,

c = mass concentration of sediment (kg/m^3)
u,v,w = flow velocity components (m/s)
$\varepsilon_{s,x}$, $\varepsilon_{s,y}$, $\varepsilon_{s,z}$= eddy diffusivities (m^2/s)
w_s = settling velocity (m/s)

The eddy viscosities are either given a constant value during the model set-up (user defined) or calculated by a turbulence closure model. For cohesive sediment (e.g. mud) the vertical mixing coefficient for sediment equals to the vertical mixing coefficient for water. Therefore, $\varepsilon_{s,z}=v_{e,z}$, where $v_{e,z}$ is the vertical eddy viscosity. Based on the hydrodynamic results, the local flow velocities as well as the eddy diffusivities can be implemented in equation (16).

The sediment fluxes between water column and bed are calculated by the exchange of fluxes from the bottom computational layer to the bed and vice versa using the formula of Partheniades-Krone:

$$E = M\left(\frac{\tau_b}{\tau_{cr,erosion}}-1\right) \quad (17)$$

$$D = w_s c_b \quad (18)$$

$$c_b = c\left(z=\frac{\Delta z_b}{2}\right) \quad (19)$$

Where,

E = erosion flux (kg/(m^2 s))
M = user defined erosion parameter(kg/(m^2 s))
τ_b = bed shear stress (Pa)
$\tau_{cr,erosion}$ = user defined critical erosion shear stress
c_b = average sediment concentration in the near bottom computational layer

The calculated erosion or deposition flux is then applied to the near bottom computational cell by means of a sediment sink or source. This is the procedure of the bed level update at every time step.

Integrated form of advection - diffusion equation

Since the standard modeling practice used in this thesis is a 2DH model, reference must be made to the equation that describes the movement of sediment particles; integrating the advection- diffusion equation over depth, the mass balance equation for suspended sediment reads:

$$\frac{\partial(h\bar{c})}{\partial t}+\frac{\partial(h\bar{u}\bar{c})}{\partial x}+\frac{\partial(h\bar{v}\bar{c})}{\partial y}-\frac{\partial}{\partial x}\left(\varepsilon_{s,x}\frac{\partial h\bar{c}}{\partial x}\right)-\frac{\partial}{\partial y}\left(\varepsilon_{s,y}\frac{\partial h\bar{c}}{\partial y}\right)=D-E \quad (20)$$

The depth-averaged suspended sediment concentration yields from solving equation (20). The reasoning is the same as in the 3D case (equations 16-20). The difference now is that since there are no layers over the vertical, a single depth-averaged value is representative for the concentration in the water column; the latter is used for the determination of the deposition flux (equation 18).

2.5.3 Morphological update

The hydrodynamic processes taking place within the model have a timescale that is 1 to 2 orders of magnitude smaller than their respective morphodynamic timescales (Wang et al., 1991). In other words, many time steps are needed before a morphological change becomes apparent. In literature several techniques relative to computational time optimization are available; Latteux (1995), for instance, introduces the concept of the morphological tide, where the tidal-averaged net sediment transport is used for the bed level update at each time step.

During this thesis the online approach is adopted; bed level changes are multiplied by a morphological factor at each time step:

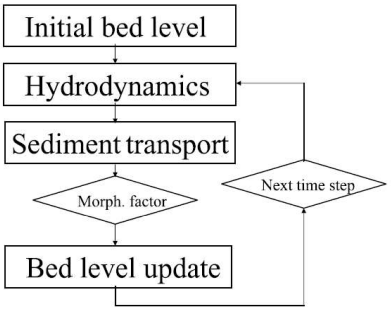

Figure 12 - Morphological update scheme (Wegen and Roelvink, 2008)

2.6 Area of interest

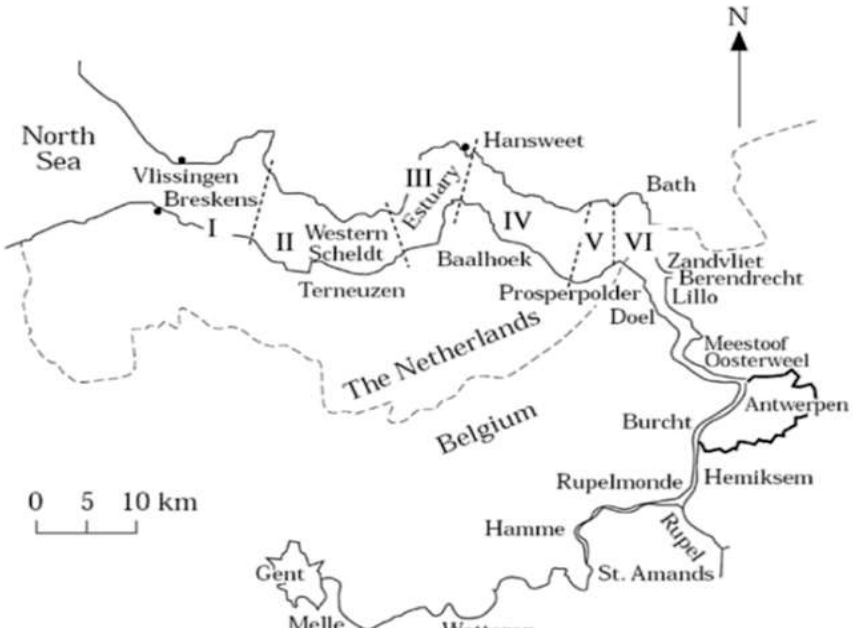

Figure 13- The Scheldt estuary (Fettweis et al., 1988)

2.6.1 Hydrodynamics and salinity

The W.S. estuary is categorized as tide-dominated; the river discharge is negligible compared to the tidal prism and wave energy is comparatively low. According to measurements, more than 109 m^3 of water enters the estuary per half tidal cycle. When this is compared to the average river discharge per tidal cycle (i.e. 5million m^3), river discharge is only 0.5% of the tidal prism.

Furthermore, waves entering the estuary from the North Sea are losing their energy due to depth and width-induced dissipation and as a result they decrease in amplitude. Maximum values found under storm conditions are in the range of 2-3m.

Following (Pritchard, 1955; Cameron and Pritchard, 1963), the regimes with regards to the vertical distribution of salinity can be seen in Figure 14:

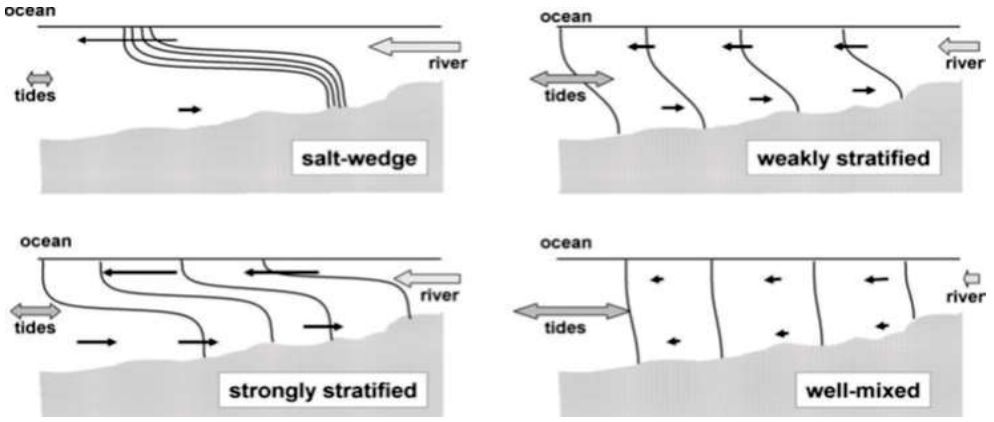

Figure 14 - Vertical distribution of salinity (Pritchard, 1955; Cameron and Pritchard, 1963)

This classification is possible by comparing the buoyant force of the river discharge with the mixing force of the tide. Given the fact that tide dominates over the river discharge, not significant salinity differences are formed over depth; all in all, the W.S. estuary can be classified as well-mixed.

2.6.2 Bed layers

In addition to Exner equation (15), layer-structured beds are becoming more attractive especially when using more than a single sediment fraction. The idea behind models that use this concept is based on the use of an active layer combined with several under layers below this layer; sediment is transported, eroded and deposited to the active layer depending on the availability of mass of sediment in this layer. In such a set up, the bed responds quicker to the hydro-sedimentary changes and history effects are incorporated.

In the current model, the height of the active layer is set to 10cm while the bed consists of a total number of 20 bookkeeping layers, found under the active layer, each with a fixed height of 1m. When deposition occurs and bed level exceeds 10cm, which is the user-defined height of the active layer, another active layer is created on top of the previous one; when bed level change reaches up to 1m, an under layer is created on top of the previous one. Following the same reasoning the adjustment of the layers during erosion takes place accordingly.

3

MODEL SET UP FOR A SCHEMATIZED TIDAL EMBAYMENT

3.1 Introduction

Over the years, the existence of mud in estuarine systems has been associated with high environmental and ecological importance. Moreover, knowledge around the siltation rates of mud at port areas makes the planning of dredging possible, thus, leading to successful port management. Considering an area that reflects all these needs increases the relevance of the current study. Therefore, the Western Scheldt estuary is chosen as the area of interest since it incorporates all these necessities.

Prior research done by Van der Wegen, Roelvink and Dam (2012, 2013) has proved the ability of process-based models to accurately predict long-term morphological estuarine development. Starting from a flat bathymetry, which basically reduces the spin-up time to approximately zero, they were able to predict the most important morphological changes happening in the Western Scheldt during a hindcast of 110 years (Van der Wegen, Roelvink and Dam, 2012). The latter implies a positive feedback loop between tidal forcing, sediment transport and morphological development that results in characteristic morphological patterns (viz. the channel-shoal formation).

Within the scope of the PhD research of Gerard's Dam (viz. long-term modelling of the morphology of estuaries using process-based models), the current model aims to investigate the influence of mud on the long-term estuarine morphological development, under tidal and fluvial forcing.

3.2 Assumptions and restrictions of the model

In order to be able to draw safe conclusions regarding the influence of mud on the results, parameters that have an effect on morphological development should be minimized. In other words, the numerical model should be as simplified as possible, in a way that certain patterns (e.g. sediment transport or morphology) can be credited to certain forcing mechanisms. Following this principle, the interpretation of model output can be more reliable.

The simplifications made during this model set up are the following:

- Most of the theoretical analysis and their applications are based on a 2DH approach
- The estuary is considered to be well-mixed: no horizontal or vertical salinity gradients; density driven currents are neglected
- The estuary is tide-dominated: river discharge is too small compared to the tidal prism and as a result negligible
- The period of the semidiurnal tidal constituent (M2) is considered as the tidal period for the numerical analysis
- The effect of flocculation is not taken into account (settling velocity is uniform for marine and fluvial sediment fractions)
- Consolidation is not taken into account (no effect on the critical shear stress)
- No initial amount of mud on the bed- amount of mud limited by boundary conditions – starved bed
- Wind is not taken into account; wind-induced currents are neglected
- Waves are not implemented in this model; the effect of waves on the sediment stirring due to shear stress is therefore neglected

3.3 Schematized estuary

3.3.1 Schematization

The long-term morphodynamic evolution of a schematized basin is investigated with the use of the process-based Delft3d software, developed by Deltares.

The schematization contains a rectangular basin (80 x 2.1km) and a river part (20km x 150m). A linearly slopping bed is used in the basin and a uniform bed is used in the river. The size of the rectangular grid cell is set to Δx=200m and Δy=150m. The bed level at the seaside is set to MSL- 10m and it is linearly decreasing to MSL- 4m at the end of the basin while it is uniformly set to MSL-8m at the river section. The system is forced by a semi-diurnal tide (M2) at the seaward boundary and by a river discharge at the landward boundary.

Figure 15 - Schematized situation, top view

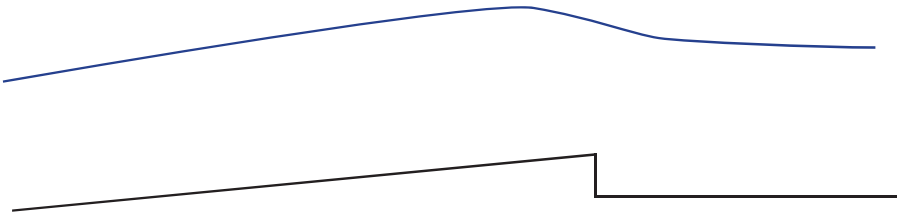

Figure 16 - Schematized situation, side view

3.3.2 Geometry and configuration of the sand model (S1)

The idea behind this schematization as well as the relevant dimensioning is to reflect as close as possible the Western Scheldt estuary, while at the same time to keep the complexity at a low level; for instance, the width is not represented exponentially decreasing landwards, as it is the case in reality, is that it would significantly complicate the interpretation of model results.

The model consists of two artificial boundaries, namely, the seaward and the landward. At the seaward boundary, the tidal amplitude and period of the forcing equals 1.75m and 12.42h respectively. As far as sediment is concerned, a Neumann boundary condition (zero flux) is applied on the concentration of sand; this implies that concentration is constant along the boundary and as a result deposition or erosion is locally minimized ($\partial c/\partial x$=0).

A Dirichlet boundary condition (i.e. discharge) is applied at the landward end, namely, 300m^3/s. No flow or transport is allowed at this boundary or at the sides of the model domain ($\partial u/\partial x$=0). In addition, regarding wall roughness, a free slip condition is applied, which means that shear stresses at the sidewalls of the model are neglected. Therefore, a uniform flow velocity over the width is to be expected.

The basin area consists of 400x14 computational cells while the river part, which is set up using a single cell over width, comprises a number of 100x1 cells.

3.3.3 Morphological factor

The starting point of simulations is chosen to be a linearly slopping bed. The bed level update is according to the online approach; hence, a morphological factor is applied after each time step.

Van der Wegen and Roelvink (2008) conducted a sensitivity analysis on the morphological factor in order to examine its effect on model output. In more detail, they used a 2D model with a basin width of 2.5km that closely relates to the model of the current thesis. The results showed that as long as bed level changes are not too large compared to the water depth, the morphological results acquired using a morphological factor of 10 do not considerably differ from the ones acquired using a factor of 400.

In addition, during this thesis, the sensitivity of the morphological factor was tested; several runs were carried out by varying the morphological factor and increasing (decreasing) the simulation time accordingly. The analysis showed that the end result was the same when using a factor of 50 or a factor of 400.

Based on this conclusion and taking into account that mud dynamics are linked with longer time scales compared to sand, this model uses a factor of 400.

3.3.4 Model runs timeframe

The strategy with regards to simulation is as follows: at first, the model is only forced by sand for the first 100 years; the created bathymetry is then used as a starting point for the simulation of mud dynamics. Therefore, the starting bathymetry regarding the 4 scenarios mentioned in *chapter 1.4 Approach*, is the 100 years bathymetry:

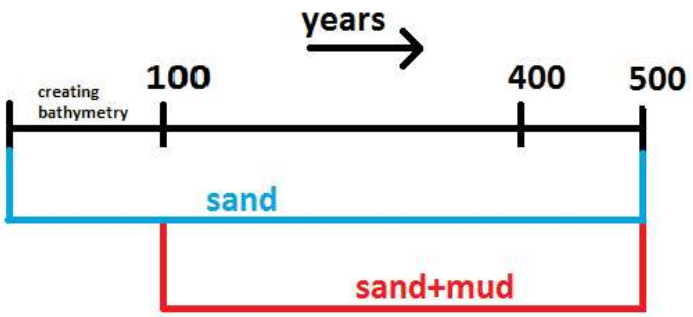

Figure 17 - Model runs timeframe

4

MODEL RUNS

This chapter deals with the model runs; several scenarios are created and compared in terms of bed level development and sediment transport. In addition, a sensitivity analysis is done so as to realise the influence of each parameter on the model output.

There is a plotting error in the model runs that is visible in the results of all the following analysis. It is evident in Figure 18, where the cross-sectional bed level is not uniformly set to 10m, but there is a peak instead at one of the two banks (i.e. where bed level is 0). This error already took place at the first stage of the analysis (i.e. creating bathymetry) and as a result it inevitably affected future plots. However, this flaw has only visually affected the results and has no consequence to the numerical computations.

4.1 Creating bathymetry

At first, bed levels have to disturbed. Consequently, local discontinuities are created that force flow acceleration and deceleration thereby causing erosion and sedimentation respectively. As a result, morphological development is accelerated. Figure 18 depicts the initial perturbed bed levels as well as the development after 100 years of simulation:

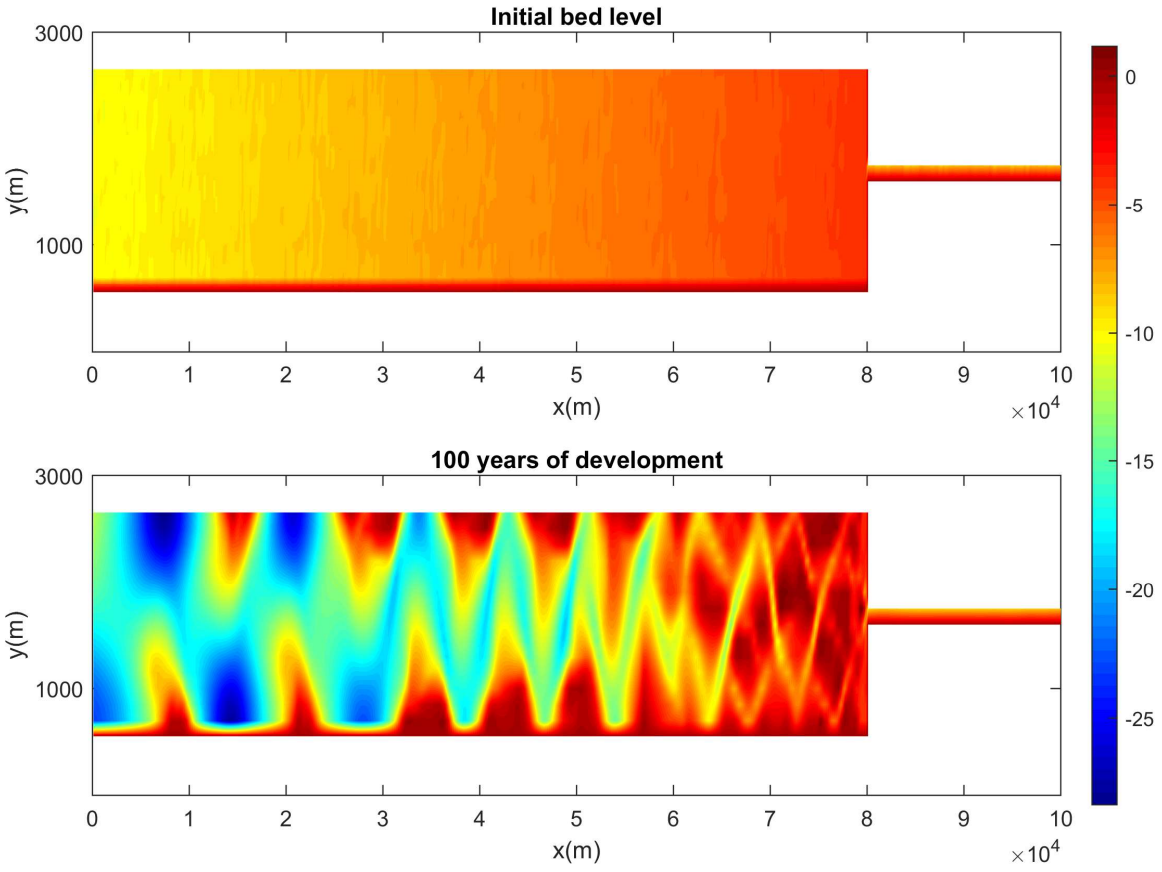

Figure 18 – Creating bathymetry

PHYSICAL PARAMETERS			
Constants		Roughness	
Gravity	Water density	Bottom	Wall
9,81m/s^2	100kg/m^3	0.023	free
Sediment			
Specific density	Dry bed density	D50	Initial sediment thickness on bed
2650kg/m^3	1600kg/m^3	200μm	30m
Morphology		Viscosity	
Morphological factor	Spin-up time	Eddy viscosity	Eddy diffusivity
400	12h	1m^2/s	10m^2/s
Morph. simulation duration			
100y			
BOUNDARIES			
Hydrodynamic		Sediment	
Sea	River	Sea	River
α_{M2}	Q	$\partial C_{sand}/\partial x=0$	$\partial C_{sand}/\partial x=0$
1,75m	300m^3/s		

Table 2 - Creating bathymetry specifications

After the end of the simulation period certain patterns have developed; the forcing imposed at the boundaries combined with the disturbed bed levels in the basin have led to the formation of a deep channel with distinct bends along the estuary. In addition, the formation of shallow bars has emerged at the sides of the main channel.

The results qualitatively resemble previous studies on the long-term morphodynamic simulation in the Western Scheldt; Van der Wegen and Roelvink (2012) showed that a process-based model is capable of reproducing the estuarine channel-shoal pattern on the long-term, using the Western Scheldt geometry and starting from a flat bottom. In relation to this, the current study also reproduces similar morphological patterns. The reason behind this is the influence that the combination of tidal forcing, sediment availability and basin geometry has on the morphological development of the basin.

4.2 Sand model (S1)

Starting from the 100year bathymetry, the model is forced by the tide and the river discharge using only sand as the representative sediment fraction. The morphological development after 400 years is visible in Figure 19:

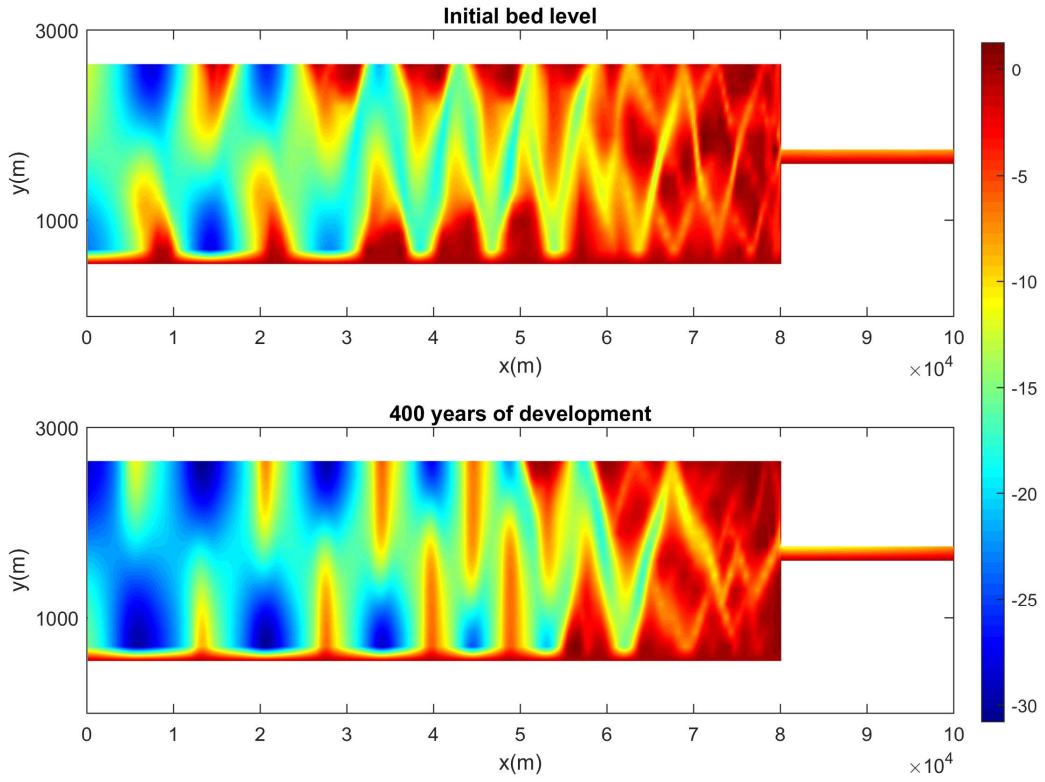

Figure 19 - 400 years of morphological development with sand

PHYSICAL PARAMETERS			
Constants		Roughness	
Gravity	Water density	Bottom	Wall
9,81m/s^2	100kg/m^3	0.023	free
Sediment			
Specific density	Dry bed density	D50	Initial sediment thickness on bed
2650kg/m^3	1600kg/m^3	200µm	30m
Morphology		Viscosity	
Morphological factor	Spin-up time	Eddy viscosity	Eddy diffusivity
400	12h	1m^2/s	10m^2/s
Morph. simulation duration			
400y			
BOUNDARIES			
Hydrodynamic		Sediment	
Sea	River	Sea	River
α_{M2}	Q	$\partial C_{sand}/\partial x=0$	$\partial C_{sand}/\partial x=0$
1,75m	300m^3/s		

Table 3 - Sand model specifications

4.3 SandMud model (S4)

So far, only sand was implemented in the model runs; in this specific run, mud is applied at both boundaries of the domain, with a uniform concentration of 0,05kg/m3. The illustration of bed levels after 400 years of simulation follows (Figure 20):

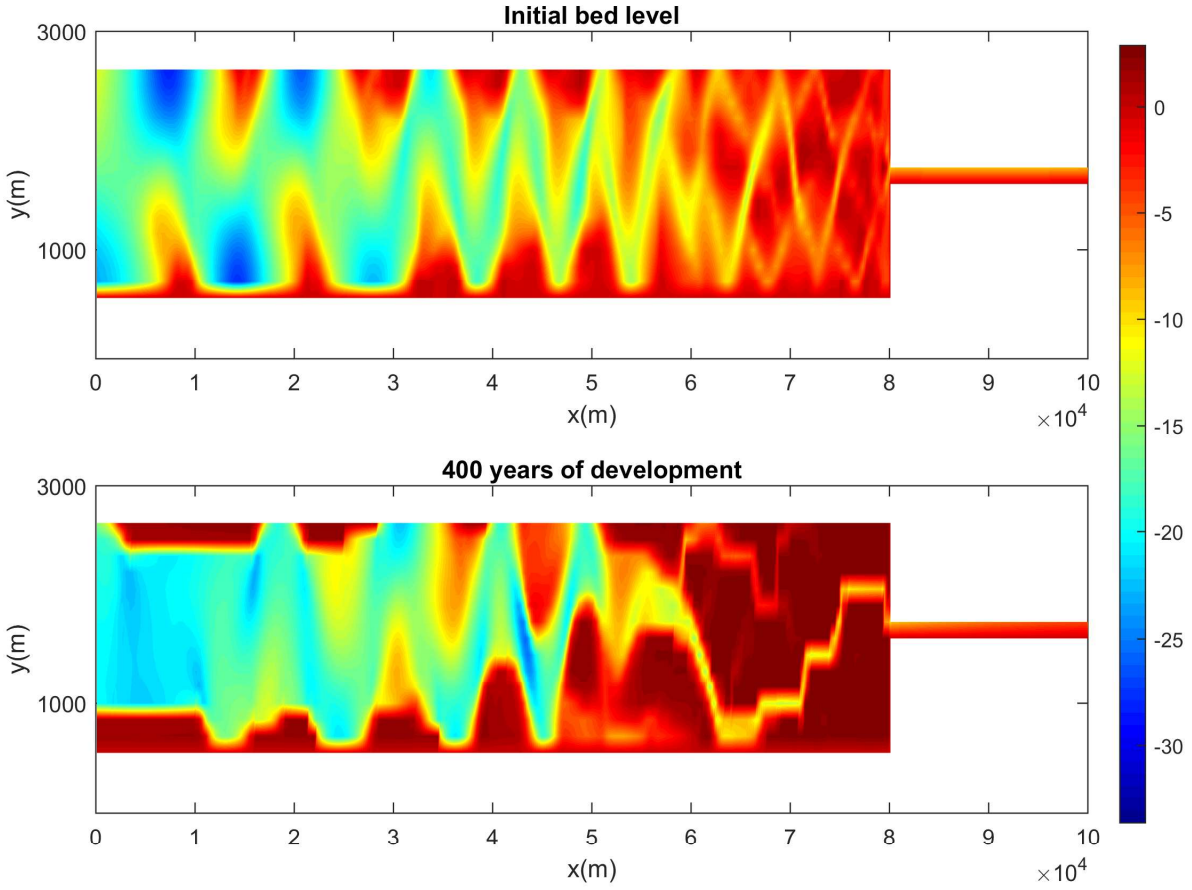

Figure 20 - 400 years of morphological development with sand and mud

PHYSICAL PARAMETERS			
Constants		Roughness	
Gravity	Water density	Bottom	Wall
9,81m/s^2	100kg/m^3	0.023	free
Sediment			
Specific density	Dry bed density	D50	Initial sediment thickness on bed
2650kg/m^3	1600kg/m^3	200μm	30m
2650kg/m^3	500kg/m^3	Marine mud	0
2650kg/m^3	500kg/m^3	Fluvial mud	0
Morphology		Viscosity	
Morphological factor	Spin-up time	Eddy viscosity	Eddy diffusivity
400	12h	1m^2/s	10m^2/s
Morph. simulation duration			
400y			
Mud specifications			
Crit. shear stress for erosion	Marine mud		Fluvial mud
	0,25Pa		0,25Pa
Erosion parameter	1,00E-05		1,00E-05
Settling velocity	0,5mm/s		0,5mm/s
BOUNDARIES			
Hydrodynamic		Sediment	
Sea	River	Sea	River
α_{M2}	Q	$\partial C_{sand}/\partial x=0$	$\partial C_{sand}/\partial x=0$
1,75m	300m^3/s	Cmud=0,05kg/m^3	Cmud=0,05kg/m^3

Table 4 - SandMud model specifications

4.4 3D SandMud model

In this chapter a 3D model is set up in order to detect the differences in morphological development between a 2D and a 3D approach. Salinity differences are implemented in the computational domain; a value of 30ppt is set at the seaward boundary, which implies saline water, while a value of 0ppt is set at the landward boundary signifying fresh water. Consequently, density driven currents are not neglected anymore and as a result they have an effect on residual sediment transport, thus, influencing morphology. Bed level development can be observed in Figure 21:

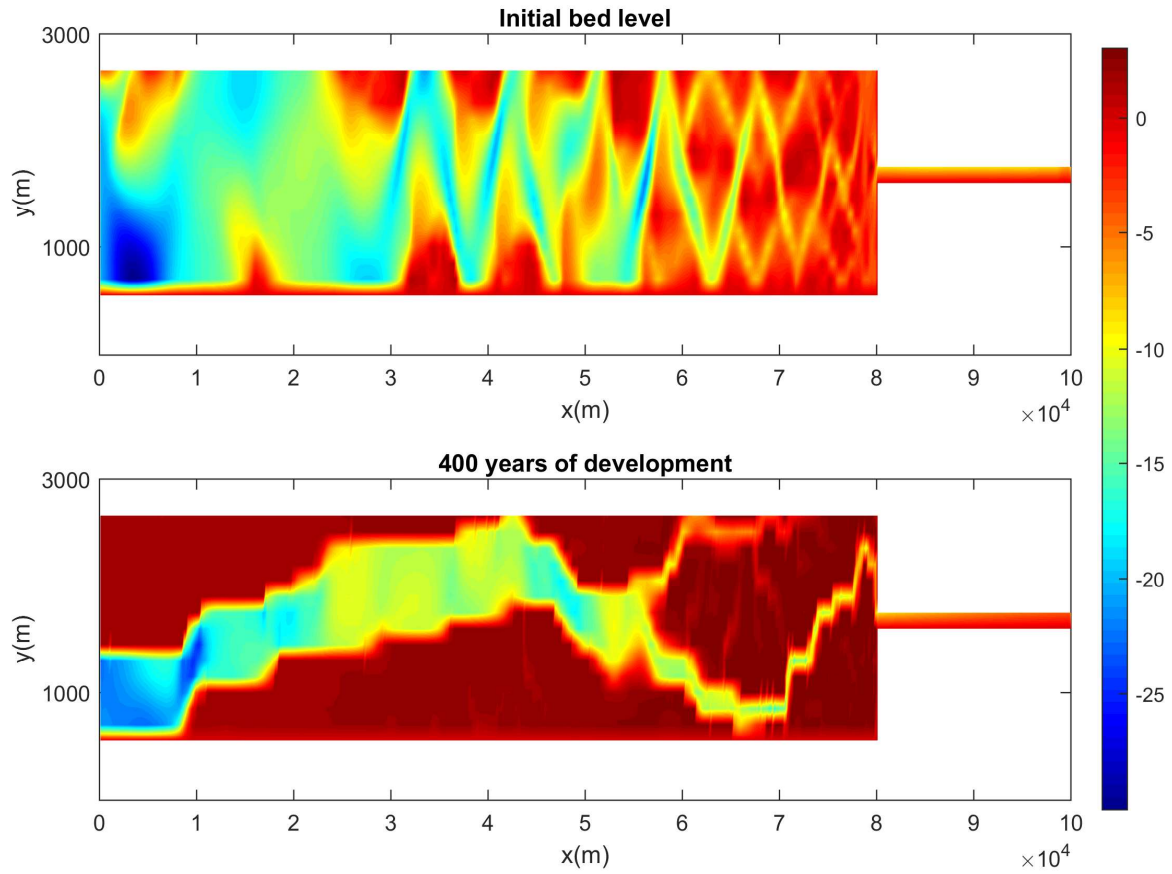

Figure 21- 400 years of morphological development with sand and mud (3D)

PHYSICAL PARAMETERS			
Constants		Roughness	
Gravity	Water density	Bottom	Wall
9,81m/s^2	100kg/m^3	0.023	free
Sediment			
Specific density	Dry bed density	D50	Initial sediment thickness on bed
2650kg/m^3	1600kg/m^3	200μm	30m
2650kg/m^3	500kg/m^3	Marine mud	0
2650kg/m^3	500kg/m^3	Fluvial mud	0
Morphology		Viscosity	
Morphological factor	Spin-up time	Hor. Eddy visc.	Hor. Eddy diffusivity
400	12h	1m^2/s	10m^2/s
Morph. simulation duration		Vert. Eddy visc.	Vert. Eddy diffusivity
400y		0,001m^2/s	0,001m^2/s
Mud specifications			
Crit. shear stress for erosion	Marine mud	Fluvial mud	
	0,25Pa	0,25Pa	
Erosion parameter	1,00E-05	1,00E-05	
Settling velocity	0,5mm/s	0,5mm/s	
BOUNDARIES			
Hydrodynamic		Sediment	
Sea	River	Sea	River
α_{M2}	Q	$\partial C_{sand}/\partial x=0$	$\partial C_{sand}/\partial x=0$
1,75m	300m^3/s	Cmud=0,05kg/m^3	Cmud=0,05kg/m^3
Salinity			
Sea		River	
30ppt		0ppt	

Table 5 - 3D SandMud model specifications

4.5 The effect of fluvial mud on the sediment transport

4.5.1 Model run

At this section, the importance of fluvial mud is assessed; comparing the standard S4 scenario, which entails mud at both boundaries, with S2 scenario (i.e. no fluvial mud), the influence of fluvial mud can be detected.

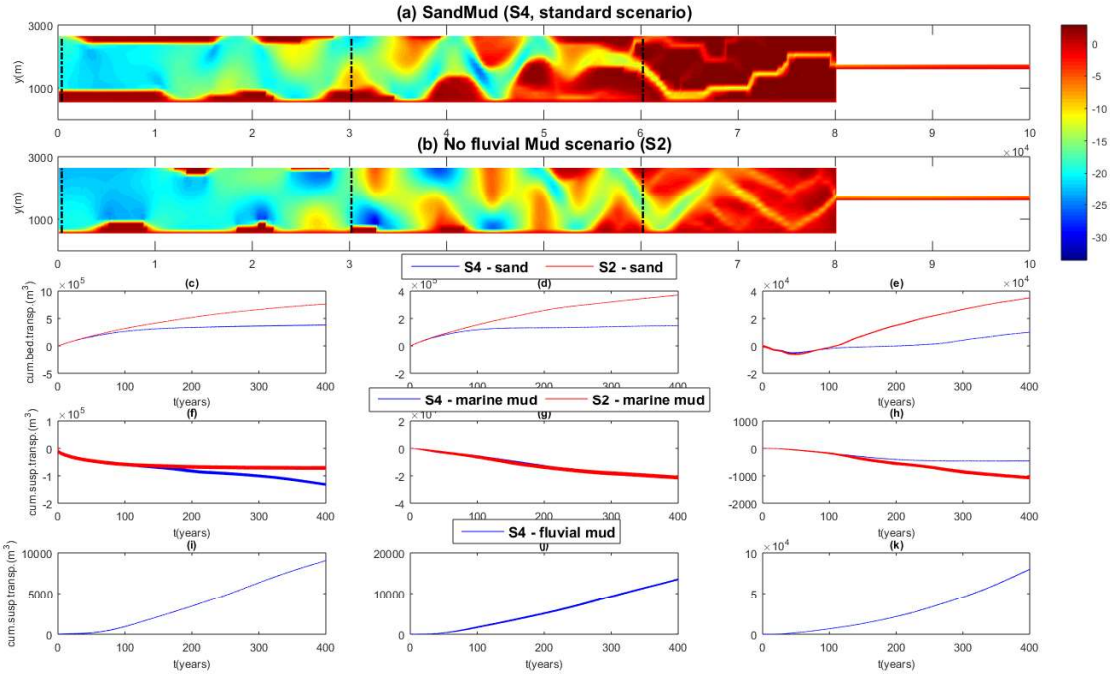

Figure 22 - Bed level development for two different scenarios and the corresponding cumulative sediment transport for 400 years of simulation, at three cross-sections. A positive transport implies a net export of sediment (i.e. seawards)

Figure 22 depicts the 400-year morphological development of the S4 standard scenario (a) versus S2 scenario (b). Cumulative sediment transports for three transects are plotted; the first column, namely, graphs (c),(f),(j) corresponds to the seaward transect that is visible with black dashed line. Graphs (d), (h), (k) are related to the middle transect while (e), (i), (l) relate to the transect at the landward side of the basin. Furthermore, graphs (c), (d), (e) depict cumulative bed load, graphs (f), (h), (i) depict cumulative transport of marine mud while graphs (j), (k), (l) show the cumulative transport of fluvial mud.

4.5.2 Conclusions

As far as the transport of sand is concerned (Figure 22c, d and e), a decreased export when fluvial mud is present takes place at all three cross-sections. The latter can probably be explained by the hiding-exposure concept; the existence of fluvial mud increases the mud volume fraction on the bed thereby reducing the concentration of sand. This in turn leads to less export of sand in case fluvial mud is present.

Another reason is that the accumulation of fluvial mud reduces the tidal storage thereby reducing tidal velocities. Accordingly, transport rates are reduced (i.e. decreased export).

With regards to marine mud transport, different sediment transport patterns at different cross-sections are observed. In more detail, at the seaward cross-section (Figure 22f), the existence of fluvial mud enhances marine mud import. That seems to be happening after 200 years of evolution.

At the most landward part of the basin (Figure 22h), marine mud transported by the tide is counteracted by fluvial mud discharged by the river. This balance of forces has an effect on marine mud import (i.e. a diminished cumulative import of marine mud in case fluvial mud is present).

Furthermore, no difference in cumulative marine mud transport is observed at the middle cross-section (Figure 22g) between the two scenarios; hence, the influence of fluvial mud is negligible at this section of the basin.

4.6 The effect of mud on the sediment transport of sand

4.6.1 Model run

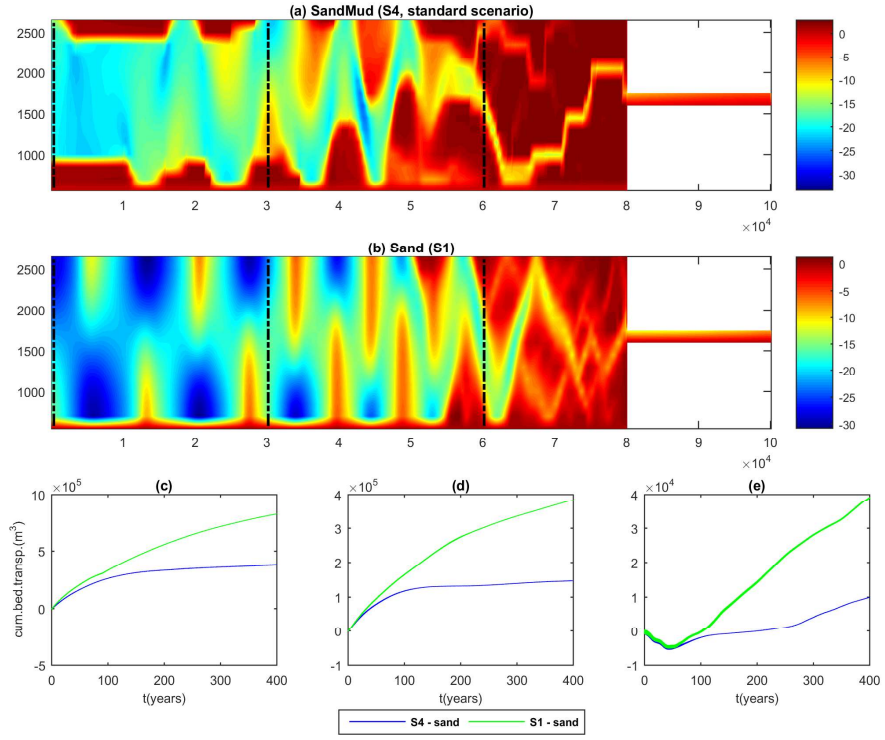

Figure 23 - Bed level development for two different scenarios and the corresponding cumulative bed transport for 400 years of simulation, at three cross-sections. A positive transport implies a net export of sediment (i.e. seawards)

Figure 23 introduces bed level development after 400 years of morphological evolution for two scenarios, namely, SandMud (Figure 23a) and Sand (Figure 23b). The illustrated black dashed lines define the three main transects where analysis takes place. Cumulative bed load transport for these two scenarios is depicted for the three different cross-sections (Figure 23c, d and e). Graphs c, d and e correspond to the seaward, middle and landward cross-section respectively.

Reduced export of sand, when mud is present, is observed in all three cross-sections. At chapter 6.1 The effect of mud on the sediment transport of sand, further analysis is being done towards the understanding of the underlying mechanisms behind this phenomenon.

4.7 2D versus 3D model

4.7.1 Model run

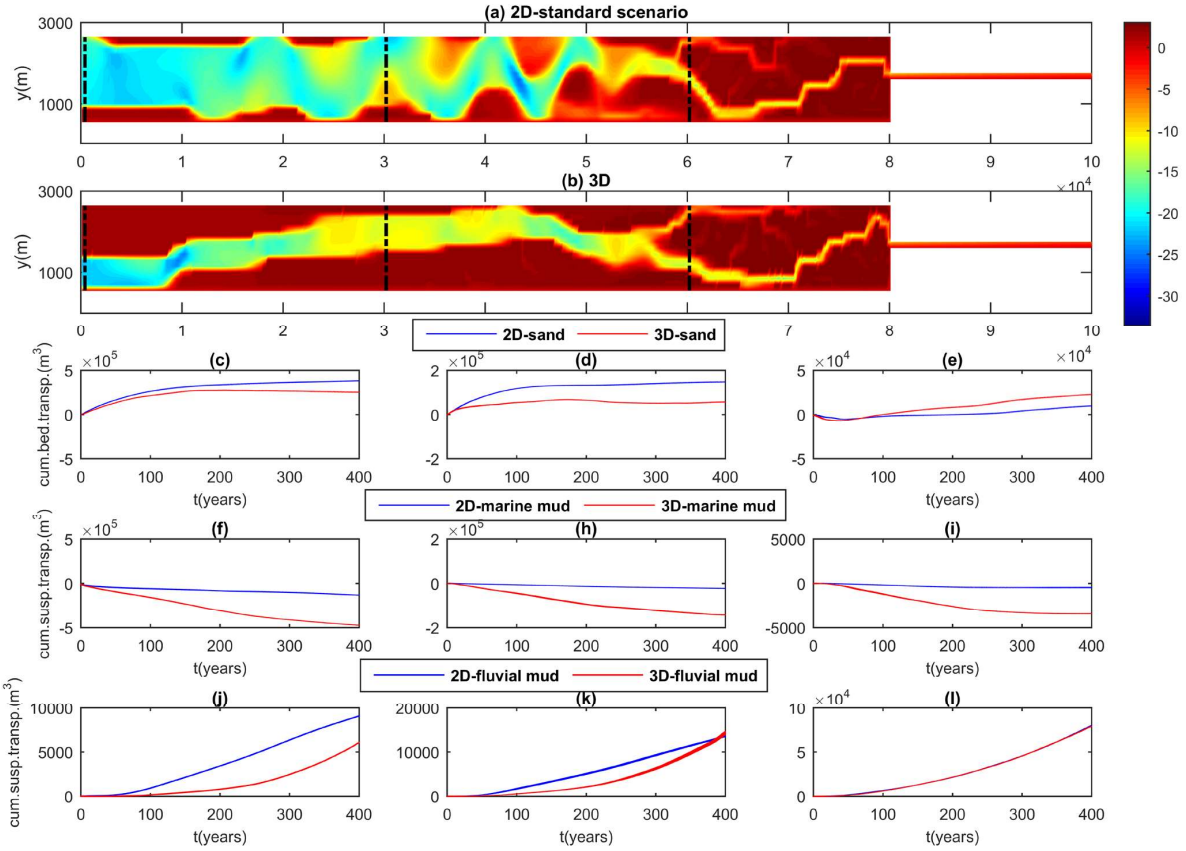

Figure 24 - Bed level development for two different scenarios and the corresponding cumulative transports for 400 years of simulation, at three cross-sections. A positive transport implies a net export of sediment (i.e. seawards)

In Figure 24 the standard scenario (S4) is compared to the 3D scenario. Bed level development after 400 years of morphological evolution for the two different set-ups is displayed in graphs a and b. The formation is similar to Figure 23; graphs c-k indicate the cumulative cross-sectional transport of sand, marine and fluvial mud for three transects along the estuary.

Figure 24c, d and e suggest a decreased export of sand in the 3D case compared to the 2D. This may be due to salinity-induced residual sediment transport (i.e. estuarine circulation); in case salinity is not neglected, (vertical) stratification takes place with fresh water flowing higher in the water column and saline water sinking at larger depths. This circulation eventually leads to a net import of sediment thereby reducing the export of sand. Moreover, horizontal salinity gradients can lead to residual sediment transport as well.

Longitudinal salinity profiles are plotted over time to indicate the vertical salinity stratification of the model (Figure 25).

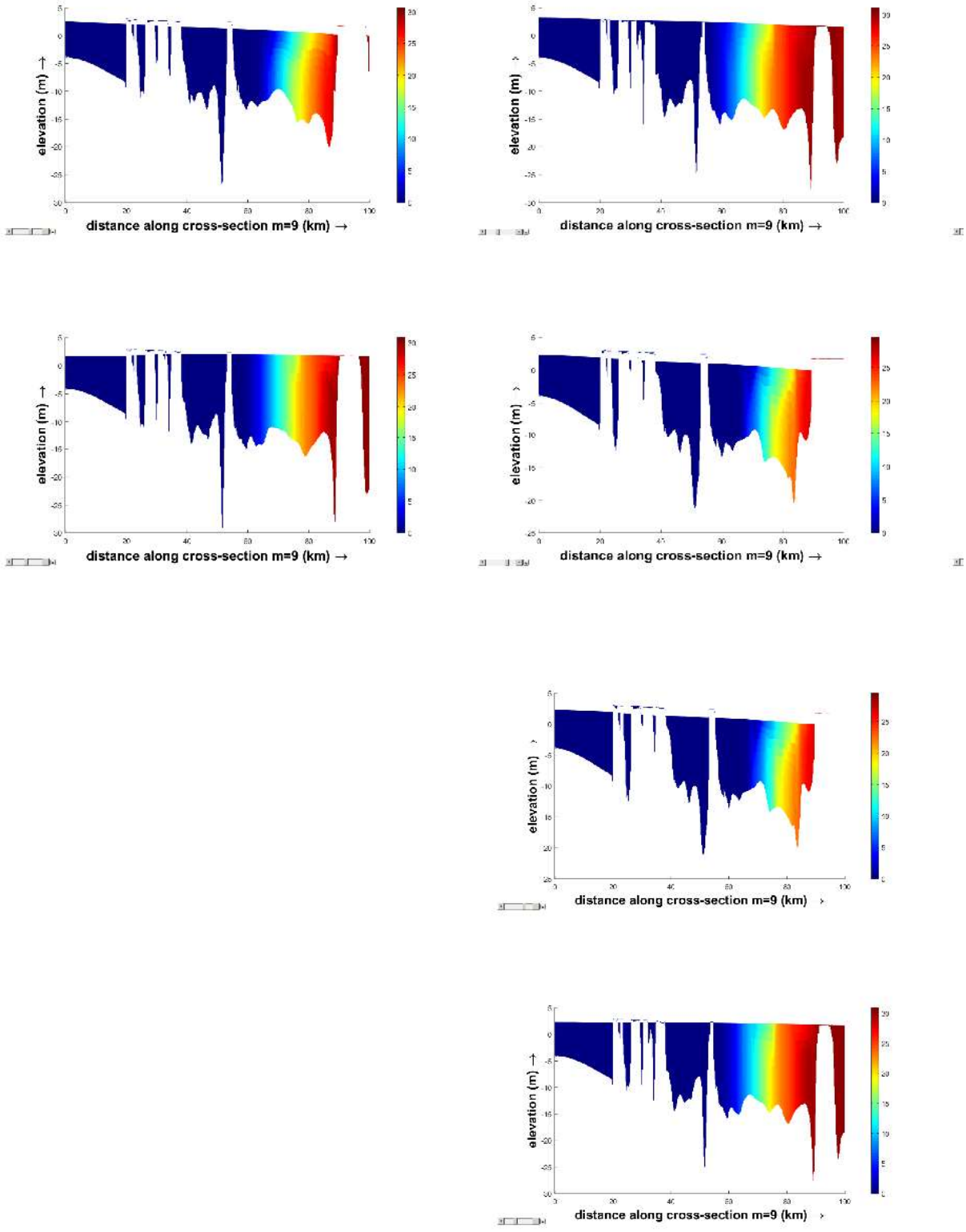

Figure 25 - Salinity profiles along a longitudinal cross-section

4.7.2 Conclusions

It is evident from the salinity profiles (Figure 25) that the estuary can be classified either as well mixed or as weakly stratified; at times the distribution of salinity is vertical (i.e. well-mixed) and at times a weak gradient develops. Due to this gradient, a salinity-induced circulation is possible to be initiated, hence, leading to a net import of sediment. However, the fact that mud is present in the system complicates the hydrodynamics and the sediment transport processes to a large extent. In addition, many settings differ when switching from a 2D to a 3D model.

Therefore, it is difficult to draw safe conclusions with regards to the influence of salinity on the reduced export of sand happening in the 3D setting. To be able to identify the importance of salinity-induced residual transport, a 3D run without salinity should be performed. Then by comparing 3D-without to 3D-with salinity, the influence of estuarine circulation on residual sediment transport can be understood.

Yet, answering this question lies out of the scope of the current MSc thesis and accordingly it will not be studied into further detail.

Still, some hypothesis on the reasons responsible for the model results can be made:

- The reduced export of sand in the 3D case can be associated with the increased accumulation of mud
    - What is possible to be happening is that massive deposition of mud leads directly to the reduction of tidal storage volume; this in turn leads to the reduction of flood and ebb velocities thereby reducing the erosion rate. Therefore, the export of sand is significantly smaller in this case.
    - Another reason might be the decreased volume fraction of sand on the bed due to the existence of mud, known as the hiding exposure effect. Mud is effectively covering the upper layers of the bed and as a result, less sand is available for export.
- The increased accumulation of mud in the 3D scenario can be associated with:
    - Salinity-induced circulation
    - Differences in bed exchange settings between the two models
        - Lag effects are more important in 3D than in 2D
          The latter can most possibly explain the increased import of marine mud in the 3D setting.
        - The deposition flux is larger in the 3D case
          In the 2D model, the deposition flux is calculated using a depth-averaged concentration (i.e. $w_s * \bar{c}$).
          In the 3D model, the near bed concentration is used instead.

4.8 Sensitivity analysis

4.8.1 Model runs

To realise how sensitive model results are to certain parameters, sensitivity analysis is conducted. As a matter of fact, sensitivity analysis is a valuable procedure that leads to several realizations. Firstly, it gives an impression on the dynamics between input and output parameters of the model. In addition, by revealing which parameters cause significant uncertainty in the output, it is a useful tool in uncertainty reduction. In addition, parameters of no influence on the output are detected and excluded from further analysis.

The effect of sediment properties is evaluated by testing a range of settling velocities w_s, critical shear stresses for erosion τ_{crit}, as well a number of erosion parameters M. In addition, the effect of hydrodynamics is investigated by varying the river discharge. Further, the effect of mud concentration is explored; different concentrations are imposed at the boundaries and their influence on the morphological development is analyzed.

Figure 26 - Figure 29 indicate sensitivity analysis results. At each of the figures a certain parameter is tested; bed level development is plotted for different values of this parameter and accordingly, its influence on the results is realized by visual comparison.

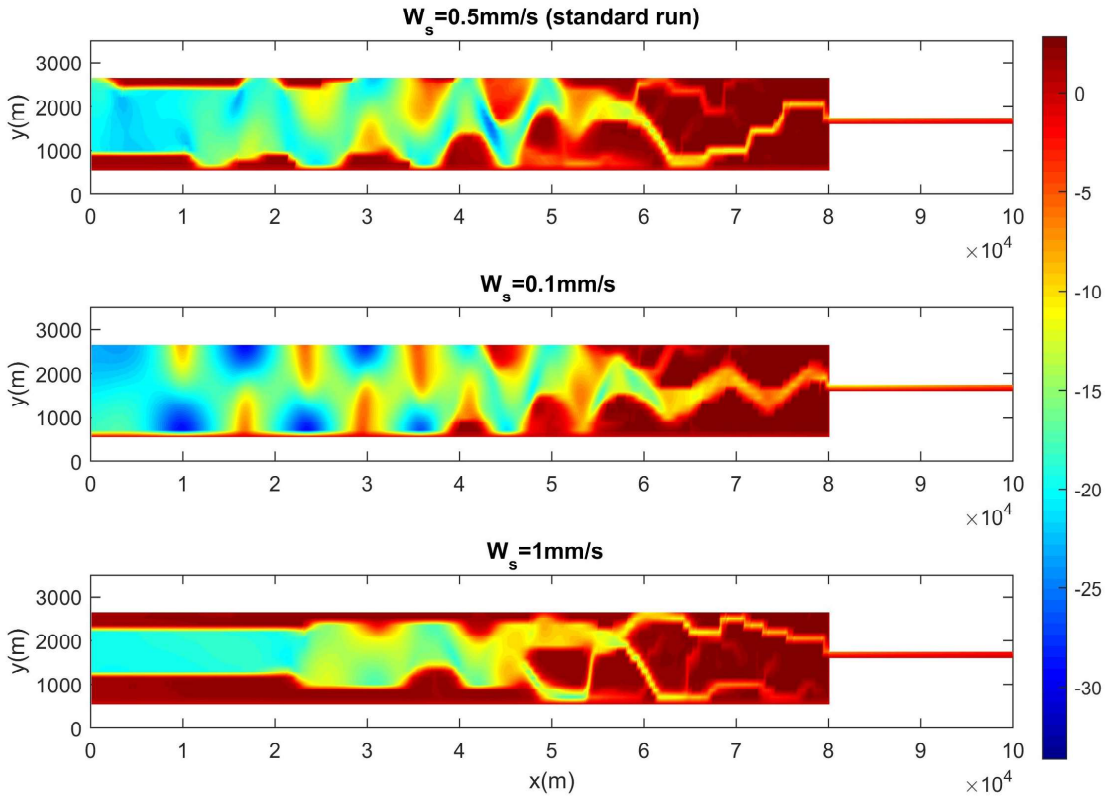

Figure 26 – Sensitivity analysis, testing fall velocity

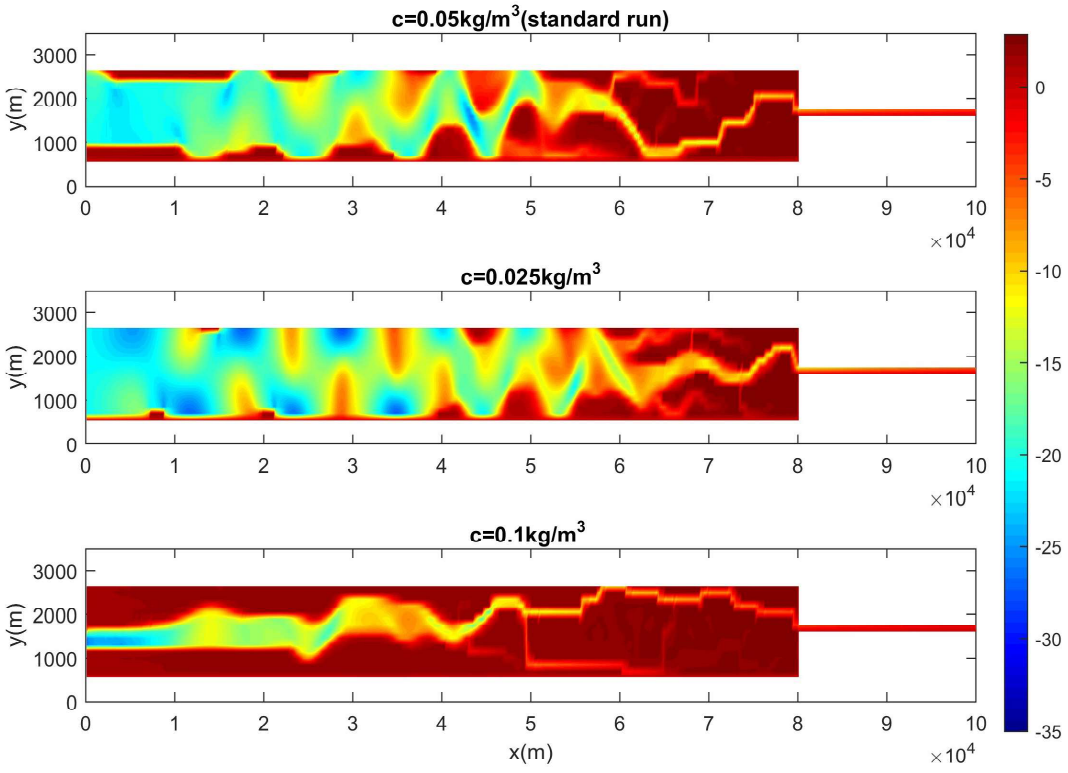

Figure 27 - Sensitivity analysis, testing mud concentration (at both boundaries)

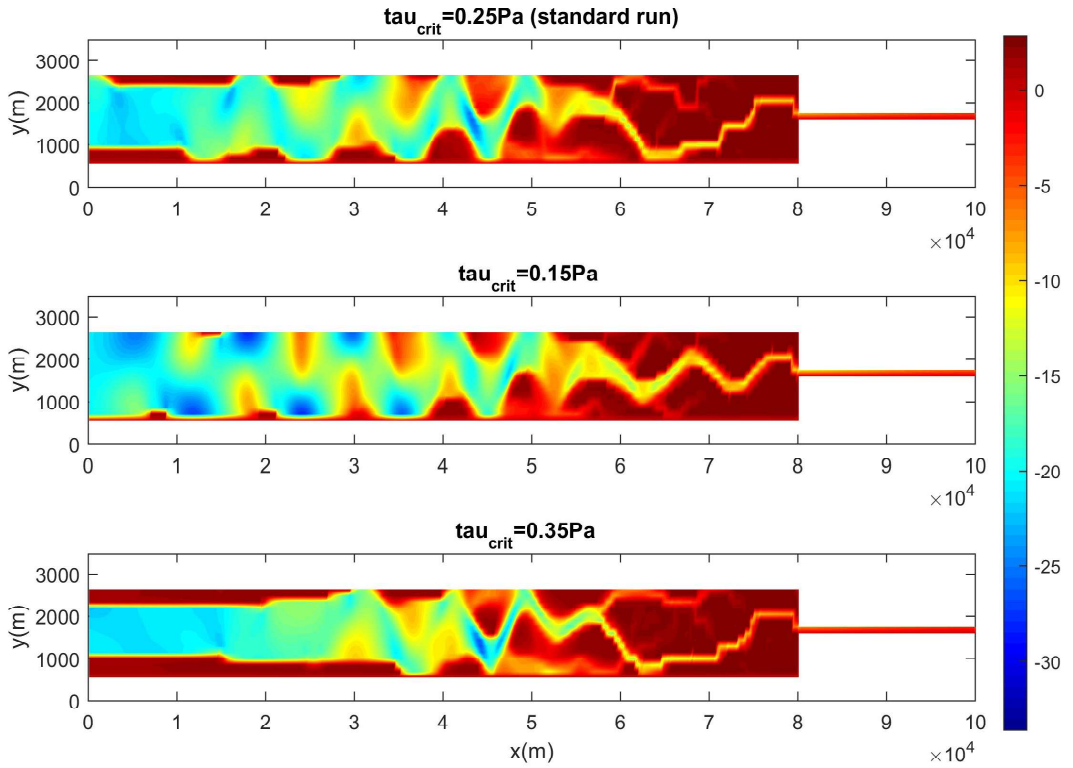

Figure 28 - Sensitivity analysis, testing crit. Shear stress for erosion

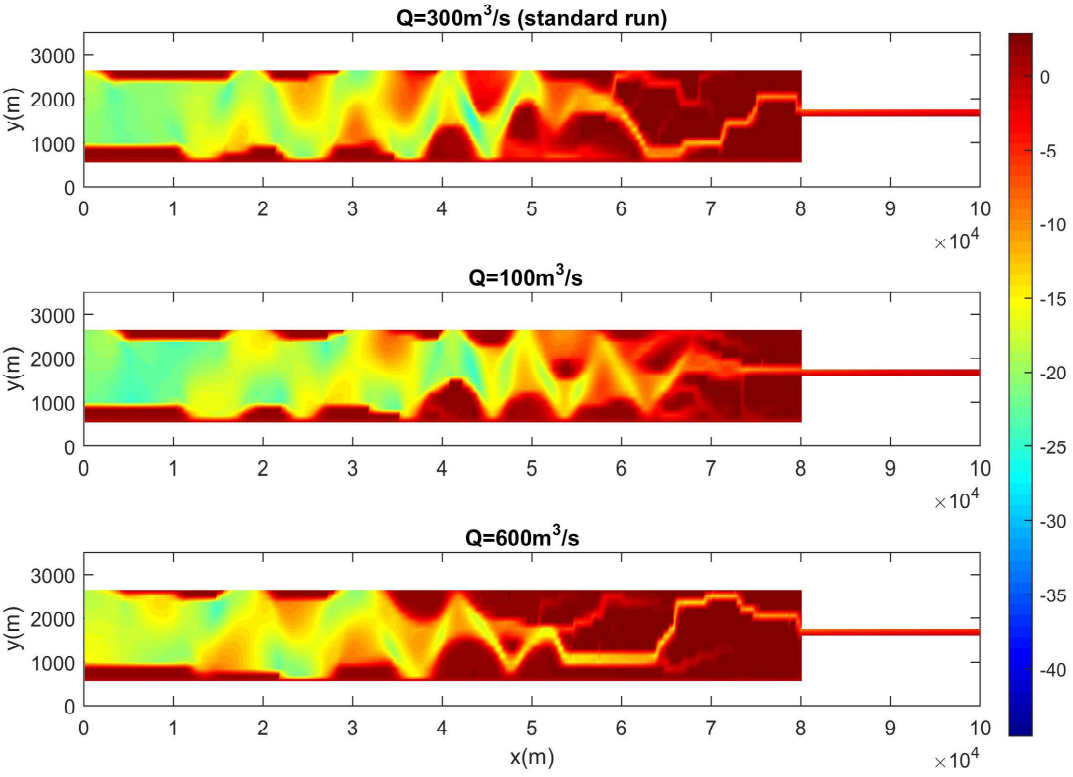

Figure 29 - Sensitivity analysis, testing river discharge

4.8.2 Conclusions

Figure 26, Figure 27, Figure 28 and Figure 29 depict bed level development for 400 years of morphological evolution. More specifically, at each figure, a single parameter is tested (e.g. fall velocity, river discharge etc.). The base scenario (SandMud) is compared to two other scenarios (i.e. one with smaller and one with larger value).

Figure 26 suggests that accumulation of mud increases in case settling velocity is increased. Using a fall velocity of 1mm/s, massive deposition takes place and the estuary gets muddy. In contrast, when a smaller value is used (e.g. 0.25mm/s) mud cannot settle anymore during the tidal cycle but it remains in suspension thereby moving in and out with the tide.

Furthermore, model results are very sensitive to the imposed concentration of mud at the boundaries (Figure 27). A large value of 0.1kg/m^3 leads to a large amount of imported mud during a tidal period and as a result, to significant accumulation. Therefore, the estuary gets muddy. On the contrary, by decreasing the value of imposed concentration at the boundaries to one fourth, much less mud becomes available to the system and as a result accumulation is limited.

Next, critical shear stress for erosion is analysed; Figure 28 suggests the estuary gets muddier when critical shear stress for erosion is increased. This is to be expected since higher velocities are needed so that critical shear stress is exceeded and sediment comes in suspension. As a result, erosion is less.

Last, the influence of river discharge on the model results is accessed (Figure 29); bed level development does not change considerably with the discharge. This leads to the conclusion that model results are less sensitive to river discharge. This does not seem logical taking into account that an increased river discharge equals with an increased fluvial mud concentration in the system. In other words, more mud is added in the basin. Differences in accumulation are more pronounced at the part of the basin close to the river, which implies that fluvial mud does not reach the seaward part of the estuary.

5

THE INFLUENCE OF TIDAL ASYMMETRY ON THE RESIDUAL SEDIMENT TRANSPORT

The asymmetric tidal velocity profile gives rise to residual sediment transport, thus, leading to morphological change. During model runs, the system was forced by a symmetrical semi-diurnal tide at the seaward boundary (M2). Due to the geometrical configuration of the model, shallow water tides were generated from the non-linear interaction of the tide with itself, mainly through the non-linear advective term and bottom friction. As a consequence, higher harmonics were formed by the model itself.

5.1 The influence of tidal asymmetry on the residual transport of sand

5.1.1 Tidal analysis

Conducting a harmonic analysis can highlight the role of tidal asymmetry on the sediment transport; this can be achieved by applying Fourier decomposition of the water level signal. Keeping the bed invariant during a model run, a direct relation between sediment transport and hydrodynamics is possible. More specifically, by analysing the variation of the tidal amplitudes of higher harmonics (e.g. M4, M6) and the phase differences between M2, M4 and M2, M6 over the model domain, conclusions with regards to the effect of tidal distortion on sediment transport can be drawn.

Bolle, Wang, Amos and De Ronde, 2010 used the latter methodology towards investigating the influence of changes in tidal asymmetry on the residual sediment transport in the Western Scheldt. However, the latter paper only focuses on the sediment transport of sand while the current MSc thesis is also interested in the transport of fines.

The water level profile was analysed using Matlab (developed by MathWorks), while at the same time taking advantage of the free open source developed by Deltares (viz. Open Earth Tools). The results of this analysis are related to the cross-section of the maximum bed level (Figure 30) and are visible in Figure 31:

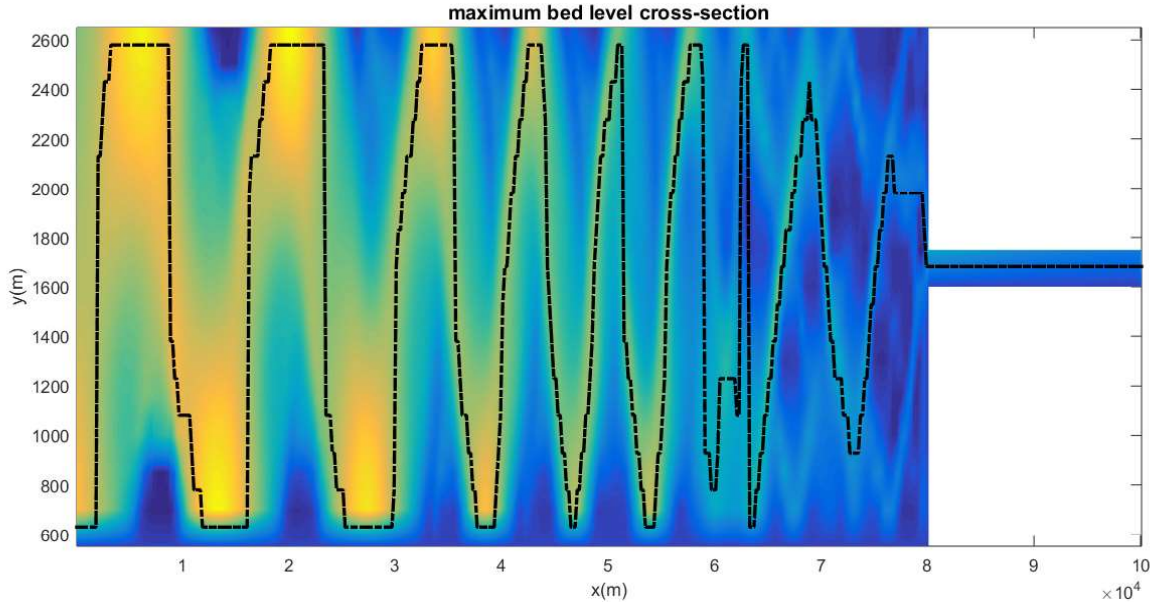

Figure 30 - The black dashed line indicates the cross-section along which bed level is maximum

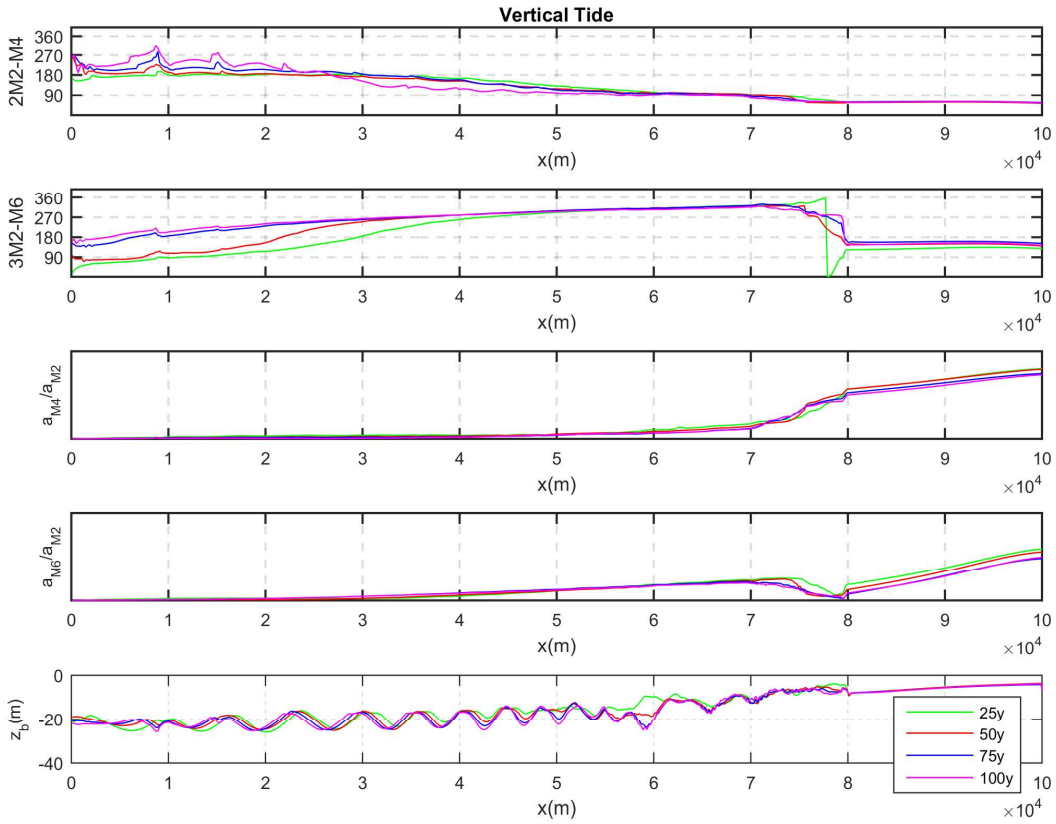

Figure 31- The evolution of the amplitude ratio and the phase difference between M2, M4 and M2, M6 tidal constituent for different bathymetries

Figure 31 depicts the evolution of the phase difference between the semi-diurnal and quarter-diurnal component (viz. M2, M4) and semi-diurnal and sixth-diurnal (viz. M2, M6) along the cross-section depicted in Figure 30. Furthermore, the development of the amplitude ratio is visible in the same figure. The character of the tide (e.g. flood/ebb dominant) can be understood by the phase difference between the tidal constituents, while the intensity of it by the amplitude ratio.

The asymmetric velocity profile leads to residual sediment transport. Therefore,A the phase difference between the M2 and M4 (M2 and M6) velocity components rather than the surface elevation components is essential for relating to residual sediment transport. Since the phase difference between water levels and velocities is not constant in space and time, it is not reliable to relate tidal distortion to residual sediment transport just by looking at the water levels.

In *chapter 6. Further analysis*, supplementary investigation on the horizontal tide is conducted and conclusions are drawn relative to the impact of tidal asymmetry on residual transport of sand.

5.2 The influence of tidal asymmetry on the residual transport of mud

5.2.1. Slack duration asymmetry

As it has already been mentioned during *chapter 2. Literature review*, tidal distortion is not only an important driver for the residual sediment transport of coarse but also of fine sediment. Slack duration asymmetry arguably influences the net transport of fines. To that end, some analysis on the asymmetric velocity signal will be done in order to investigate whether there is a relation between hydrodynamics and sediment transport.

The velocity profile is plotted at three different cross-sections (Figure 32, Figure 33, Figure 34) in order to investigate slack duration asymmetry development (i.e. $du/dt_{HWS} \neq du/dt_{LWS}$). Each of the figures depicts the velocity record during a run of 10 tidal cycles (i.e. 5days), with an invariant bed, for 5 different bathymetries (i.e. 25, 50, 75, 100, 200years); each column stands for a different bathymetry.

5.2.2 Calculating critical flow velocities

In Figure 32, Figure 33 and Figure 34 slack duration asymmetry is given in numbers. In more detail, the first line of the figure corresponds to the depth-averaged flow velocity while the second line gives the slack tide duration, during high and low water. Estimating the time when flow velocity ranges between critical and zero velocity do the quantification of this period. Positive and negative critical flow velocities are depicted by red and blue circles respectively; during this time span, flow is too weak to transport sediment and settling of fines occurs:

$$\tau_{crit} = \rho c_f \bar{u}^2 \quad (21)$$

$$c_f = \frac{g}{C^2} \quad (22)$$

$$C = \frac{1}{n} h^{1/6} \quad (23)$$

Where,

τ_{crit} = critical shear stress for erosion (N/m^2)
u = depth averaged velocity in x direction (m/s)
ρ = water density (kg/m^3)
c_f = friction coefficient
g = gravitational acceleration (m/s^2)
C = Chezy friction coefficient ($m^{1/2}/s$)
n = Manning' s coefficient ($m^{-1/3}s$)
h = water depth (m)

Using these equations and taking into account the (user-defined) critical shear stress for erosion (i.e. τ_{crit}=0.25N/m^2) the calculation of critical flow velocities is possible:

$$\bar{u}_{crit} = \sqrt{\frac{\tau_{crit}}{\rho g}} C \quad (24)$$

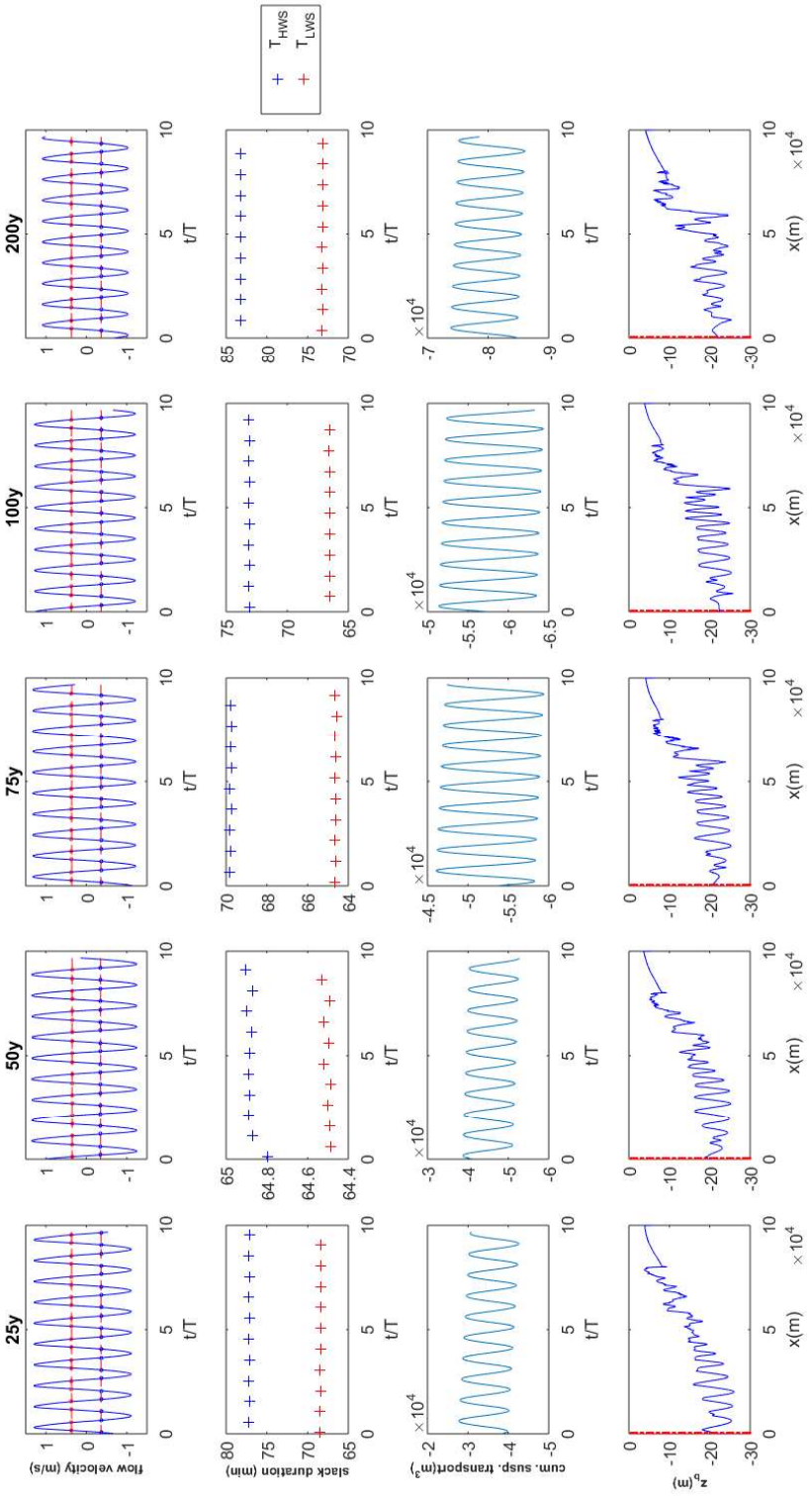

Figure 32 - Slack Duration Asymmetry at the seaward cross-section. A positive transport implies a net export of sediment (i.e. seawards)

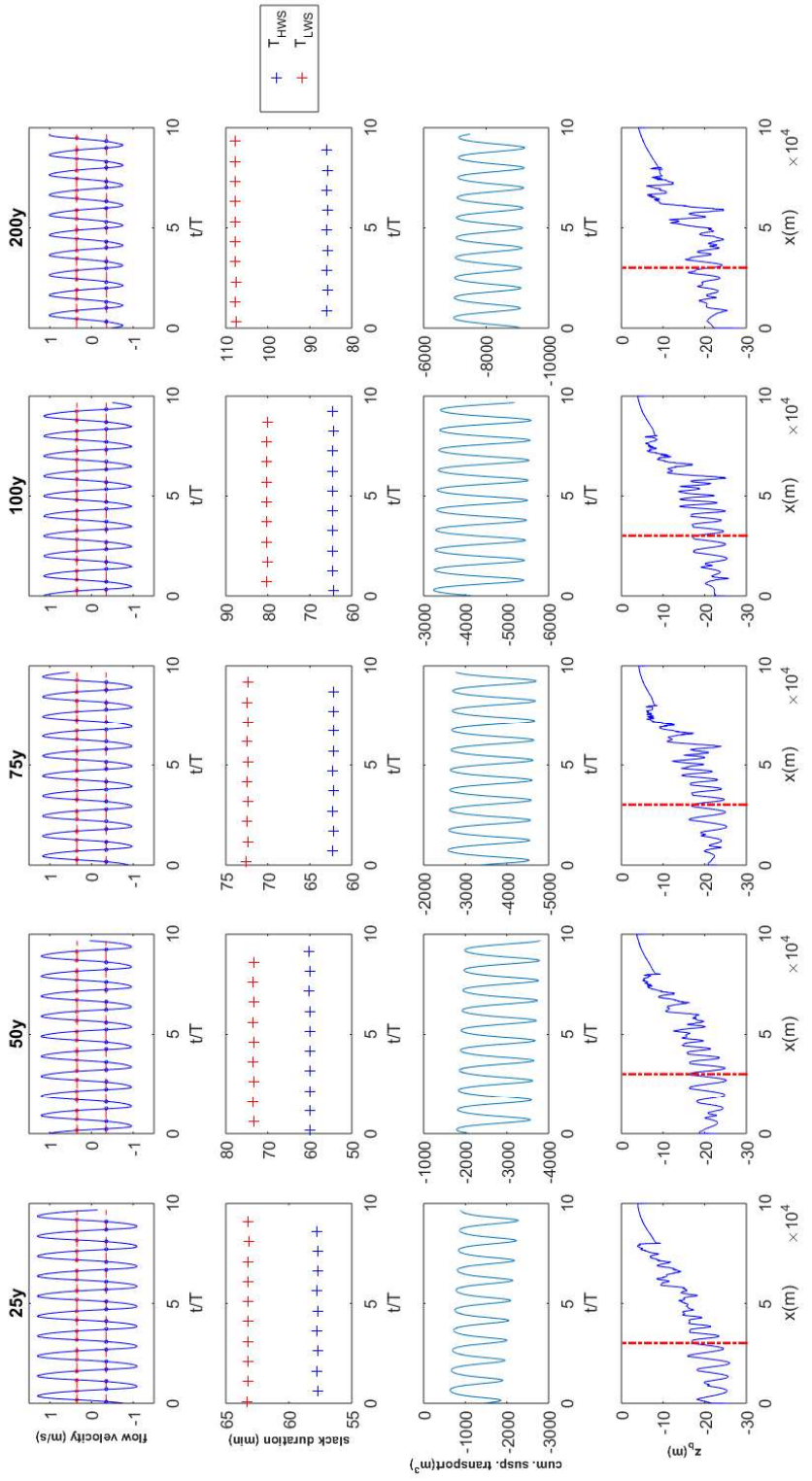

Figure 33 - Slack Duration asymmetry at the middle cross-section. A positive transport implies a net export of sediment (i.e. seawards)

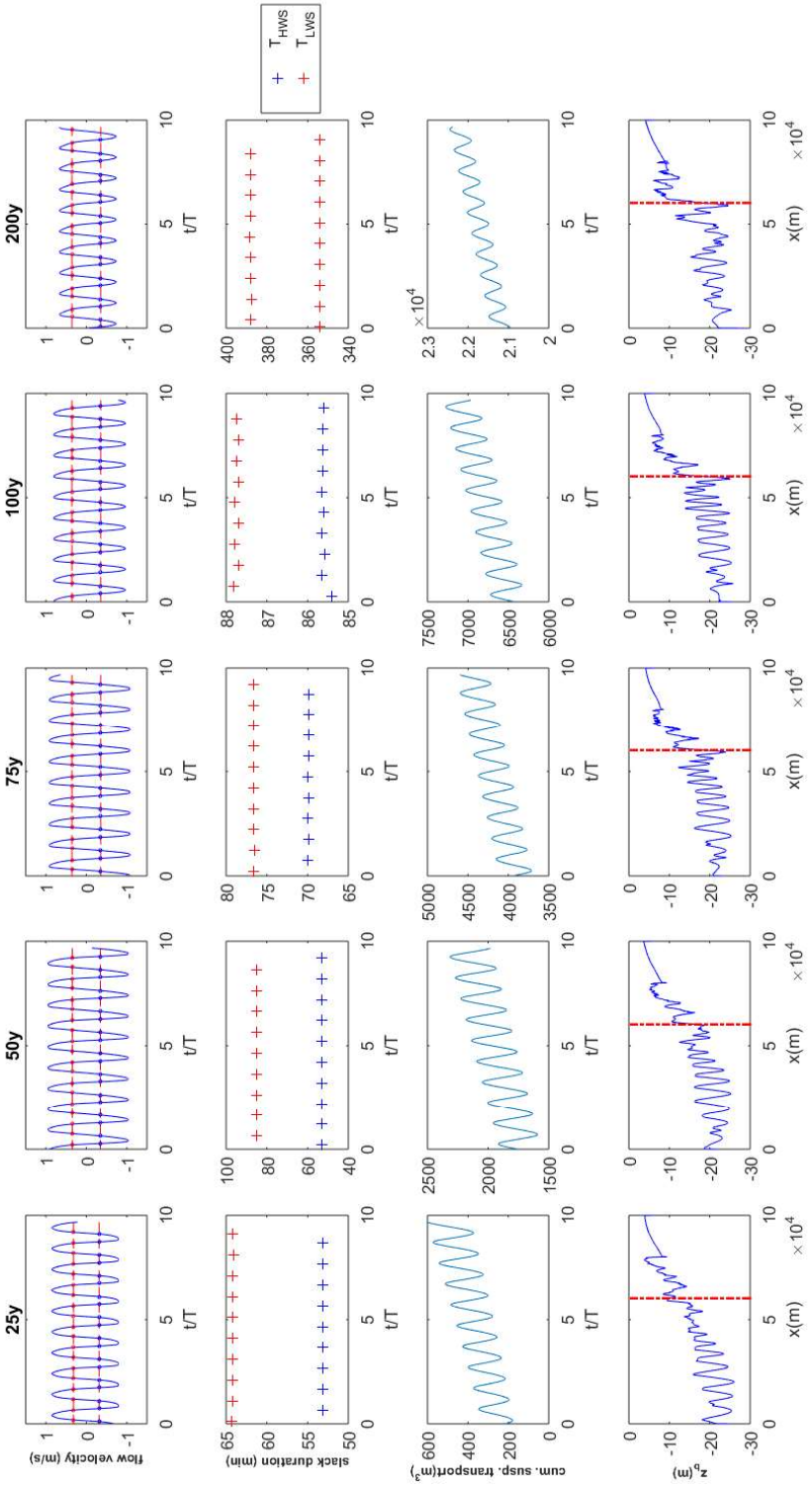

Figure 34 - Slack Duration asymmetry at the landward cross-section. A positive transport implies a net export of sediment (i.e. seawards)

5.2.3 Conclusions

The duration of flow reversal during low tide (HWS) and during high tide (LWS) is visible with the red and blue crosses respectively (Figure 32, Figure 33 and Figure 34).

Figure 32 depicts slack duration asymmetry at the seaward cross-section. More specifically, HWS is longer than LWS; this is the case for all different bathymetries (e.g. 25, 50, 75, 100, 200 years). A longer HWS implies a net import of fines; there is more time for sediment to settle during flood flow and as soon as the tide reverses (i.e. ebb flow), concentration is significantly reduced. This in turn leads to a reduced export. Therefore, averaged over a tidal cycle, a net import is expected. Theory comes in agreement with model output; a cumulative import of suspended sediment is happening in all scenarios except the 200-year scenario where a net export is observed.

In Figure 33 the middle cross-section is analysed; LWS is longer than HWS at this transect. Again this holds for all the scenarios (e.g. different bathymetries). In this case a next export of fines is to be expected. Looking at the cumulative suspended transport plots of Figure 33, an import of fines can be observed instead of an export; this might be due to the fact that the flow velocity record is representative for a single observation point while the cumulative sediment transport accounts for the whole cross-section. In addition, asymmetries in sediment properties might be responsible for this disagreement between hydrodynamics and residual transport.

Furthermore, Figure 34 depicts slack duration asymmetry at the landward cross-section. LWS is longer and as a result a net export of fines is anticipated at this section of the estuary. Indeed, cumulative suspended transport plots suggest a net export.

It has to be said that slack tide duration is not the only driver of residual transport of fines. Local depth during flood and ebb flow can have a counteracting effect, especially in case the wet surface of the basin is much larger at high water than at low water (e.g. deep channels with large intertidal area). For instance, if the depth during ebb flow is significantly smaller than during flood flow, more sedimentation will occur during ebb flow no matter the asymmetry in the hydrodynamics. The relaxation time scale for sedimentation is given by:

$$T_{sed} = \frac{h}{w_s} \quad (25)$$

Where,

h=local water depth (m)

w_s=fall velocity (m/s)

All in all, it can be concluded that residual transport of mud is difficult to be determined only by slack duration asymmetry. The reason is that net transport depends on several parameters (e.g. sediment properties, hydrodynamics, local bathymetry) and as a result, it cannot be sufficiently described by a single parameter.

6

FURTHER ANALYSIS

6.1 The effect of mud on the sediment transport of sand

During the previous chapter (viz. *4.6 The effect of mud on the sediment transport of sand*) the influence of mud on the exporting sand volume was made apparent. More specifically, Figure 23 suggested the different sand exporting magnitudes for the two scenarios (i.e. SandMud versus Sand). In order to explain the reduced export of sand in the SandMud scenario, further analysis needed to be made with regards to the hydrodynamics as well as the sediment properties governing each of the models.

In the next chapters analysis of certain parameters that influence residual sediment transport takes place; the idea is to compare results between the two models and extract useful conclusions relative to the importance of each parameter.

6.1.1 Investigating hydrodynamics

The cross-sectional depth averaged velocity is plotted at the three cross-sections under consideration for both the SandMud and the Sand model (Figure 35 and Figure 36 respectively); peak flow asymmetry is depicted at the three cross-sections of interest along the estuary. More specifically, each column stands for a different cross-section; the first column (i.e. blue colour) corresponds to the seaward cross-section while the second (red) and the third (green) to the middle and the landward cross-section respectively.

The effect of mud is in general on reducing both peak flood and ebb velocities without changing the character of the tide. This is to be expected since the accumulation of mud reduces the tidal storage; this in turn leads to the reduction of tidal velocities (e.g. flood/ebb). The latter is evident when comparing Figure 35 to Figure 36.

At the seaward cross-section the tidal signal is flood-dominant for both models while at the landward it is ebb-dominant. Lastly, at the middle cross-section, the signal is switching from ebb to flood dominant during the 400 years of evolution.

Plotting flow velocity at a certain transect can give an overall idea with regards to the local residual sediment transport. However, as stated earlier, this flow record consists of several components and it is highly likely that these components have opposing effects on the residual sediment transport.

The most important drivers of residual sediment transport, as mentioned in chapter 2.3.2, are: residual flow (i.e. Stokes drift return current, river discharge) as well as higher frequency components of the flow velocity (i.e. tidal asymmetry). In order to be able to make a distinction between each of these mechanisms and its contribution to sediment transport, additional investigation has to be done for each component separately.

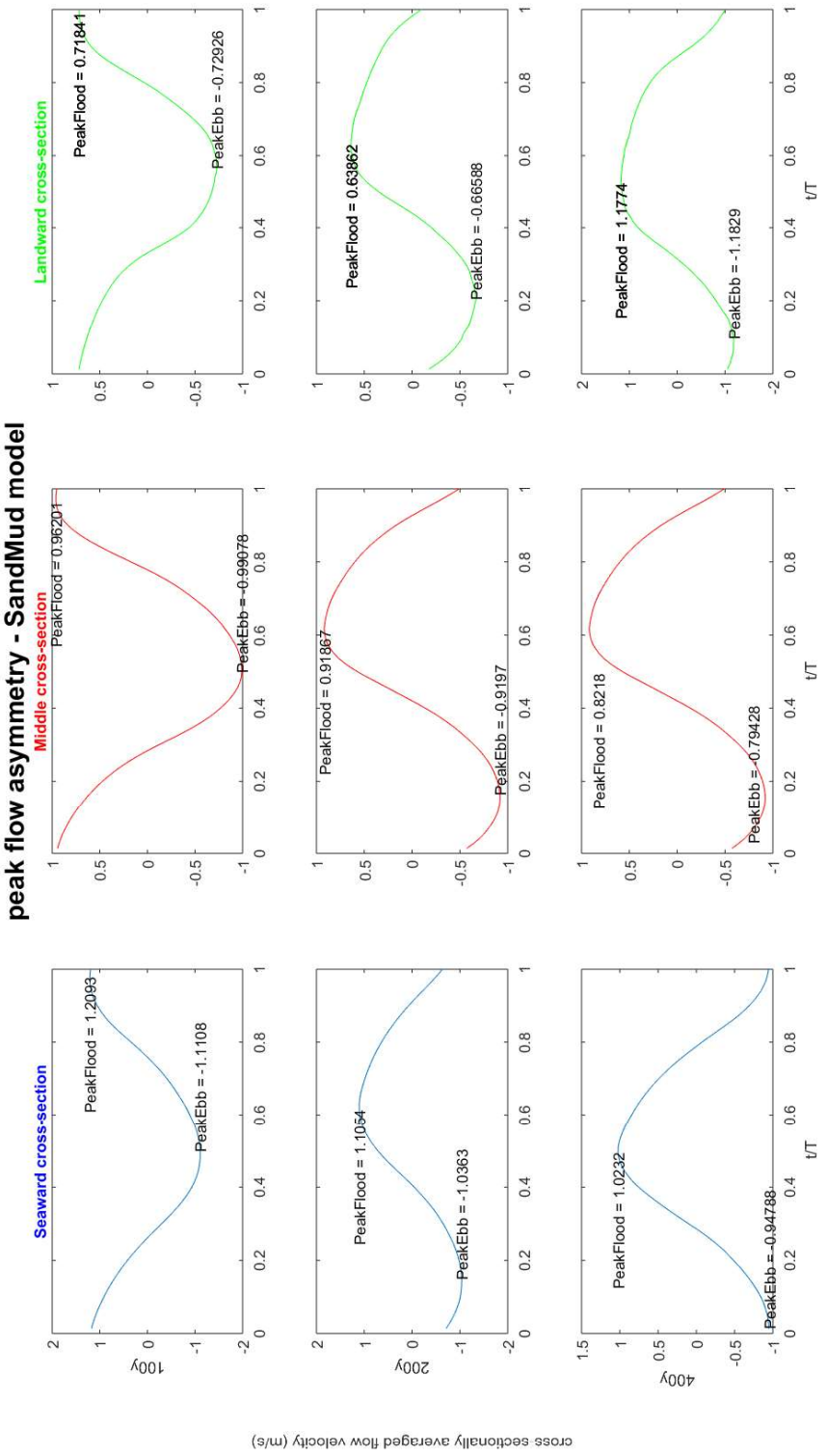

Figure 35 - Peak flow asymmetry, SandMud model

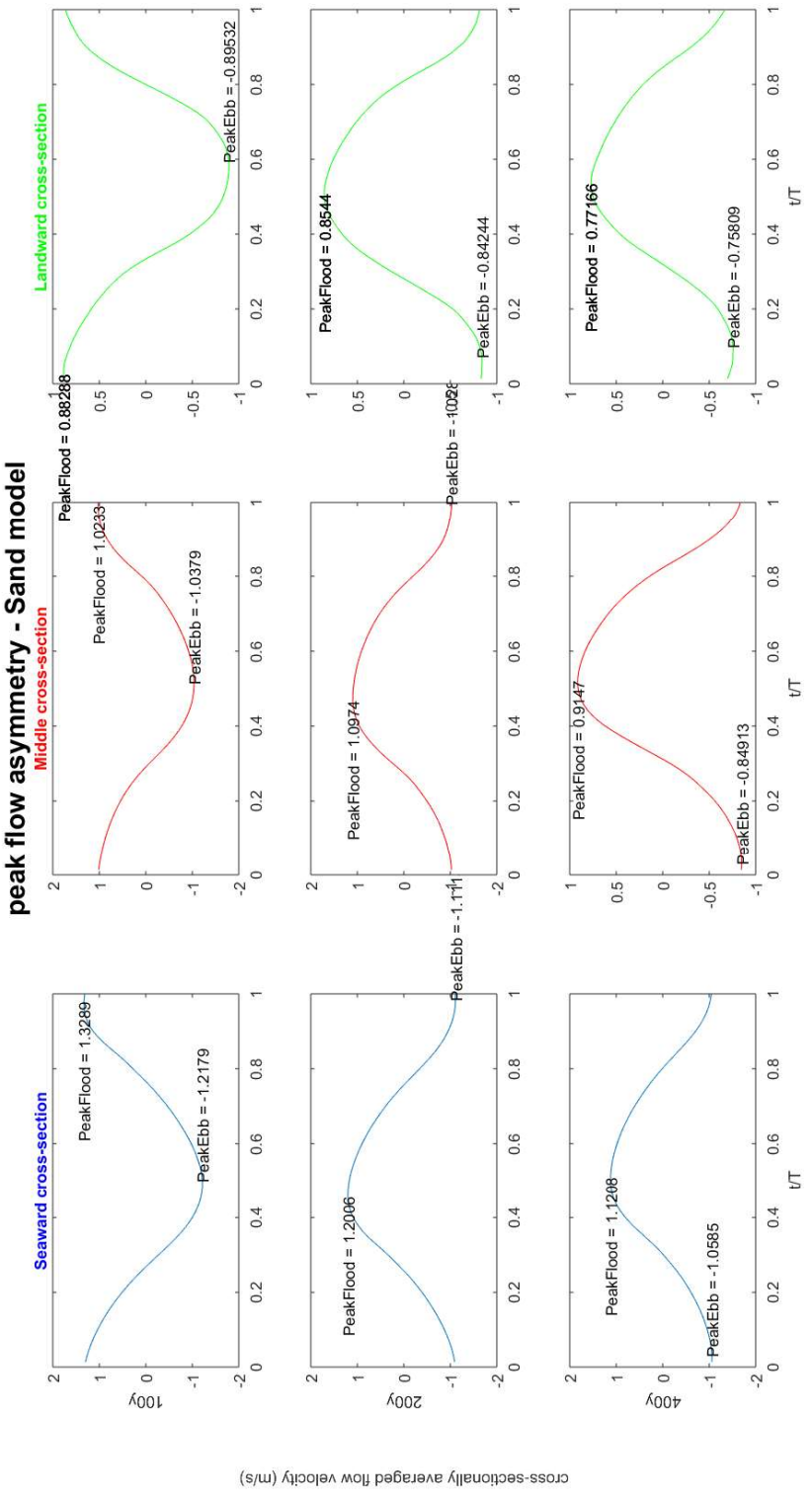

Figure 36 - Peak flow asymmetry, Sand model

6.1.2 Investigating Tidal Asymmetry

It is known from literature that tidal asymmetry is one of the main drivers of residual sediment transport in estuarine environments (Dronkers, 1986). The tidal wave is getting distorted as soon as it approaches shallow water due to the following phenomena (Van Rijn, 2010):

- Reflection
- Amplification
- Deformation
- Damping

As a result, tidal surface elevations as well as velocities diverge from an ideal sinusoidal case. Due to the nonlinear dependence between velocity and sediment transport, the net sediment transport averaged over a tidal cycle is not zero anymore; this implies a change in morphology.

The concept of tidal asymmetry is particularly applicable for coarse sediment (i.e. sand) and less applicable for fines, where lag effects take over, making the interpretation of results less trivial.

To be able to draw any conclusion with regards to the relation between tidal asymmetry and residual sediment transport, the bed has to be constant. Hence, further analysis is going to be done using 3 different bathymetries (namely, during 100, 200 and 400 years). In more detail, starting from a certain bathymetry the model will run for 5days (approximately 10 tidal cycles). During these runs the morphological factor is set to 1 so the bed is practically invariant. A schematic representation is given for a better understanding (Figure 37):

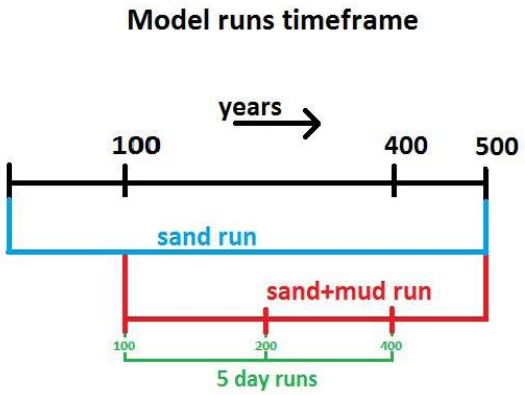

Figure 37 - Schematic representation of runs timeframe

In the next figures the temporal variation of the vertical tidal asymmetry will be analysed for both scenarios (i.e. SandMud, Sand). There are two characteristic parameters that can be used for the investigation of tidal asymmetry in the estuary: the phase difference between semidiurnal and quarter-diurnal component (2M2-M4) as well as the amplitude ratio of these components (a_{M4}/a_{M2}). The phase difference signifies the character of the tide (e.g. flood/ebb dominant) while the amplitude ratio suggests the intensity of the asymmetry.

Figure 38, Figure 39, Figure 40 depict bed level development as well as phase difference between M2 and M4 components at 100, 200 and 400 years for both the Sand and the SandMud model. The three cross-sections are visible with black dashed line.

Tidal asymmetry at a certain part of the estuary is related to the asymmetry at the seaward boundary (Van der Spek, 1994). Similarly, the hypothesis is made that the residual sediment transport at a cross-section can be related to the change in the tidal asymmetry at this section rather to the tidal asymmetry itself (Wang, Jeuken, de Vriend, 1999).

The change of the character of the phase difference throughout the years is induced by the changing morphology. What is thought to be happening is that, in general, estuaries tend to import sediment via a flood-dominant velocity signal; this leads to growth of intertidal area, which in turn modifies the tidal signal to ebb-dominant and hence, urges sediment export. Later on, shoals are eroded and the estuary moves back to its initial state. This process applies mostly for coarse sediment where an instantaneous sediment response to the flow is assumed.

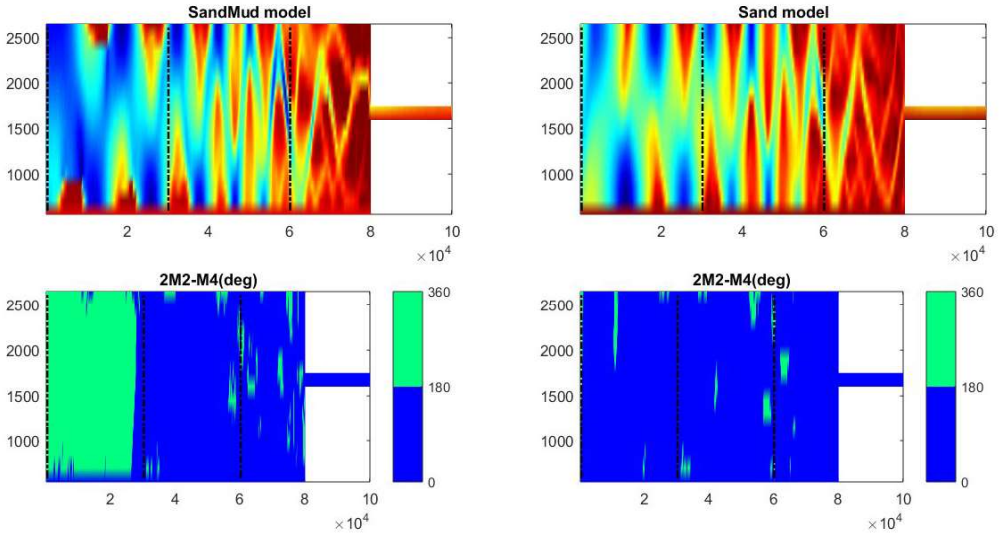

Figure 38 - Phase Difference 2M2-M4 at 100 years

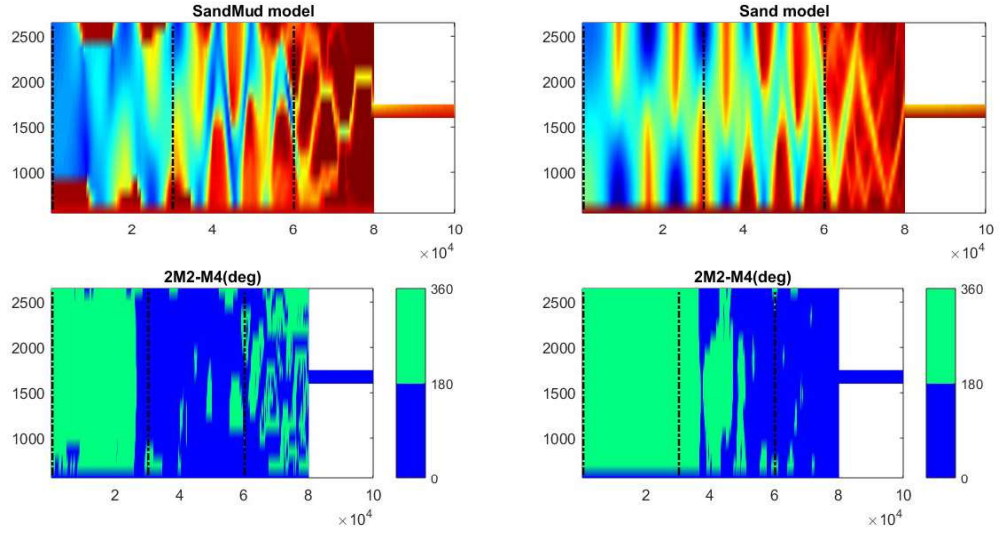

Figure 39 - Phase Difference 2M2-M4 at 200 years

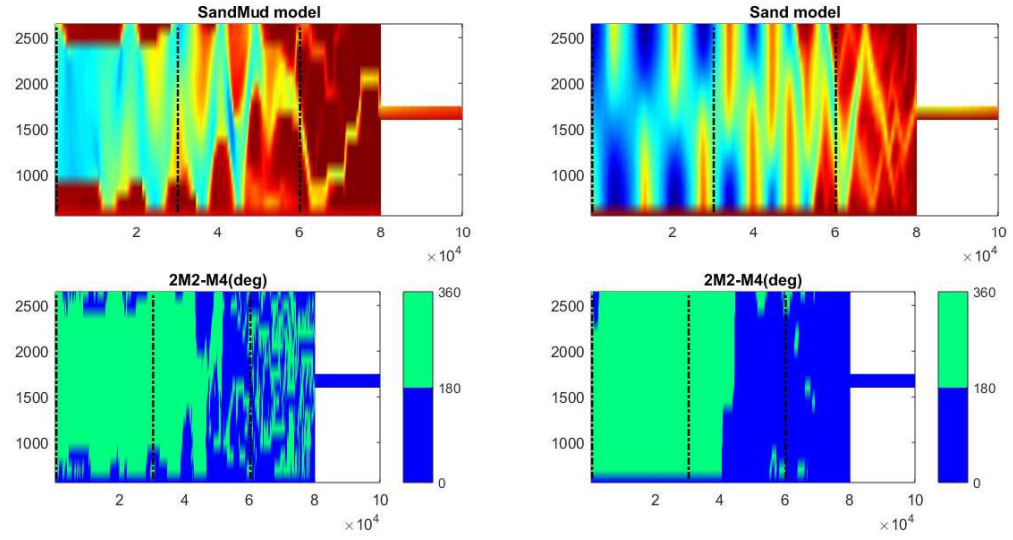

Figure 40 - Phase Difference 2M2-M4 at 400 years

The plots of the intertidal area over time might give an insight into tidal asymmetry development (Figure 41):

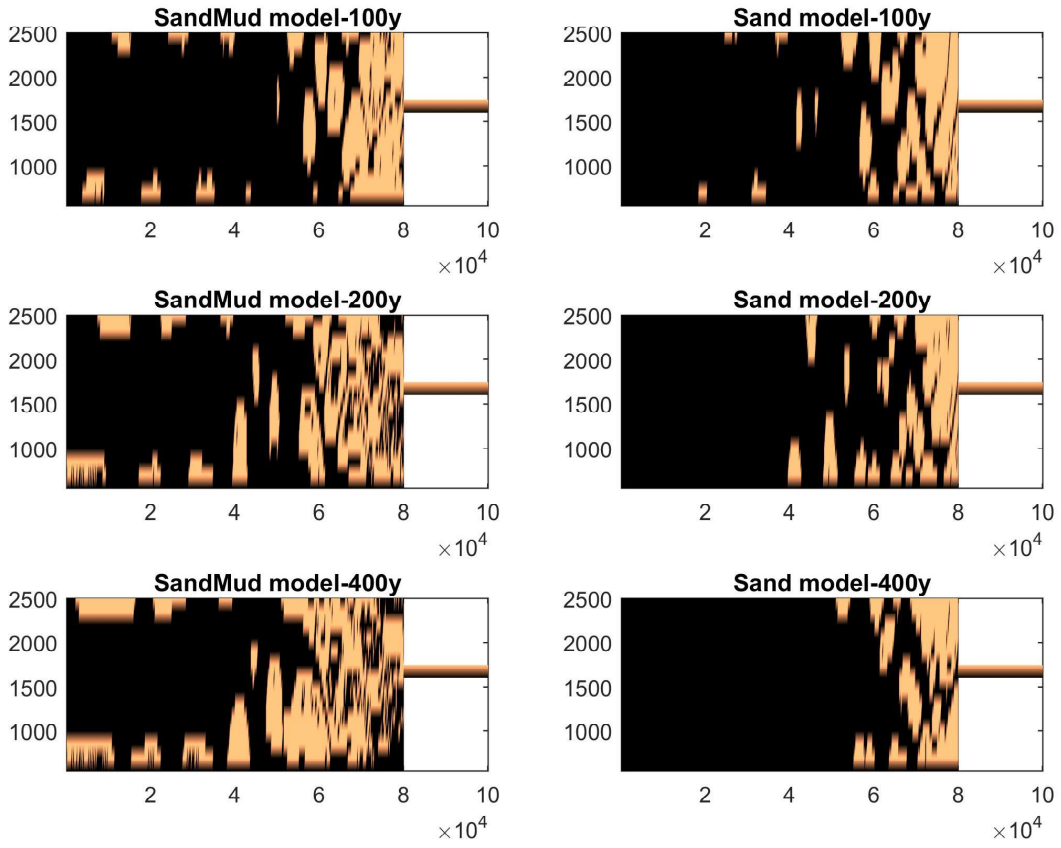

Figure 41 - Intertidal area for both models at 100y, 200y, and 400y

Residual sediment transport is directly related to the asymmetric velocity signal (in this model via the Engelund-Hansen formula). The latter formula suggests that sediment transport is proportional to the velocity to the power 5 ($S \propto u^5$). This non-linear dependency leads to residual sediment transport in case asymmetry develops.

Previously, an attempt was made to relate local vertical tidal asymmetry to residual sediment transport. In fact, local horizontal tidal asymmetry depends on the vertical asymmetry happening in the whole storage area (i.e. landwards from the area of interest). However, it is not possible to draw any safe conclusions by looking at the asymmetry in the water levels. The reason is that the phase difference between horizontal and vertical tide is not constant along the estuary. Accordingly, a certain vertical tidal signal cannot be securely translated into a certain horizontal tidal signal.

A harmonic analysis of the horizontal tidal signal might give a clearer picture in this respect. The cross-sectional averaged velocity will be used as an input for the harmonic analysis. Accordingly, the temporal development of the phase difference between M2 and M4 as well as the amplitude ratio between the two components will be analysed at the three cross-sections of interest; namely, at the seaward (x=0km), middle (x=30km) and landward (x=60km) cross-section.

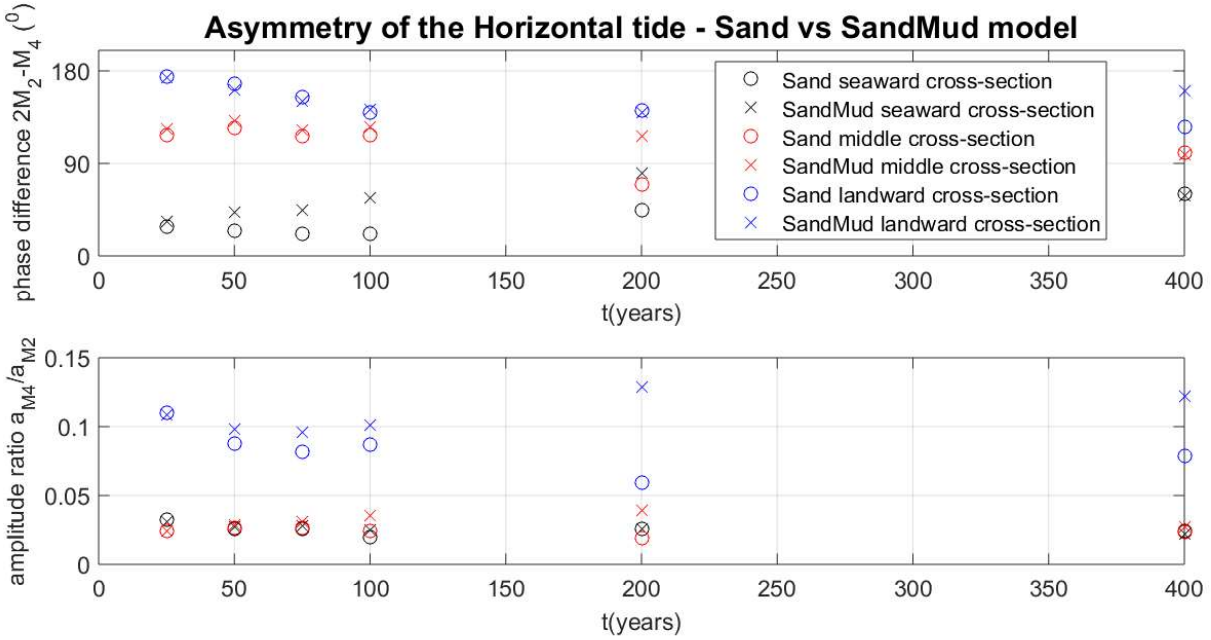

Figure 42 - Phase difference 2M2-M4 and amplitude ratio aM4/aM2 of the horizontal tide, for the SandMud and Sand model

Figure 42 shows the development of the asymmetry of the cross-sectional depth-averaged velocity, for three cross-sections, for the SandMud and the Sand model. In more detail, for each cross-section, flow velocity was calculated using the following formula:

$$\bar{u}_{cr} = \frac{\sum_{i=1}^{n}(u_i * h_i)}{\sum_{i=1}^{n} h_i} \quad (26)$$

In which,

u_{cr} = the cross-sectional depth averaged velocity
u_i = the x velocity component at the observation point i
h_i = the water depth at the observation point i

The model has been set up such that each cross-section along the estuary consists of 12 observation points. Hence, the cross-sectional velocity is calculated using the weighted arithmetic mean of these velocity points. By doing that the influence of lateral depth variation is taken into account.

As a general observation it can be said that, in both models, the effect of tidal asymmetry on the residual sediment transport of sand is an export at the middle and landward cross-section (e.g. ebb-dominance) and an import at the seaward cross-section (e.g. flood-dominance). Therefore, mud does not change the character of tidal asymmetry. In addition, the intensity of tidal distortion, which is introduced by the amplitude ratio, is not significantly altered in case of mud; the trends are similar and the value of the ratio is comparable in both scenarios. Therefore, all in all, it can be concluded that the existence of mud does not have a major effect on tidal asymmetry.

Furthermore, the latter findings can be related to the actual residual transport of sand happening at the three cross-sections in Figure 23. Model results show an export of sand at all three cross-sections. Obviously the importing effect of tidal distortion at the seaward cross-section is counteracted by other exporting mechanisms (i.e. Stokes drift return current, river discharge).

Moreover, the phase difference between M2 and M4 tidal constituents at the three cross-sections can be used as an indication for the influence of tidal asymmetry on the residual transport of fines. The fact that it ranges between 0 and 180 degrees implies that LWS is longer than HWS at all three transects. The latter is verified by the flow velocity plots; it is true for the middle (Figure 33) and landward cross-section (Figure 34) but not for the seaward cross-section (Figure 32), where the signal shows a longer HWS.

However, it can be argued that the asymmetric velocity profile is not only controlled by the M2 M4 phase difference; literature suggests the difference between M2 and M6 is also important for the hydrodynamics. Furthermore, this disagreement between theory and model results can also be credited to the fact that Figure 32, Figure 33 and Figure 34 relate to the velocity at a single observation point whereas Figure 42 relate to the cross-sectional velocity.

6.1.3 Investigating Stokes Drift

Tidal distortion is an important driver of morphological development but cannot be exclusively used for predicting future morphology. Another important physical process taking place in estuaries and has an impact on residual sediment transport is Stokes Drift.

Similarly to wind waves, Stokes drift can take place in tidal waves as long as the character of the wave is partly progressive. A residual mass flux in the wave propagation direction will occur if more than half of the flood tide coincides with water levels above MSL. This net inflow must be compensated by a seaward-directed flow, much like undertow (Bosboom and Stive, 2013); typical values of this return current in the Western Scheldt range around 5cm/s.

The existence of mud in the system has already been linked with a reduced export of sand compared to the Sand scenario (Figure 23). Further analysis with regards to the difference in the return current between the two models should be able to provide an answer to the question whether Stokes Drift is an important driver towards this behaviour or not.

The return current in a depth-averaged sense can be calculated accordingly:

$$\bar{u}_{return} = -\frac{\langle q \rangle}{h_0} = 0.5\frac{\hat{\eta}}{h_0}\hat{u}\cos\varphi \qquad (27)$$

In which,

$\hat{\eta}$ = tidal amplitude (m)
h_0 = water depth (m)
φ = phase difference between horizontal and vertical tide (rad)
$\hat{u}$ = peak tidal velocity (m/s)

The results of this analysis can be seen in Figure 43. The first line of the figure shows bed level development after 400 years of morphological evolution. The second line depicts the average phase difference between vertical and horizontal tide while the third line introduces peak flood velocities. The fourth line stands for the depth averaged return current.

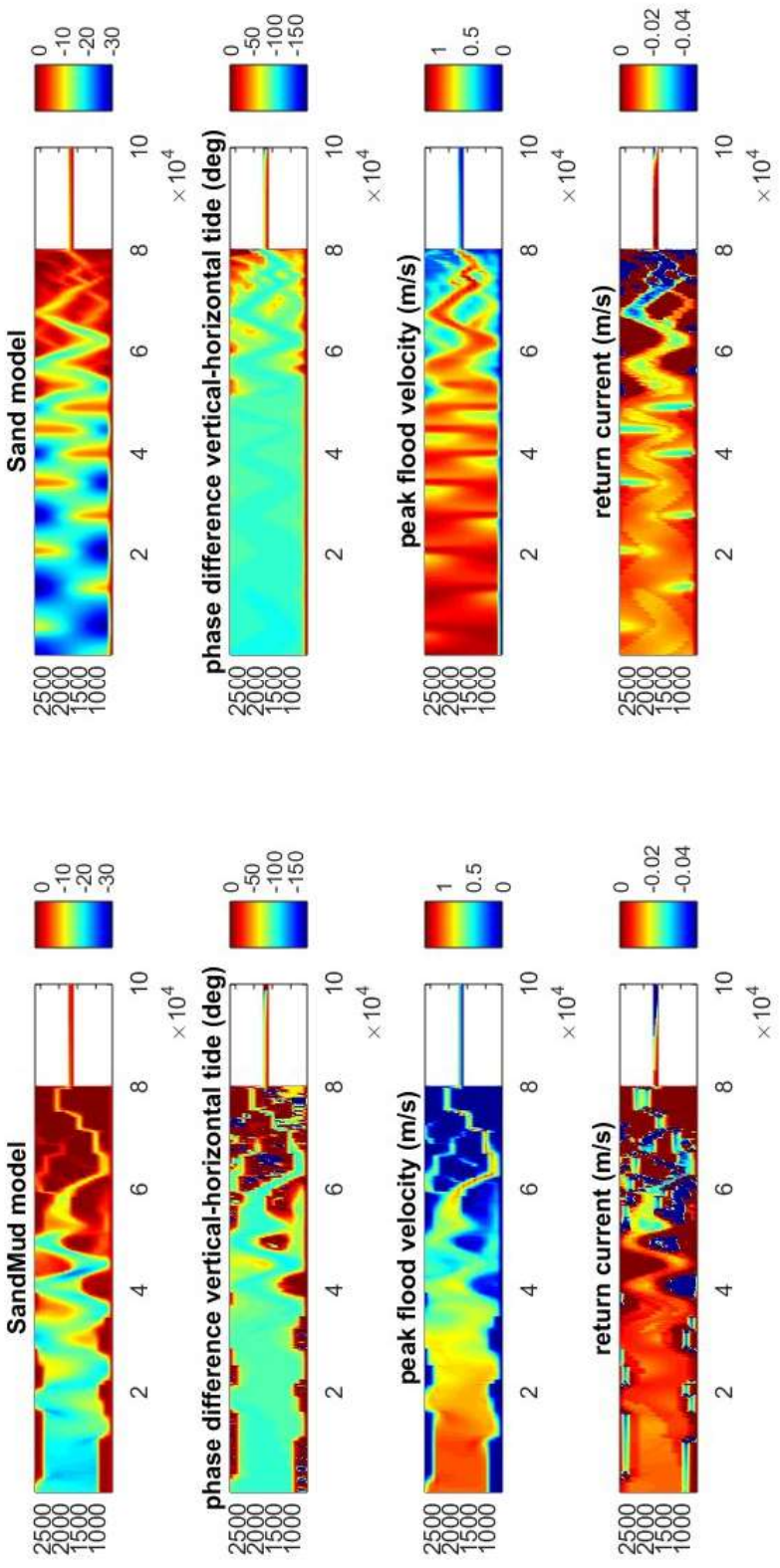

Figure 43 - Stokes Drift return current for the two models at 400years of development

As expected, the accumulation of mud reduces the storage area and as a result peak flood velocities. This of course has an influence on the return current; model results show smaller velocities in the SandMud scenario compared to the Sand scenario. This in turn means that the erosion induced by the Stokes drift return current is lower when mud is present in the system.

The comparison of the return current between the two models and over the years is illustrated (Figure 44):

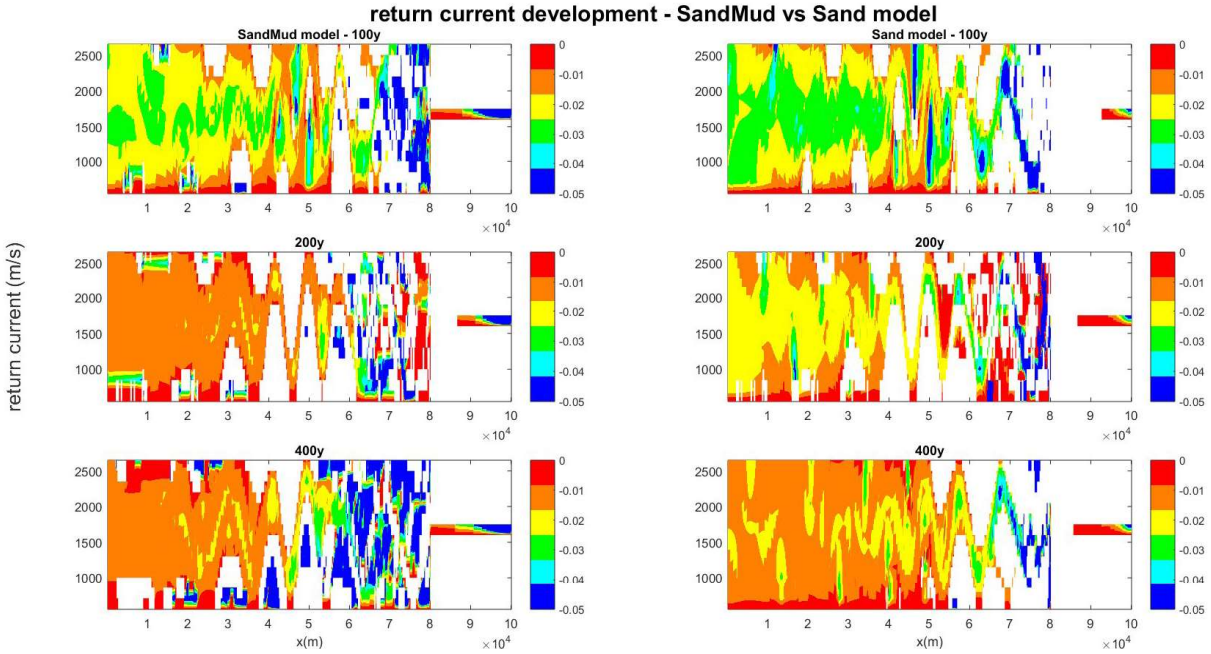

Figure 44 - Return current development in the two models

Figure 44 is indicative for the mud-induced decrease in the Stokes drift return current. For a better understanding, relevant values are given in Table 6:

Decrease in Stokes drift return current				
Cross-section	Distance from mouth	Years		
		100y	200y	400y
Seaward	0 km	25%	65%	9%
Middle	30 km	24%	70%	-4%
Landward	60 km	4%	18%	-27%

Table 6 - Decrease in Stokes drift return current due to mud

As a final conclusion, it can be said that Stokes drift return current is another mechanism responsible for the reduced export of sand (Figure 23).

6.2 Investigating the reduced sand export at the seaward cross-section

Peak flow asymmetry plots between the two models (Figure 35, Figure 36) show that the influence of mud is on decreasing both peak flood and ebb velocities. Therefore, averaged over a tidal period, this leads to a difference in the residual transport of sand. However, the reduced export of sand (in the Sand scenario) might not be solely based on the difference in the hydrodynamics between the two models.

Another reason, which might justify the reduced sand export, is the sediment fraction availability on the bottom. This is to say, the increased volume fraction of mud in a computational cell on the bed equals to a reduced volume fraction of sand in the same cell (i.e. covering effect). Since every sediment transport formula is a function of the concentration times the velocity, a reduced sand concentration would in turn mean a reduced export of sand. Gaining insight towards sediment fraction availability requires further analysis into bed stratification.

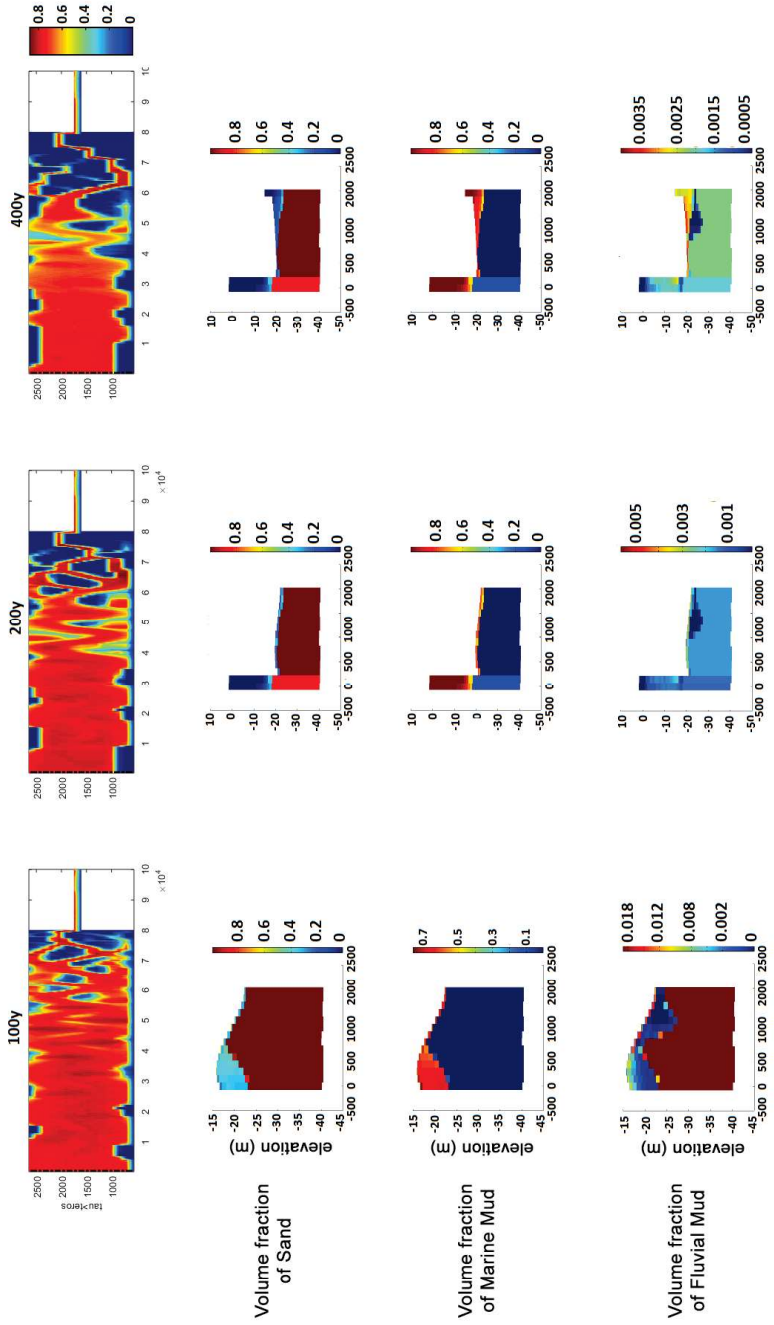

Figure 45 - Bed composition at the seaward cross-section at 100, 200 and 400 years

In Figure 45 bed stratification development at the seaward cross-section is depicted. In more detail, each of the 3 columns corresponds to a different 5-day run (i.e. during 100y, 200y and 400y). The first row indicates the percentage of time over a tidal cycle when critical shear stress for erosion is exceeded. In other words, it signifies the areas where mud is eroded from the bed and areas where the flow is too weak to erode the fines. The second row indicates the percentage of sand volume in the bed while the third and the fourth row show the percentage of marine and fluvial mud in the bed layers respectively.

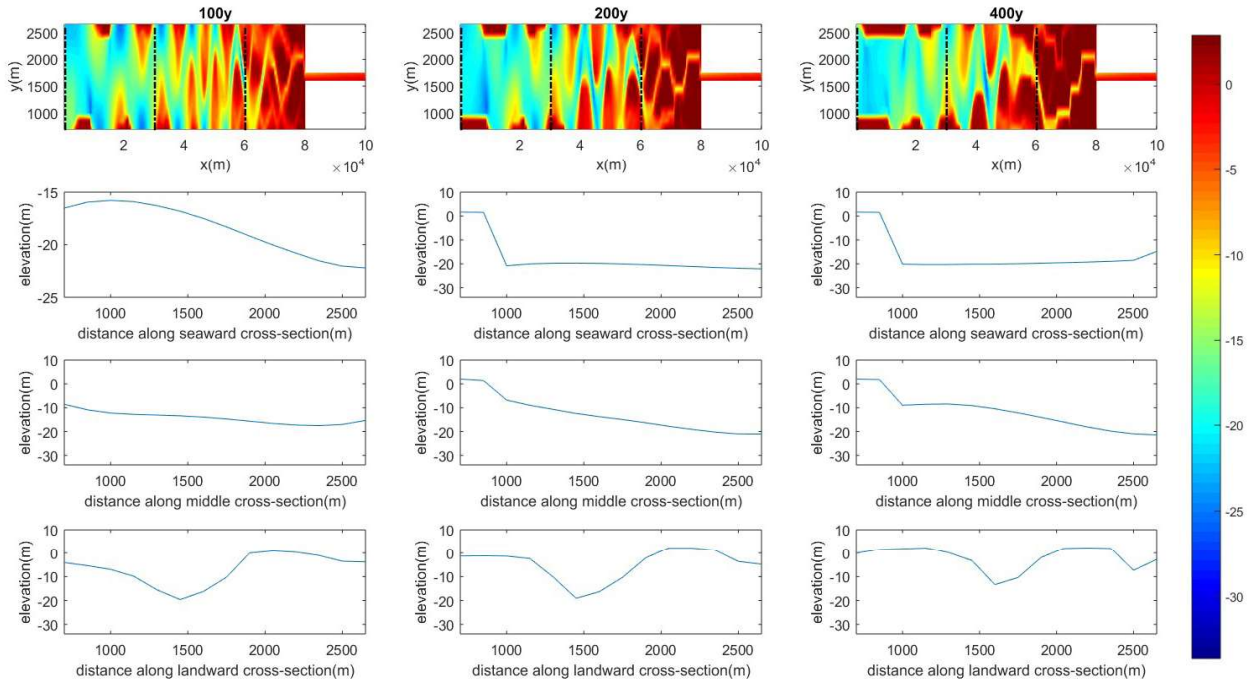

Figure 46 - Cross-sectional bed level development

Figure 46 depicts bed level development at the three cross-sections of interest. Each column represents a different model run (i.e. 100, 200 and 400 years) while each row stands for a different cross-section (i.e. seaward, middle, and landward).

At 100 years, sand concentration in the upper layers is already reduced by 60% due to the presence of marine mud (first column, Figure 45); the fluvial mud content is very low. Mud settles mainly at the shallow part of the cross-section (Figure 46). This makes sense since the deposition of mud depends on the fall velocity that is a function of the grain size; fines have a small fall velocity (compared to coarser sediment) and as a result it is less likely to settle at deeper parts.

At 200 years (second column, Figure 45) sand concentration (in the upper layers) has been reduced even more due to the increased concentration of mud.

At 400years, more mud has accreted at the shallow parts of the cross-section compared to 200y run.

A general observation for every run is that mud is mainly settling at the shallow areas of the cross-sections. However, it is clear that deeper parts are also covered to some extent by mud (less than in the case of the shallow). In total, the existence of mud on the bed is effectively reducing the concentration of sand, thereby reducing the export rate. Therefore, this mechanism can be used to explain the reduced export of sand, in the SandMud model, at the seaward cross-section (Figure 23).

6.3 Investigating the reduced sand export at the middle cross-section

The character of the tide is ebb-dominant throughout the years (Figure 35, Figure 36); this realisation can explain the exporting tendency at this cross-section for both SandMud and Sand model (Figure 23d). Nonetheless, the difference in exporting volume between the two models cannot be solely explained by the difference in the hydrodynamics.

Sediment fraction availability on the bed might be of importance here. To really understand what is happening, bed stratification plots are essential.

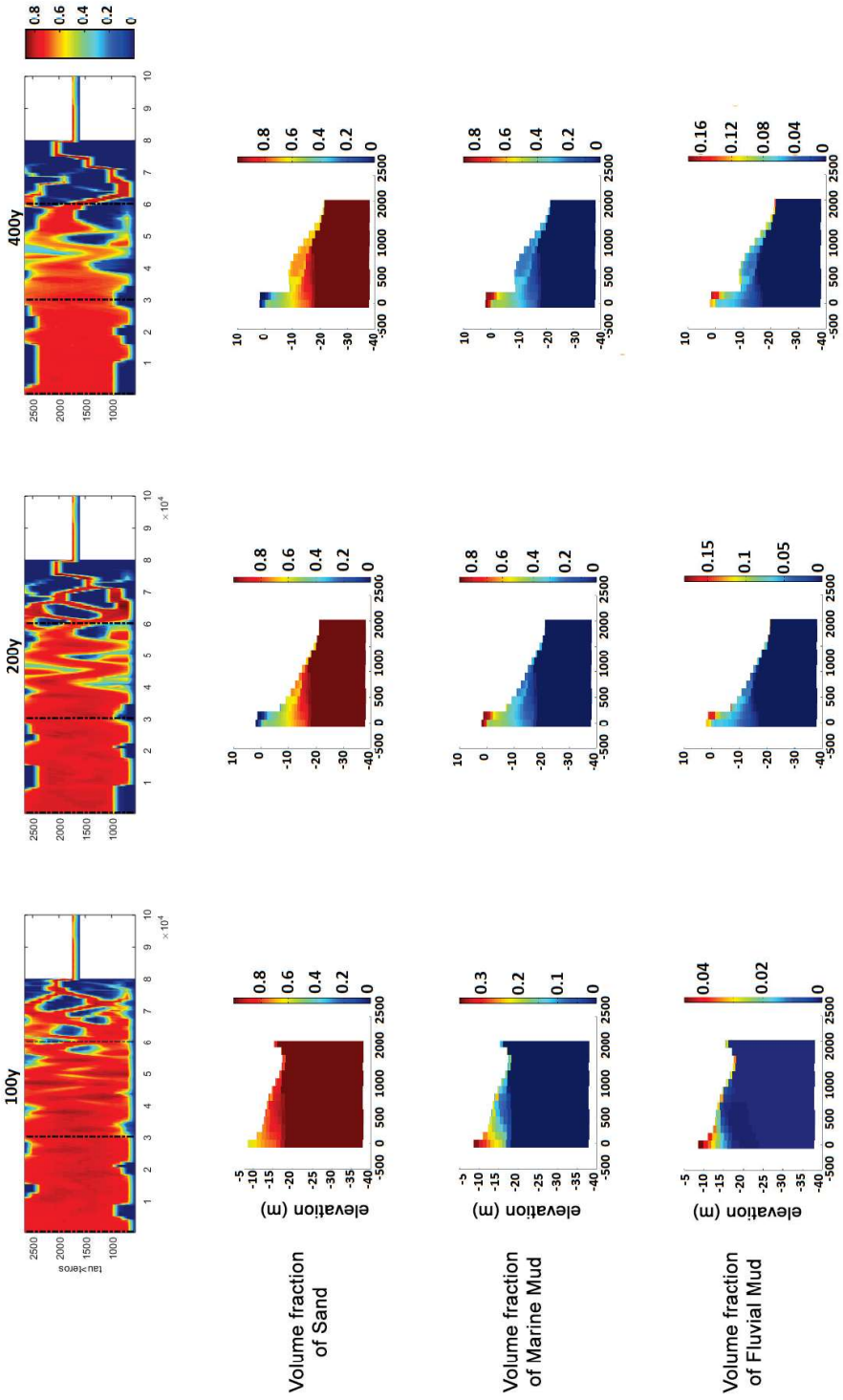

Figure 47 - Bed composition at the middle cross-section at 100, 200 and 400 years

The development of bed stratification is visible at Figure 47. At 100 years of evolution, the bed is mostly covered by sand (more than 80%); marine mud is responsible approximately for the rest 20%. Fluvial mud concentration remains at low levels (around 2%). At 200 years and 400 years of evolution, the formation of the shallow area close to the bank (Figure 46) attracts a lot of mud (≈80%) while the rest of the area concentrates significantly less mud (30% at most).

The conclusion that can be drawn is that marine mud fraction effectively reduces the sand volume fraction thereby leading to reduced sand export. Moreover, as far as fluvial mud is concerned, it is evident that its concentration is not capable of influencing the results to a large extent. Therefore, marine mud is still responsible for the differences in cumulative sand transport between the two models.

6.4 Investigating the reduced sand export at the landward cross-section

Peak flow asymmetry plots suggest a velocity signal that is exporting sand throughout the 400 years of evolution. The influence of mud on the hydrodynamics is on reducing peak flood and ebb velocities; the latter might not justify the reduced export of sand to its full extent. Similarly to the approach followed for the other two cross-sections, bed stratification plots will give an insight into volume fraction availability on the bed.At the landward cross-section (i.e. 60 km from the mouth), sediment volume fraction plots for different runs (e.g. 100, 200 and 400 years) indicate the development of bed stratification (Figure 48).

At 100 years of evolution, the bed consists mostly of sand (≈85-90%). However, at 200 years, fluvial mud has covered more than 70% of the upper layers; the rest 30% remains sandy (marine mud has not reached this region ≈2%). At 400 years, even more fluvial mud has deposited at this section, making the upper layers fully muddy (approximately 80-90%). This can be linked with the reduction in the sand exporting volume that happens after the first 100 years (Figure 23e). As a matter of fact, the increasing difference in the exporting volumes (blue and green line) can be credited to the increasing fluvial mud content.

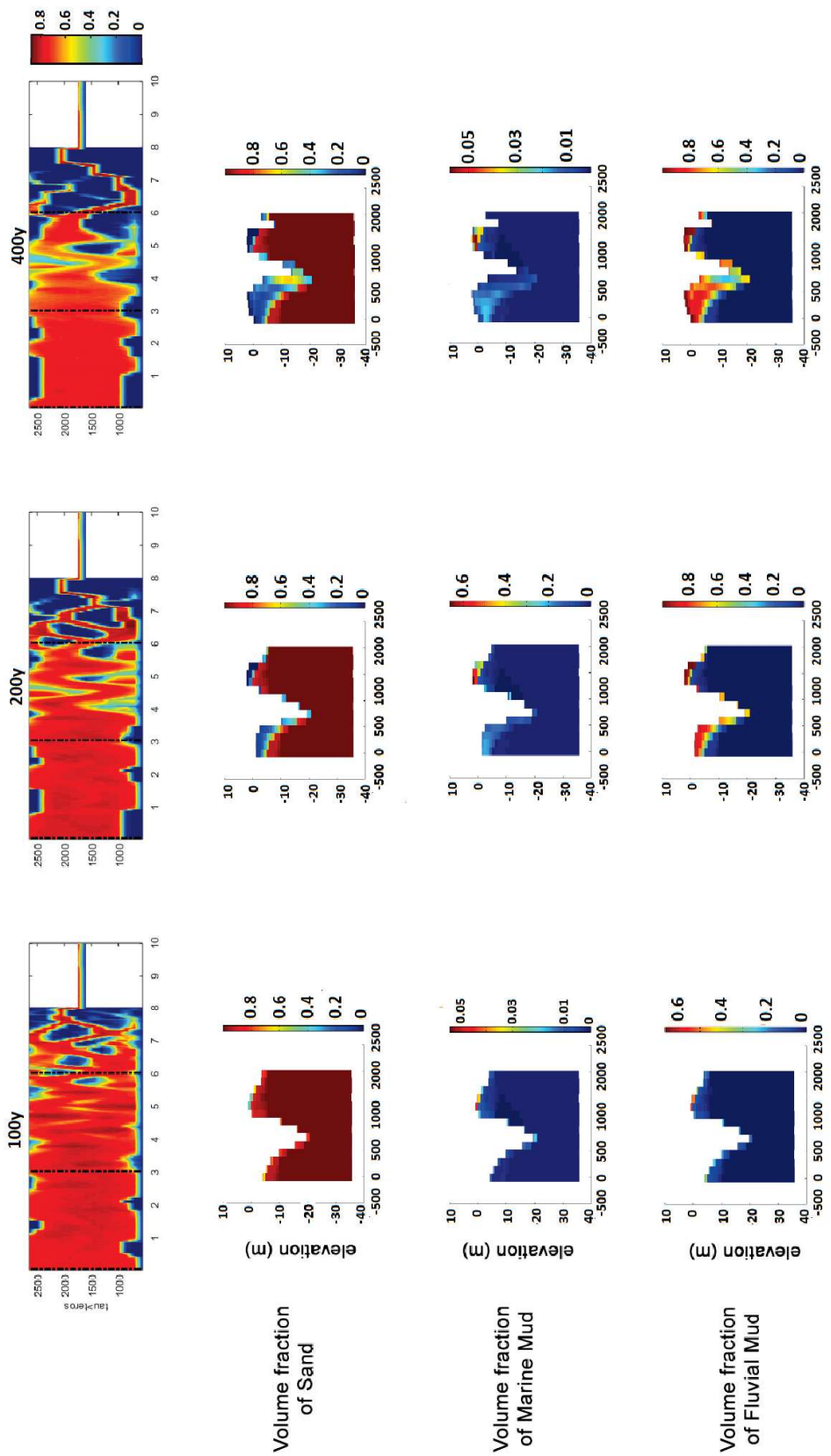

Figure 48 - Bed composition at the landward cross-section at 100, 200 and 400 years

7

CONCLUSIONS

Analysis proved that both the SandMud and the Sand model are characterized by export of sand throughout the 400 years of morphological development (Figure 23).

In order to explain the export of sand, mechanisms that have an influence on residual sediment transport have been defined and analysed. The most important are thought to be the following three:

- Tidal asymmetry (i.e. interaction between M2 and M4 tidal constituents)

  Peak flow asymmetry is of importance here since higher velocities relate non-linearly to the sediment transport thus, averaged over the tide, leading to import or export. This asymmetry is crucial for the residual transport of coarse sediment (i.e. sand), which responds instantaneously to the flow, while it is less relevant for finer sediment where lag effects need to be taken into account.

  Figure 42 show that tidal asymmetry enhances ebb-dominance at the middle and landward cross-section (export) and flood-dominance (import) at the seaward cross-section. The import close to the mouth is counteracted by an ebb-directed residual flow (e.g. Stokes drift return current, river discharge).

- Stokes drift return current

  Ebb-directed velocities up to 5cm/s lead to a tidal averaged net export of sand.

- River Discharge

  Averaged over the tide, the seaward-directed river velocities lead to a net export of sand.

Figure 23c and d show a net export throughout the 400 years of evolution while Figure 23e show an import during the first 50 years, followed by an export. The combined effect of the aforementioned mechanisms is thought to be responsible for the exporting behaviour of the schematized estuary.

7.1 Research questions

The research questions as defined in *chapter 1.3 Research questions*, are listed below:

Q1. What is the influence of mud on the morphological development?

Q2. What is the sensitivity of model output to changes in certain parameters?

Q3. What is the impact of mud on the hydrodynamics?

Q4. What is the impact of mud on the residual transport?

7.1.1 The influence of mud on the morphological development

The conclusion from the analysis is that the accumulation of mud reduces the accommodation space and the tidal storage of the estuary; this leads to a reduction in tidal velocities and as a result to a reduction in sediment transport rates ($S \propto u^5$). The estuary is exporting less sand and as a result it fills with sediment; this can be well understood by looking at Figure 23 where the SandMud scenario is compared to the Sand scenario.

In addition, mud has another effect on the sediment transport of sand; mud deposition reduces the volume fraction of sand on the bed (Figure 45, Figure 47 and Figure 48) thereby reducing the sand transport rate. As a result, less sand is exported and the estuary fills with sediment.

However, a distinction has to be made between numerical and physical reality. In other words, it has to be clarified whether the latter effect is only due to the model or it can also happen in the physical system of interest (i.e. the Western Scheldt estuary).

What physically happens is that deposited mud is mixing with sand thereby strengthening the bed. Accordingly, critical shear stress for erosion increases and sediment transport rate decreases. Therefore, although the final effect is the same (i.e. sediment transport rate is reduced), it is caused by two different mechanisms.

7.1.2 The sensitivity of model output to changes in certain parameters

Sensitivity analysis was conducted in *chapter 4.8 Sensitivity analysis*. The conclusions can be summarised as follows:

- The model is sensitive to fall velocity. An increase in fall velocity leads to more deposition of mud than in the case of smaller fall velocity. This is reasonable since the relaxation time scale for sedimentation decreases. In the physical system, coarser grains (i.e. larger fall velocity) accumulate faster than finer and as a result morphology is anticipated to resemble the case with larger fall velocity (Figure 26). Therefore, numerical results can be linked to physical results in this case. The mudflats area in the outer estuary suggest that, qualitatively, the standard value of 0.5mm/s is the more appropriate, as it reflects best to the Western Scheldt.
- The imposed concentration of mud at the boundaries is set to 0.05kg/m^3 for the standard SandMud scenario. However, when concentration is doubled, significant deposition takes place (Figure 27); the bed level plot suggest that the estuary is choked by mud while in the case, where the concentration is halved (0.025kg/m^3), much less deposition is observed. Model results are reasonable in this case because a larger concentration at the boundaries equals with more mud in the system.
- The user-defined critical shear stress for the erosion of fines is set to 0.25Pa for the standard SandMud scenario. An increase leads to more deposition (extensive mudflats in the outer estuary) since sediment is more difficult to be eroded from the bed; a decrease imply increased erosion; more sediment is entrained from the bed and remains in suspension during the tidal cycle (almost no mudflats in the outer estuary) (Figure 28). Qualitatively, it can be said that using the standard value of 0.25Pa the model resembles best the Western Scheldt estuary.
- The standard value for the river discharge is set to 300m^3/s. This value is larger compared to the average Scheldt river discharge (120m^3/s). However, model runs suggest that results are not sensitive to the river discharge. The differences in accumulation are more pronounced at the part of the estuary close to the river (Figure 29), which implies that mud from the river does not reach the seaward part.

7.1.3 The impact of mud on the hydrodynamics

The deposition of mud has an effect on morphology; it leads to a reduction of the tidal storage which in turn has an impact on water levels and velocities. The effect of mud on velocities can be well understood by comparing Figure 35 to Figure 36, where the cross-sectional velocity is plotted throughout 400 years of evolution for the SandMud and Sand model respectively. In conclusion, mud reduces both peak flood and ebb velocities.

7.1.4 The impact of mud on the residual transport

This chapter explains the mechanisms responsible for the decreased export of sand observed in the SandMud model compared to the Sand model (Figure 23, blue and green line respectively).
The accumulation of mud has a double effect on the sediment transport of sand; first, the existence of mud on the bed decreases the available volume fraction of sand thereby decreasing its export rate; this numerical process can be physically associated with the strengthening of the bed caused by the mixing of sand and mud. Second, the change in morphology, induced by mud, has an influence on the hydrodynamics (e.g. velocities); this in turn has an influence on the residual transport.

The most important drivers of residual sediment transport, as mentioned in *chapter 2.3.2 Influence of tidal asymmetry on residual sediment transport*, are residual flows (i.e. Stokes drift return current, river discharge) as well as higher frequency components of the flow velocity (i.e. tidal asymmetry).
The influence of mud on each of the latter parameters is realised by analysing each parameter separately comparing the SandMud to the Sand scenario. The conclusions can be summarised as follows:

- Reduction in tidal velocities

  The accumulation of mud decreases the tidal storage of the estuary thereby decreasing tidal velocities (both peak flood and ebb); this can be understood by comparing Figure 35 to Figure 36. As a result, the sediment transport rate decreases and the export of sand is diminished.

- Covering (hiding) of sand by mud

  The existence of mud has a direct effect in reducing the concentration of sand on the bed. As a result less sand is available for export since the upper layers consist mostly of mud (Figure 45, Figure 47 and Figure 48). Therefore, this covering is contributing to the reduced export of sand.

- Tidal asymmetry

  Comparing the asymmetry development in both models (Figure 42) it can be said that mud has no significant effect neither on the character of the distortion nor in the intensity. Therefore, tidal asymmetry is not considered an important mechanism towards the reduced export of sand.

- Stokes drift return current

  Another effect of mud is the decrease of the Stokes drift return flow (Figure 43, Figure 44). This leads to an additional decrease in the exporting sand volume thereby making the difference between the two models larger.

BIBLIOGRAPHY

Dam, G., Van Der Wegen, M., Bliek, B. and Cleveringa, J. (2016). Long-term sand-mud modeling of the Scheldt estuary. Abstract for the 18th Physics of Estuaries and Coastal Seas Conference, 2016.

Hibma, A., de Vriend, H.J. and Stive, M.J.F. (2003). Numerical modeling of shoal pattern formation in well-mixed elongated estuaries. Estuarine, Coastal and Shelf Science 57 (2003), 981-991.

Van Der Wegen, M., Dastgheib, A., Jaffe, B.E. and Roelvink, D. (2010). Bed composition generation for morphodynamic study of San Pablo Bay in California, USA.

Valle-Levinson, A. (2010). Definition and classification of estuaries. Contemporary issues in Estuarine Physics.

Wang, Z. B., Jeuken, C., and De Vriend, H. (1999). Tidal asymmetry and residual sediment transport in estuaries: a literature study and application to the Western Scheldt. Technical report, Deltares (WL).

Winterwerp, J.C. (2013). On the response of tidal rivers to deepening and narrowing, Risks for a regime shift towards hyper-turbid conditions.

Van Kessel, T., Vanlede, J. and de Kok, J. (2010). Development of a mud transport model for the Scheldt estuary. Continental Shelf Research Vol. 31, 165-181.

Van Der Wegen, M. (2013). Numerical modeling of the impact of sea level rise on tidal basin morphodynamics. Journal of Geophysical Research: Earth Surface Vol. 118, 447-460.

Mehta, A.J., Hayter, E. J., Parker, W. R., Krone, R. B., Teeter, A. M. Cohesive Sediment Transport. Journal of Hydraulic Engineering, Vol.115, No. 8, August, 1989.

Geleynse, N., Storms, J. E. A., Stive, M. J. F., Jagers, H. R. A., Walstra, D.J. R. (2010). Modeling of a mixed-load fluvio-deltaic system. Geophysical Research Letters, Vol. 37.

Bolle, A.,Wang, Z. B., Amos, C., and De Ronde, J. (2010). The influence of changes in tidal asymmetry on residual sediment transport in the Western Scheldt. Continental Shelf Research Vol. 30, 871–882.

Van Der Wegen, M. and Roelvink, J. A. (2008). Long-term morphodynamic evolution of a tidal embayment using a two-dimensional, process-based model. Journal of Geophysical Research, Vol. 113.

Dronkers, J. (1986). Tidal asymmetry and estuarine morphology. Netherlands Journal of Sea Research, 20(2/3): 117-131.

Van Maren, D. S. and Winterwerp, J. C. (2012). The role of flow asymmetry and mud properties on tidal flat sedimentation. Continental Shelf Research Vol. 60, 71-84.

Van Der Werf, J. J. and Briere, C. D. E. The influence of morphology on tidal dynamics and sand transport in the Scheldt estuary. Deltares, 2013

Mertens, T., DeWolf, P., Verwaest, T., Trouw, K., De Nocker, L. and Coudere, K.
An integrated master plan for Flanders future coastal safety.

Dam, G., Van Der Wegen, M. and Roelvink, D. (2013). Long-term performance of process-based models in estuaries.

Van Kessel, T., Valende, J., Eleveld, M. A., Van Der Wal, D. and De Maerschalck, B. Validation and Application of Mud Model Scheldt Estuary in the framework of LTV. Deltares, 2011.

Van Der Wegen, M. and Roelvink, J. A. (2012). Reproduction of estuarine bathymetry by means of a process-based model: Western Scheldt case study, The Netherlands. Geomorphology Vol. 179, 152-167.

Bosboom, J. and Stive,M. J. (2012). Coastal Dynamics I: Lectures Notes CIE4305 . VSSD, Delft.

Deltares (2011a). Delft3D-FLOW user manual.

Duan, J. G. and Nanda, S. K. (2005). Two-dimensional depth-averaged model simulation of suspended sediment concentration distribution in a groyne field. Journal of Hydrology Vol. 327, 426-437.

Amoudry, L. (2008). A Review on Coastal Sediment Transport Modeling.

Scheel, F., van Ledden, M., van Prooijen, B.C., & Stive, M.J.F. (2012). Simulating the large-scale spatial sand-mud distribution in a schematized process-based tidal inlet system model.
University of Twente, NCK-days 2012: Crossing borders in coastal research. 191-195.

Parker, B. B. (2007). Tidal Analysis and Prediction, Chapter 3: Methods of Tidal Analysis and Prediction.

Van De Kreeke, J. and Robaczewska, K. (1993). Tide induced residual transport of coarse sediment; application to the Ems estuary. Netherlands Journal of Sea Research Vol. 31, Netherlands Institute for Sea Research, 209-220.

Verlaan, P. A. J., 2000. Marine vs fluvial bottom mud in the Scheldt estuary. Estuarine,
Coastal and Shelf Science 50 (5), 627-638.

McLaren, 1994. Sediment transport in the Westerschelde between Baarland and Rupelmonde. GeoSea Report. GeoSea Consulting, Cambridge, United Kingdom.

Friedrichs, C. T. and Aubrey, D. G. (1988). Non-linear tidal distortion in Shallow Well-mixed estuaries: a Synthesis. Estuarine, Coastal and Shelf Science Vol.27, 521-545

Speer, P. E. and Aubrey, D. G. (1985). A study of non-linear propagation in shallow inlet/estuarine systems. Part II; theory. Estuarine, Coastal and Shelf Science Vol. 21, 207-224.

Wang, Z. B. (1989). Mathematical Modeling of Morphological Processes in Estuaries. Communications on hydraulic and geotechnical engineering, Faculty of Civil Engineering, Delft University of Technology, report nr. 89-1

Pritchard, D. W. (1955). Estuarine circulation patterns. Proceedings of the American Society of Civil Engineers 81 (717), 1 - 11.

Cameron, W. M. and Pritchard, D. W. (1963) Estuaries. In: Hill, M. N. (editor) The Sea Vol. 2, John Wiley and Sons, New York, 306–324.

Dronkers, J. (1986). Tidal asymmetry and estuarine morphology. Netherlands Journal of Sea Research, Vol.20, 117-131.

Van Rijn, L. C. (2010). Tidal phenomena in the Scheldt Estuary. Deltares